

Biostratigraphy and sequence stratigraphy of the Toarcian Ludwigskanal section (Franconian Alb, Southern Germany)

Gernot Arp¹, Sebastian Gropengießer¹, Christian Schulbert², Dietmar Jung³, Andreas Reimer¹

¹ Georg-August-Universität Göttingen, Geowissenschaftliches Zentrum, Abteilung Geobiologie, Goldschmidtstraße 3, 37077 Göttingen, Germany

² Friedrich-Alexander-Universität Erlangen-Nürnberg, GeoZentrum Nordbayern, PaläoUmwelt, Loewenichstraße 28, 91054 Erlangen, Germany

³ Bayerisches Landesamt für Umwelt, Geologischer Dienst, Hans-Högn-Str. 12, 95030 Hof/Saale, Germany

<http://zoobank.org/257141A1-1F3E-47AE-8D6F-8F08FDF4CBA0>

Corresponding author: Gernot Arp (garp@gwdg.de)

Academic editor: A. Nützel ♦ Received 6 July 2020 ♦ Accepted 2 February 2021 ♦ Published 17 June 2021

Abstract

Extensive construction work at the canal cutting of the Ludwigskanal near Dörlbach, Franconian Alb, provided the opportunity to re-investigate a scientific-historical and biostratigraphically important reference section of the South-German Toarcian. The 16 m thick section, described bed by bed with respect to lithology and macrofossils, starts within the Upper Pliensbachian Amaltheenton Formation, covers the Toarcian Posidonienschiefere and Jurensismergel Formation, and ends in basal parts of the Opalinuston Formation. Carbonate contents are high in the Posidonienschiefere and successively decline within the Jurensismergel to basal parts of the Opalinuston. The high carbonate contents in the Posidonienschiefere are associated with comparatively low organic carbon contents. However, organic carbon contents normalized to the silicate fraction are similarly high if compared to other regions in Germany. Only the persistence of high organic carbon levels into middle parts of the Upper Toarcian differs from those of most regions in central Europe.

Ammonite biostratigraphy indicates a thickness of >9 m for the Upper Pliensbachian, 1.15–1.20 m for the Lower Toarcian, 5.04 m for the Upper Toarcian, and >0.5 m for the Lower Aalenian. Despite the low sediment thickness, all Toarcian ammonite zones and almost all subzones are present, except for major parts of the Tenuicostatum Zone and the Fallaciosum Subzone.

On the basis of discontinuities, condensed beds, and correlations with neighbouring sections in Southern Germany, a sequence stratigraphic interpretation is proposed for the Toarcian of this region: (i) The Posidonienschiefere Formation corresponds to one 3rd order T-R sequence, from the top of the Hawskerense Subzone to a fucoid bed at the top of the Variabilis Subzone, with a maximum flooding surface at the top of the Falciferum Zone. (ii) The Jurensismergel Formation exhibits two 3rd order T-R sequences: The first ranges from the basis of the Illustris Subzone (i.e., the Intra-Variabilis-Discontinuity) to the top of the Thouarsense Zone, with a maximum flooding surface within the Thouarsense Zone. The “belemnite battlefield” reflects a transgressive “ravinement surface” within the first Jurensismergel Sequence, not a maximum regression surface at its basis. The second sequence extends from the erosive basis of the Dispansum Zone to the top of the Aalensis Subzone, with a maximum flooding surface at the Pseudoradiosa-Aalensis Zone boundary. Finally, the Opalinuston starts with a new sequence at the basis of the Torulosum Subzone. Transgressive system tracts of these 3rd order T-R sequences are commonly phosphoritic, while some regressive system tracts show pyrite preservation of ammonites. The maximum regression surfaces at the basis of the Toarcian and within the Variabilis Zone reflect a significant submarine erosion and relief formation by seawater currents, while this effect is less pronounced at the basis of the Dispansum Zone and basis of the Torulosum Subzone (i.e., the boundary Jurensismergel-Opalinuston Formation).

Kurzfassung

Umfangreiche Bauarbeiten am Kanaleinschnitt des Ludwigskanals bei Dörlbach auf der Fränkischen Alb boten die Gelegenheit ein wissenschaftlich-historisch und biostratigraphisch wichtiges Referenzprofil des süddeutschen Toarciums neu zu untersuchen. Das 16 m mächtige Profil, dessen Lithologie und Makrofossilien Schicht für Schicht beschrieben werden, beginnt innerhalb der Amaltheenton-Formation des Oberpliensbachiums, umfasst die Posidonienschiefere- und Jurensismergel-Formationen des Toarciums und endet mit basalen Teilen der Opalinuston-Formation. Die Karbonatgehalte sind im Posidonienschiefere hoch und nehmen innerhalb des Juren-

sismergels sukzessive bis in basale Teile der Opalinuston-Formation ab. Die hohen Karbonatgehalte im Posidonienschifer sind mit vergleichsweise niedrigen organischen Kohlenstoffgehalten verbunden. Die auf die Silikatfraktion normierten organischen Kohlenstoffgehalte sind jedoch im Vergleich zu anderen Regionen in Deutschland ähnlich hoch. Lediglich die anhaltend hohen organischen Kohlenstoffgehalte bis in den mittleren Teil des Oberarciums unterscheiden sich von denen der meisten Regionen Mitteleuropas.

Biostratigraphisch verwertbare Ammoniten-Funde belegen eine Mächtigkeit von >9 m für das Obere Pliensbachium, 1.15–1.20 m für das Untere Toarcium, 5.04 m für das Obere Toarcium, und >0.5 m für das Untere Aalenium. Trotz der geringen Sedimentmächtigkeiten sind alle Ammoniten-Zonen und nahezu alle Subzonen nachweisbar, mit Ausnahme großer Teile der Tenuicostatum-Zone und der Fallaciosum-Subzone.

Auf Grundlage von Diskontinuitäten, kondensierten Horizonten und Korrelationen mit Nachbarprofilen in Süddeutschland wird eine sequenzstratigraphische Interpretation für das Toarcium dieser Region entwickelt: (i) Die Posidonienschifer-Formation entspricht einer Sequenz dritter Ordnung, vom Top der Hawskerense-Subzone bis zu einem Fucoidenhorizont am Top der Variabilis-Subzone, mit einer maximalen Überflutung am Top der Falciferum-Zone. (ii) Die Jurensismergel-Formation weiß zwei Sequenzen dritter Ordnung auf: Die erste reicht von der Basis der Illustris-Subzone (d.h. der Intra-Variabilis-Diskontinuität) bis zum Top der Thouarsense-Zone. Das „Belemniteschlachtfeld“ spiegelt einen transgressiven „Auswaschungshorizont“ innerhalb der ersten Jurensismergel-Sequenz wider, keinen Meeresspiegeltiefstand an ihrer Basis. Die zweite Sequenz reicht von der erosiven Basis der Dispansum-Zone bis zum Top der Aalensis-Subzone, mit einer maximalen Überflutung an der Grenze Pseudoradiosa-Aalensis Zone. Die Opalinuston-Formation beginnt schließlich mit einer neuen Sequenz an der Basis der Torulosum-Subzone. Transgressive Phasen dieser Sequenzen dritter Ordnung sind häufig phosphoritisch ausgebildet, während regressive Phasen eine Pyriterhaltung von Ammoniten aufzeigen. Die Meeresspiegeltiefstände nahe der Basis des Toarciums und innerhalb der Variabilis-Zone sind mit einer deutlichen submarinen Erosion und Reliefbildung durch grundberührende Meeresströmungen verbunden. Dieser Effekt ist an der Basis der Dispansum-Zone und Torulosum-Subzone (d.h. der Formationsgrenze Jurensismergel-Opalinuston) weniger stark ausgeprägt.

Keywords

Ammonoidea, Jurensismergel, Lower Jurassic, Posidonienschifer, sealevel changes, Southern Germany, stratigraphy

Schlüsselwörter

Ammonoidea, Jurensismergel, Unterer Jura, Posidonienschifer, Meeresspiegel-Schwankungen, Süddeutschland, Stratigraphie

Introduction

The Franconian Alb is a classical region of Jurassic geosciences in Europe, and specifically the area of Altdorf SE of Nürnberg has been of great importance in the early times of palaeontology (von Freyberg 1958a, b, c, 1972; Schmidt-Kaler 1974; Mayr 1995; Kursawe 1995, 1996; Mäuser 2001). Indeed, the construction of the Ludwigskanal cutting at Dörlbach south of Altdorf (Fig. 1) lead 1840–1841 to the first large-scale temporary exposure of the Schwarzsula-Group in Southern Germany and corresponding fossil discoveries such as one of the worldwide first finding of a large, 1.6 m long, *Temnodontosaurus* skull (von Freyberg 1972). Furthermore, the Ludwigskanal outcrop delivered many invertebrate type fossils, among them a number of ammonoids, described in the monographs of Quenstedt (1845–1849, 1851–1852, 1856–1858, 1865–1866, 1872–1875, 1876, 1881–1884, 1882–1885a, b).

However, the only contemporary description of the exposed strata was given by Beyschlag (1841), and it took over eight decades until more details on the section were provided by Reuter (1927), Kolb (1964) and Urlich (1971),

all of them focussing on the Posidonienschifer Formation. Despite these previous descriptions, and despite that the sediment succession of the Schwarzsula Group in this region is generally well known (Reuter 1927; Meyer and Schmidt-Kaler 1996; Bloos et al. 2005), a number of crucial stratigraphic details are subject to controversial views and remained unclear to date. Above all, this applies to the extent and position of discontinuities and condensed beds. Consequently, no sequence stratigraphic interpretation of the Toarcian has been suggested for this region, except for the Posidonienschifer (Röhl and Schmid-Röhl 2005).

Slope failure at the Ludwigskanal cutting near Dörlbach and following extensive construction activities re-exposed the section in 2010–2012, allowing a re-investigation of the complete succession from the middle part of the Amaltheenton, through the Posidonienschifer and Jurensismergel, to the basis of the Opalinuston Formation (Fig. 2A, B). An overview and preliminary description of the new exposure was already given in Arp et al. (2014). Gastropods of the Amaltheenton were described by Gründel and Nützel (2015).

The aim of the present study is to provide a detailed description of the lithologic succession and its macrofossils.

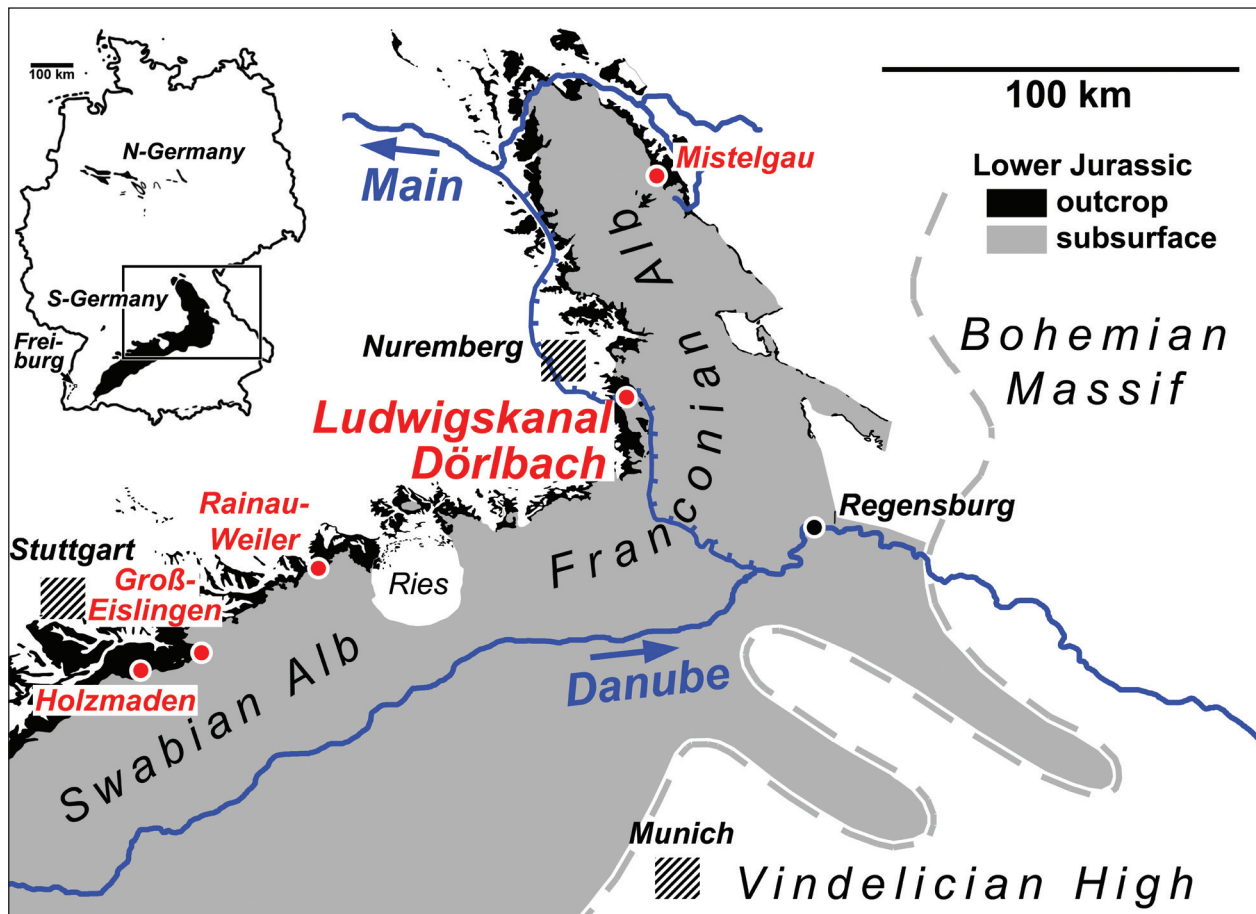


Figure 1. Geographic and geological overview with the location of the Ludwigskanal section ($49^{\circ}21.238938\text{N}$, $11^{\circ}21.534298\text{E}$) at the western margin of the Franconian Alb (S-Germany, Bavaria). Outcrop and subsurface deposits of Lower Jurassic after Freudenberger and Schwerd (1996).

The high-resolution biostratigraphy and sequence stratigraphy may form a basis for further investigations on seawater temperatures ($\delta^{18}\text{O}$ of low-Mg calcite skeletons), seawater currents, sealevel changes, and causes for the persistence of the Toarcian Oceanic Anoxic Event (T-OAE; Jenkyns 1988) in the eastern part of the NW European Epicontinental Seaway. The present study focusses on the description and stratigraphic interpretation of this section.

Location and geological overview

The Ludwigskanal cutting is located in Southern Germany, Bavaria, approximately 20 km ESE of Nürnberg (Fig. 1) in the western foreland of the middle Franconian Alb. The village Dörlbach lies 1 km W of the cutting, while Altdorf/Mfr. is located 3 km N of it. The coordinates of the section, located on the topographic map 1:25000, sheet 6634 Altdorf b. Nürnberg, are $49^{\circ}21.238938\text{N}$, $11^{\circ}21.534298\text{E}$. The region is part of the South German Scarplands (Petersen and Schröder 2010 and references therein), and the escarpment of the Franconian Alb, i.e., the edge of the Upper Jurassic limestone plateau, is located approximately 5 km E of the investigated section (Schmidt-Kaler 1974).

Geologically, the deep subsurface of the region is formed by high-grade metamorphics and plutonites of the Variscan basement (Moldanubian gneiss and granite). These basement rocks are overlain by a Mesozoic cover sequence starting with Triassic fluvial coarse siliciclastics of the Buntsandstein (63 m), Muschelkalk (45 m) and Keuper Group (270 m) (drilling Eschertshofen: Salger and Schmid 1982). After a stratigraphic gap comprising the Rhaetian, the Lower Jurassic Schwarzsula Group (47–69 m) starts with fluvial arkoses of the Bayreuth Formation, followed by marine near-shore sandstones of the Gryphaeensandstein Formation, condensed dolomitic limestones of the Numismalismergel Formation, monotonous claystones of the Amaltheenton Formation, condensed bituminous limestones and shales of the Posidonienschlieren Formation, and finally fossiliferous marls of the Jurensismergel Formation (Schmidt-Kaler 1974; Salger and Schmid 1982; Fig. 3). The Middle Jurassic Braunjura Group (125 m) is composed of marine, monotonous claystones (Opalinuston Formation), iron-ore-bearing sandstones (Eisensandstein Formation) and a condensed, highly fossiliferous succession of iron-oolites and glauconitic siltstones (Sengenthal Formation). Up to 70 m of the Upper Jurassic Weißjura Group are preserved

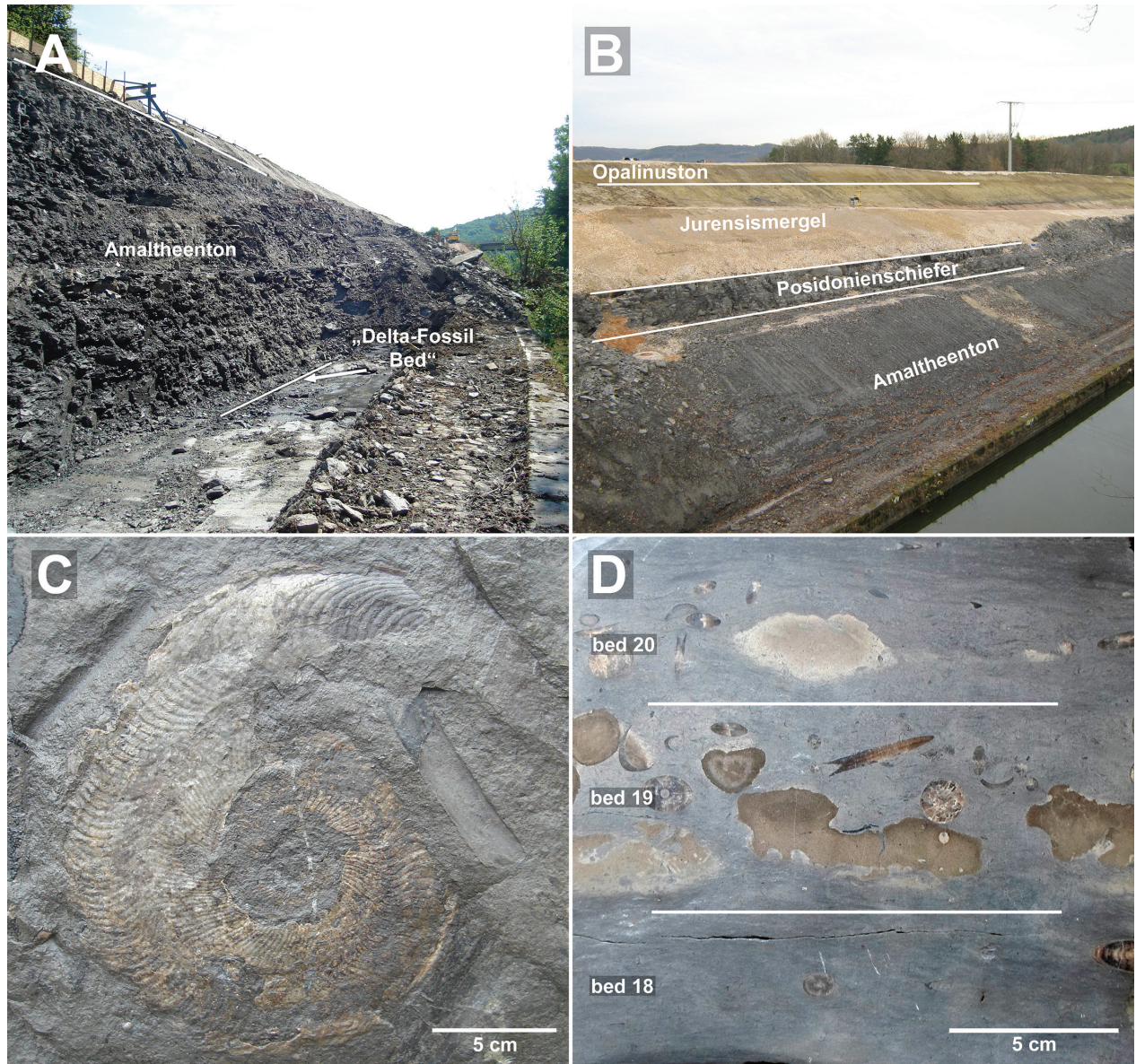


Figure 2. Field images of the Ludwigskanal section and ammonites. **A.** Western section of the canal cutting, showing basal parts of the exposure, from the “Delta-Fossil Bed” to the basis of the Posidonienschifer Formation. **B.** Eastern section of the canal cutting, showing the Amaltheenton, Posidonienschifer, Jurensismergel, and basal parts of the Opalinuston Formation. **C.** *Harpoceras falciferum* (Sowerby), “Falciferum Shale”, bed 10, field image (specimen not recovered). **D.** Polished section of rock sample, from “Fucoid Bed” (bed 17), basal marl of Jurensismergel (bed 18) and “Belemnite Battlefield” (bed 19) to the “Main Phosphorite Bed” (bed 20).

in the Altdorf region, with bedded marine limestones and sponge-microbialite mounds, some of them dolomitized (Schmidt-Kaler 1974). Subaerial exposure, erosion and karstification during Cretaceous and Tertiary times led to the present-day landscape (Wagner 1960; Hofbauer 2001; Peterk and Schröder 2010).

Material and methods

Fieldwork and sampling was carried out on 16 days between September 2010 and August 2014. Lithological descriptions are based on field observation and binocular observations on hand specimens, supplemented by 21

thin sections between 5×7.5 cm and 7.5×10 cm in size, and about 80 µm thick.

Total carbon (C_{tot}), nitrogen (N_{tot}), and sulfur (S_{tot}) of bulk rock samples were analysed with a Euro EA 3000 Elemental Analyser (HEKATEch, Wegberg, Germany) applying 2,5-bis(5-tertbenzoxazol-2-yl)thiophene (BBOT) and atropine sulfate monohydrate (IVA Analysetechnik, Meerbusch, Germany) as reference material. Organic and carbonate carbon ($C_{\text{org}}, C_{\text{carb}}$) contents were determined by a LECO RC612 (Leco, St. Joseph, MI, USA) multi-phase carbon and water analyser. For calibration, Leco synthetic carbon (1 and 4.98 carbon %) and Leco calcium carbonate (12 carbon %) standards were used. All analyses were performed as duplicates. Analytical accuracy of all analyses was bet-

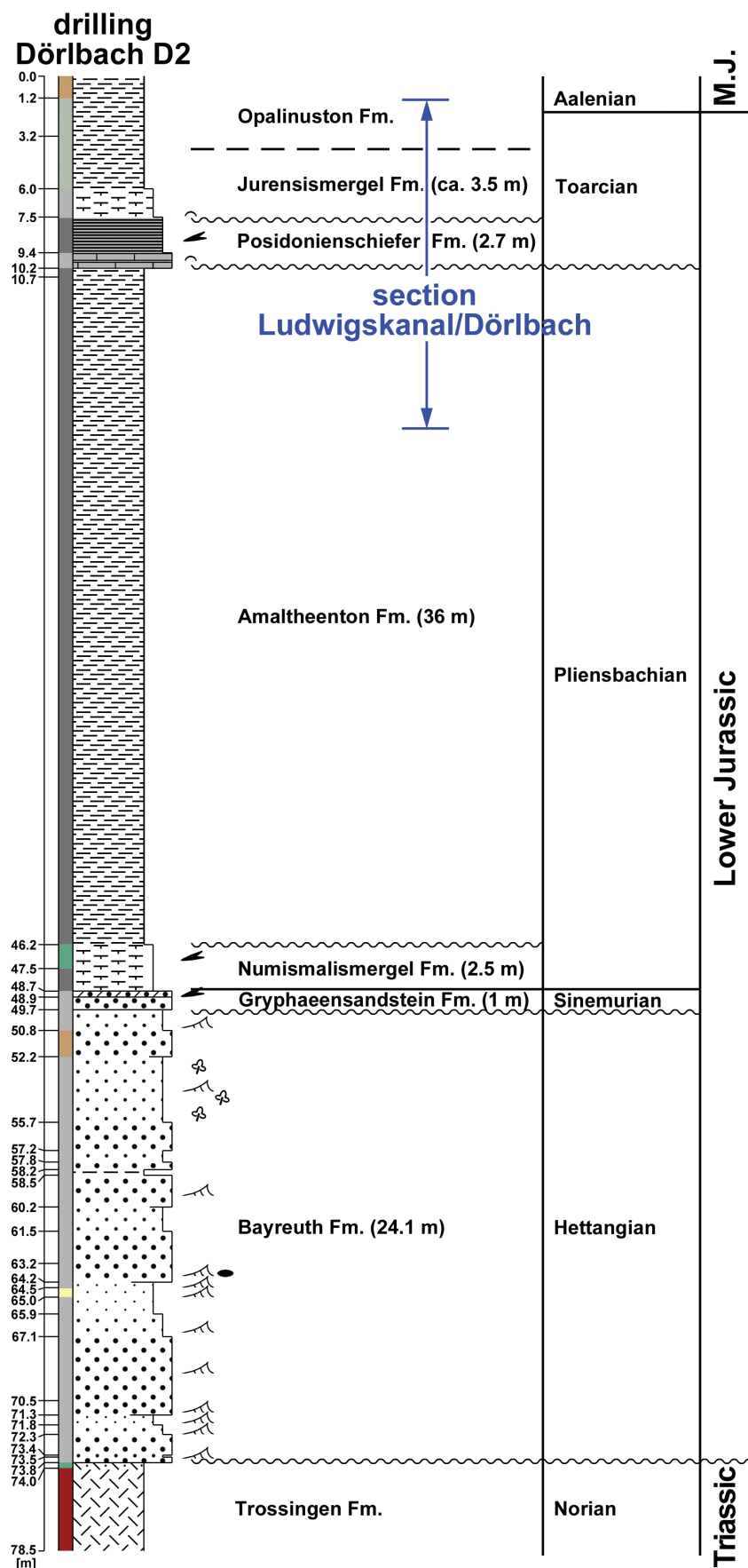


Figure 3. Overview of the Lower Jurassic Schwarzscura Group, Drilling Dörlbach D2 (top ground surface 436 m a.s.l., 49°21.679543N, 11°21.797843E; topographic map sheet 6634 Altdorf b. Nürnberg; unpublished drilling report), ca. 750 m N of the Ludwigskanal/Dörlbach section. For legend see Fig. 7.

ter than 3%. The carbonate-free fraction was calculated from the total weight minus the CaCO_3 and C_{org} content.

Biostratigraphy is based on approximately 425 determinable ammonites that were recovered *in situ*. Few additional ammonites recovered by private fossil collectors were taken into account. Ammonite determinations follow the systematic descriptions in Howarth (1958, 1978, 1992), Gabilly (1976a, b), Schulbert (2001a), Rulleau (2007), Hoffmann (2010, 2015), Arp (2010), and Di Cencio and Weis (2020).

Repository: The material is stored in the Museum and Collection of the Geoscience Centre, University of Göttingen, under the numbers GZG.INV.45641–GZG.INV.45644 and GZG.INV.70496–GZG.INV.70650.

Data Availability Statement: All data used in this publication are stored on the Göttingen Research Online Data repository (<https://doi.org/10.25625/8PLFNS>).

Figure captions: unless otherwise noted, all specimen are coated by ammonium chloride prior to photography. **Abbreviations:** diameter (d), diameter of penultimate half whorl (di), umbilical width (u), whorl height (wh), whorl breadth (wb), primary ribs per half whorl (rb/2).

Results

Description of the section

Informal bed names are given in quotation marks. From bottom to top:

Amaltheenton Formation:

Bed 1: >100 cm	bluish-grey, well bedded claystone;
Bed 2: 0–15 cm	“Septaria Bed”: grey marlstone concretions with mm-thick, calcite-cemented shrinkage cracks;
Bed 3: 25 cm	bluish-grey, well bedded claystone with scattered cm-sized septarian concretions; ammonoids: at the top one juvenile <i>Pleuroceras solare</i> (Phillips);
Bed 4: 10 cm	“Delta-Fossil Bed”: bluish-grey, fissile, calcareous claystone to argillaceous marl with abundant ammonoids, belemnites, echinoderm remains and bivalves; lower part of the bed with reworked bluish-grey marlstone concretions with borings and serpulid tubes; ammonoids: <i>Pleuroceras spinatum</i> (Bruguière); <i>Amaltheus</i> sp. (juvenile), <i>Pleuroceras solare</i> (Phillips) (within reworked concretions; Fig. 10: 1), <i>Pleuroceras solare</i> var. <i>solitarium</i> (Simpson) (within reworked concretions; Fig. 10: 2), <i>Amauroceras ferrugineum</i> (Simpson) (within reworked concretions; Fig. 10: 2); other fossils: <i>Passaloteuthis</i> sp., <i>Pseudopecten equivalvis</i>

Bed 5: 800 cm

Bed 6: 0–1 cm

Posidonienschiefer Formation:

Bed 7: 5–15 cm

Bed 8: 15 cm

(Sowerby), *Eopecten velatus* (Goldfuss), *Pseudomytiloides* sp., *Nicanella pumila* (Sowerby), *Harpax spinosus* (Sowerby), *Mactromya* sp., *Ryderia doris* (d'Orbigny), *Pseudolimea* sp., *Palaeoneilo elliptica* (Goldfuss), *Oxytoma inaequivalvis* (Sowerby), *Terquemia arietis* (Quenstedt), *Palmoxytoma cygnipes* (Young & Bird), *Pleurotomaria amathei* Quenstedt, *Laeviconulus subimbricatus* (Koch & Dunker), *Leviplura blainvilliei* (von Münster), rhynchonellid brachiopods, *Amaltheocrinus* sp., echinid spines, drift wood; bluish-grey, slightly miceous, fissile claystone with scattered small bivalves; 15 and 75 cm below top layers of flat-lenticular, grey siderite nodules; ammonoids: *Pleuroceras spinatum* (Bruguière) (0.8 m, 1.5 m, 2.0 m, 3.0 m, 5.5 m, 7.25 m and 7.5 m below top: Fig. 10: 3, 4); other fossils: *Palaeoneilo* sp.; reworked flat concretions composed of bluish-grey pyrite-rich argillaceous limestone, with corroded surfaces;

“Laibstein I”: dark grey, laminated calcareous marl with coarse shell debris and one 15-cm-sized limestone concretion composed of laminated bituminous pellet packstone, with intercalated layers of coarse shell debris and fish scales; basis with reworked flat concretions from the Amaltheenton; ammonoids: *Tiltoniceras antiquum* (Wright) (1–2 cm above basis; and one juvenile specimen in middle part; Fig. 10: 5, 6); middle and upper part with *Cleviceras exaratum* (Young & Bird) (Fig. 10: 10), *Hildaites murleyi* (Moxon) (Fig. 10: 8, 9), and *Lytoceras ceratophagum* (Quenstedt) (Fig. 10: 7); other fossils: *Pseudomytiloides dubius* (Sowerby), *Nicanella* sp., scattered *Coelodiscus minutus* (Schübeler in Zieten); “Laibstein II”: dark grey, laminated bituminous limestone concretions (pellet packstone) up to 50 cm width, with abundant mm-sized holoplanktonic gastropods; ammonoids: *Cleviceras elegans* (Sowerby) (Fig. 11: 6), rare *Cleviceras* cf. *exaratum* (Young & Bird), *Phylloceras heterophyllum* (Sowerby) (Fig. 11: 5), *Harpoceras serpentinum*

	(Schlotheim) (Fig. 11: 1), “ <i>Peronoceras</i> ” <i>desplacei</i> (d’Orbigny) (Fig. 11: 4), <i>Nodicoeloceras crassoides</i> (Simpson), <i>Dactylioceras semiannulatum</i> Howarth (Fig. 11: 7), <i>Dactylioceras anguum</i> (Reinecke) (Fig. 11: 3); other fossils: <i>Meleagrinella cf. substriata</i> (von Münster), <i>Pseudomytiloides dubius</i> (Sowerby), <i>Goniomya rhombifera</i> (Goldfuss), <i>Camptonectes subulatus</i> (von Münster in Goldfuss), <i>Pleuromya</i> sp., abundant <i>Coelodiscus minutus</i> (Schübeler in Zieten);	2)), <i>Pseudolioceras</i> sp. (juvenile); other fossils: <i>Meleagrinella substriata</i> (von Münster), belemnites; grey, bituminous argillaceous limestone consisting of densely packed <i>Meleagrinella</i> shells and scattered phosphatic vertebrate microfragments; fossils: <i>Meleagrinella substriata</i> (von Münster);
Bed 9: 5–6 cm	“Fish Scale Bed”: dark grey, bituminous argillaceous fissile limestone composed of mollusc shell fragments and fish scales, with abundant belemnites; ammonoids: <i>Dactylioceras</i> sp. (upper bedding plane), <i>Cleviceras cf. elegans</i> (lower bedding plane); other fossils: <i>Meleagrinella cf. substriata</i> (von Münster), <i>Pseudomytiloides dubius</i> (Sowerby), belemnites, ichthyosaur vertebra;	grey, bituminous limestone (lumachelle) consisting of densely packed <i>Meleagrinella</i> shells, faecal pellets, and scarce phosphatic vertebrate microfragments; ammonoids: <i>Dactylioceras cf. athleticum</i> (Simpson); other fossils: <i>Meleagrinella substriata</i> (von Münster), <i>Pseudomytiloides dubius</i> (Sowerby);
Bed 10: 10 cm	“Falciferum Shale”: dark grey, laminated, bituminous marl; lower part with one dark grey, 8 × 12-cm-sized, poorly laminated bituminous limestone concretion (pellet packstone) with mollusk shell debris, few phosphatic vertebrate microfragments and abundant small <i>Dactylioceras</i> shells (spar filled); ammonoids: <i>Harpoceras falciferum</i> (Sowerby) (middle part; Fig. 2C), <i>Phylloceras heterophyllum</i> (Sowerby); other fossils: <i>Pseudomytiloides dubius</i> (Sowerby) abundant on bedding planes, drift wood; grey, bituminous argillaceous fissile limestone with abundant fish scale and shell debris; fossils: few large (2-cm-sized) <i>Meleagrinella cf. substriata</i> (von Münster);	“Bifrons Shale”: dark-grey, bituminous marl, laminated; with scattered shell debris in layers, scattered phosphatic scale and bone microfragments, abundant belemnites 26 cm and 38 cm below top; ammonoids: <i>Hildoceras semipolitum</i> Buckman (2 cm, 17 cm, 18 cm, and 22 cm below top; Fig. 12: 4, 5), <i>Pseudolioceras cf. lythense</i> (Young & Bird) (20 cm below top), <i>Phylloceras heterophyllum</i> (Sowerby) (28 cm below top); other fossils: <i>Pseudomytiloides dubius</i> (Sowerby), <i>Bositra buchi</i> var. <i>elongata</i> (Goldfuss), rare <i>Orbiculoides papyracea</i> (von Münster), <i>Lenticulina</i> sp., rare echinoderm fragments, belemnites;
Bed 11: 3–4 cm	“Variabilis Shale”: dark-grey, laminated to well bedded, bituminous marl (lower 60 cm) to calcareous marl (top 10 cm) with scattered shell debris, rare phosphatic fish scale and bone microfragments; ammonoids compressed or as pyrite casts preserved, scattered pyrite nodules up to 3 cm in size; light-grey <i>Chondrites</i> horizons 5–6 cm and 18–19 cm below top; ammonoids: <i>Denckmannia cf. rude</i> (Simpson) (1 cm below top), <i>Haugia jugosa</i> (Sowerby) (3 cm below top; Fig. 12: 9), <i>Haugia</i> sp. (7 cm and 70 cm below top), <i>Haugia variabilis</i> (d’Orbigny) (13 cm below top; Fig. 12: 8), <i>Pseudolioceras compactile</i> (Simpson) (13 cm, 19 cm, 21 cm, 24 cm, 25 cm, 37 cm, and 65 cm below top; Fig. 12: 10, 11), <i>Pseudolioceras</i> sp. (23 cm and 25 cm below top), <i>Catacoeloceras raquinianum</i> (d’Orbigny) (3 cm, 7 cm, 13 cm, 15 cm, 19 cm, 22 cm, 37 cm, 38 cm, and 53 cm below top; Fig.	“Variabilis Shale”: dark-grey, laminated to well bedded, bituminous marl (lower 60 cm) to calcareous marl (top 10 cm) with scattered shell debris, rare phosphatic fish scale and bone microfragments; ammonoids compressed or as pyrite casts preserved, scattered pyrite nodules up to 3 cm in size; light-grey <i>Chondrites</i> horizons 5–6 cm and 18–19 cm below top; ammonoids: <i>Denckmannia cf. rude</i> (Simpson) (1 cm below top), <i>Haugia jugosa</i> (Sowerby) (3 cm below top; Fig. 12: 9), <i>Haugia</i> sp. (7 cm and 70 cm below top), <i>Haugia variabilis</i> (d’Orbigny) (13 cm below top; Fig. 12: 8), <i>Pseudolioceras compactile</i> (Simpson) (13 cm, 19 cm, 21 cm, 24 cm, 25 cm, 37 cm, and 65 cm below top; Fig. 12: 10, 11), <i>Pseudolioceras</i> sp. (23 cm and 25 cm below top), <i>Catacoeloceras raquinianum</i> (d’Orbigny) (3 cm, 7 cm, 13 cm, 15 cm, 19 cm, 22 cm, 37 cm, 38 cm, and 53 cm below top; Fig.
Bed 12: 25 cm	“Dactylioceras Bed”: grey, bituminous limestone consisting of densely packed <i>Meleagrinella</i> shells and shell fragments, faecal pellets, and scarce phosphatic vertebrate microfragments; abundant sparite and micrite filled casts of <i>Dactylioceras</i> ; relictic cross-stratification in the lower part of the bed; ammonoids: <i>Dactylioceras athleticum</i> (Simpson) (abundant throughout the bed; Fig. 12: 3), <i>Dactylioceras cf. commune</i> (Sowerby) (lower bedding plane; Fig. 12: 1), <i>Hildoceras cf. lusitanicum</i> Meister (lower bedding plane; Fig. 12:	“Dactylioceras Bed”: grey, bituminous limestone consisting of densely packed <i>Meleagrinella</i> shells and shell fragments, faecal pellets, and scarce phosphatic vertebrate microfragments; abundant sparite and micrite filled casts of <i>Dactylioceras</i> ; relictic cross-stratification in the lower part of the bed; ammonoids: <i>Dactylioceras athleticum</i> (Simpson) (abundant throughout the bed; Fig. 12: 3), <i>Dactylioceras cf. commune</i> (Sowerby) (lower bedding plane; Fig. 12: 1), <i>Hildoceras cf. lusitanicum</i> Meister (lower bedding plane; Fig. 12:
Bed 13: 1–2 cm		
Bed 14: 10–12 cm		
Bed 15: 40 cm		
Bed 16: 70 cm		

	13: 2, 3), <i>Catacoeloceras</i> sp. (68 cm below top), <i>Mucrodactylites mucronatus</i> (d'Orbigny) (43 cm below top; Fig. 12: 7, 8), <i>Lytoceras</i> sp. (5 cm below top), <i>Lytoceras cf. cornucopia</i> (Young & Bird) (13 cm below top), <i>Lytoceras sublineatum</i> (Oppel) (26 cm and 38 cm below top; Fig. 13: 1), <i>Hildoceras cf. semipolitum</i> Buckman (70 cm below top); other fossils: <i>Salpingoteuthis</i> sp. (15 cm below top), further belemnites, <i>Bositra buchi</i> var. <i>elongata</i> (Goldfuss), <i>Pseudomytiloides dubius</i> (Sowerby), <i>Propeamussium pumilum</i> (Lamarck), <i>Grammatodon</i> sp., <i>Lenticulina</i> sp. (rare);	phosphorite nodules up to 1 × 3 × 6 cm and abundant belemnites; <i>Chondrites</i> burrows; ammonoids: <i>Lytoceras cornucopia</i> (Young & Bird) (Fig. 13: 8), <i>Pseudogrammoceras</i> sp., <i>Denckmannia rude</i> (Simpson) (Fig. 13: 9), <i>Osperleioceras bicarinatum</i> (Zieten) (Fig. 13: 7); other fossils: <i>Dactylosteuthis irregularis</i> (Schlotheim), <i>Chlamys textoria</i> (Schlotheim), <i>Campstonectes cf. subulatus</i> (Münster);
Bed 17: 2 cm	"Fucoid Bed": grey to white-grey, bioturbated marl, slightly phosphoritic, with <i>Chondrites</i> burrows; with compressed and deformed phosphoritic casts of ammonoids; ammonoids: abundant <i>Catacoeloceras raquinianum</i> (d'Orbigny), <i>Haugia variabilis</i> (d'Orbigny), <i>Phylloceras heterophyllum</i> (Sowerby), <i>Lytoceras cf. cornucopia</i> (Young & Bird); other fossils: <i>Pseudomytiloides dubius</i> (Sowerby), <i>Campstonectes subulatus</i> (Münster);	"Toarcensis Shale": dark grey, well bedded, bituminous marl transected by numerous small branching burrows (<i>Chondrites</i>); abundant compressed ammonoids (solely <i>Grammoceras</i>) and bivalves (solely <i>Pseudomytiloides</i>); ammonoids: <i>Grammoceras thouarsense</i> (d'Orbigny) (Fig. 14: 1) throughout the bed; other fossils: <i>Pseudomytiloides dubius</i> (Sowerby), few belemnites;
		"Belemnite accumulation": grey, poorly stratified argillaceous marl full of belemnites (<i>Dactylosteuthis</i>); nubeculariid foraminifera on shell fragments and belemnites; one compressed <i>Lytoceras</i> shell fragment with stromatolithic crust at the top inside of the body chamber; one phosphorite nodule with microbialite-like corroded upper surface; locally small lenticular phosphorite nodules; basis with flat corroded phosphorites (11 × 7 × 1 cm in size) and double-sided-corroded belemnite rostra; ammonoids: <i>Alocolytoceras cf. rugiferum</i> (Pompeckj); other fossils: <i>Liostrea erina</i> (d'Orbigny) attached to belemnite rostra, <i>Chladocrinus</i> sp.;
Bed 18: 5 cm	grey, well bedded calcareous marl; ammonoids: <i>Pseudogrammoceras subregale</i> (Pinna) (Fig. 13: 4), <i>Haugia cf. phillipsi</i> (Simpson) (Fig. 13: 5); abundant <i>Catacoeloceras raquinianum</i> (d'Orbigny); <i>Haugia cf. variabilis</i> (d'Orbigny) at basis of the bed; other fossils: <i>Bositra buchi</i> var. <i>elongata</i> (Goldfuss);	"Levesquei-Dispansum-Marl": grey, poorly bedded marl rich in nubeculariid foraminifera, shell debris, and with small phosphorite nodules; abundant mid-sized and large compressed ammonites (top 12 cm and at 20–25 cm below top); deformed phosphorite casts of smaller ammonoids, rare pyrite casts;
Bed 19: 6 cm	"Belemnite Battlefield": grey, bituminous calcareous marl with abundant bivalve shell debris (<i>Propeamussium</i>), belemnite accumulation, and reworked phosphorite nodules; at the basis reworked plate-like, bored white-grey phosphorites nodules up to 2.5 × 5 × 10 cm in size; thin burrows; ammonoids: <i>Lytoceras cf. cornucopia</i> (Young & Bird), <i>Pseudogrammoceras</i> sp., lower bedding plane with <i>Catacoeloceras raquinianum</i> (d'Orbigny) (Fig. 13: 6); other fossils: <i>Dactylosteuthis irregularis</i> (Schlotheim);	ammonoids: <i>Phlyseogrammoceras dispansum</i> (Lycett) (12–20 cm and 20–25 cm below top; Fig. 14: 5, 8), <i>Pseudolioceras cf. boulbiense</i> (Young & Bird) (12–20 cm below top; Fig. 14: 3), <i>Alocolytoceras rugiferum</i> (Pompeckj) (12–20 cm, 20–25 cm, and 29 cm below top; Fig. 14: 2, 4), <i>Hammatoceras insigne</i> (Schübeler in Zieten) (15 cm below top; Fig. 15: 10,
Bed 20: 6–7 cm	"Main Phosphorite Bed": grey, marl to calcareous marl, poorly bedded, with abundant bivalve shell debris (<i>Propeamussium</i>) with white-grey	
Bed 21: 14–15 cm		
Bed 22: 5 cm		
Bed 23: 30 cm		

Jurensismergel Formation:

Bed 18: 5 cm	grey, well bedded calcareous marl; ammonoids: <i>Pseudogrammoceras subregale</i> (Pinna) (Fig. 13: 4), <i>Haugia cf. phillipsi</i> (Simpson) (Fig. 13: 5); abundant <i>Catacoeloceras raquinianum</i> (d'Orbigny); <i>Haugia cf. variabilis</i> (d'Orbigny) at basis of the bed; other fossils: <i>Bositra buchi</i> var. <i>elongata</i> (Goldfuss);	"Levesquei-Dispansum-Marl": grey, poorly bedded marl rich in nubeculariid foraminifera, shell debris, and with small phosphorite nodules; abundant mid-sized and large compressed ammonites (top 12 cm and at 20–25 cm below top); deformed phosphorite casts of smaller ammonoids, rare pyrite casts;
Bed 19: 6 cm	"Belemnite Battlefield": grey, bituminous calcareous marl with abundant bivalve shell debris (<i>Propeamussium</i>), belemnite accumulation, and reworked phosphorite nodules; at the basis reworked plate-like, bored white-grey phosphorites nodules up to 2.5 × 5 × 10 cm in size; thin burrows; ammonoids: <i>Lytoceras cf. cornucopia</i> (Young & Bird), <i>Pseudogrammoceras</i> sp., lower bedding plane with <i>Catacoeloceras raquinianum</i> (d'Orbigny) (Fig. 13: 6); other fossils: <i>Dactylosteuthis irregularis</i> (Schlotheim);	ammonoids: <i>Phlyseogrammoceras dispansum</i> (Lycett) (12–20 cm and 20–25 cm below top; Fig. 14: 5, 8), <i>Pseudolioceras cf. boulbiense</i> (Young & Bird) (12–20 cm below top; Fig. 14: 3), <i>Alocolytoceras rugiferum</i> (Pompeckj) (12–20 cm, 20–25 cm, and 29 cm below top; Fig. 14: 2, 4), <i>Hammatoceras insigne</i> (Schübeler in Zieten) (15 cm below top; Fig. 15: 10,
Bed 20: 6–7 cm	"Main Phosphorite Bed": grey, marl to calcareous marl, poorly bedded, with abundant bivalve shell debris (<i>Propeamussium</i>) with white-grey	

Bed 24: 95 cm	12), <i>Hammatoceras</i> sp. (20–25 cm below top), <i>Dumortieria insignisimilis</i> (Brauns) (11 cm below top; Fig. 14: 6, 7), <i>Dumortieria levesquei</i> (d'Orbigny) (6 cm and 9 cm below top; Fig. 14: 11, 13), <i>Dumortieria radians</i> (Reinecke) (6 cm below top), <i>Dumortieria pseudoradiosa</i> (Branco) (4 cm below top; Fig. 14: 14), <i>Dumortieria radiosa</i> (Seebach) (4 cm below top), <i>Dumortieria striatulocostata</i> (Quenstedt) (4 cm below top), <i>Dumortieria</i> sp. (pyrite cast at 8 cm below top); other fossils: <i>Chlamys textoria</i> (Schlotheim), <i>Camptonectes subulatus</i> (Münster in Goldfuss), <i>Entolium</i> sp., <i>Eopecten velatus</i> (Goldfuss), <i>Plagiostoma giganteum</i> Sowerby, <i>Pseudolimea</i> sp., <i>Pseudomytiloides</i> sp., <i>Nicanella voltzi</i> (Hoeninghaus in Roemer), <i>Liostrea erina</i> (d'Orbigny), belemnites; grey, well bedded argillaceous marl to marl with abundant shell microdebris; lower 60 cm rich in nubeculariid foraminifera; lower 45 cm with small marcasite nodules; 40–45 cm below top accumulation of phosphorite nodules and ammonites, 70 cm below top accumulation of compressed ammonites; ammonoids: <i>Paradumortieria</i> cf. <i>tectiforme</i> Elmi & Caloo-Fortier (20 cm, 25 cm, 40–45 cm, and 50 cm below top; Fig. 15: 5), <i>Dumortieria</i> cf. <i>kochi</i> Benecke (40 cm below top; Fig. 15: 11), <i>Dumortieria moorei</i> (Lycett) (7 cm, 40 cm, and 54 cm below top; Fig. 15: 10), <i>Dumortieria</i> cf. <i>moorei</i> (Lycett) (5 cm and 40 cm below top), <i>Dumortieria pseudoradiosa</i> (Branco) (40–45 cm and 70 cm below top), <i>Dumortieria</i> cf. <i>pseudoradiosa</i> (Branco) (65 cm and 94 cm below top), <i>Dumortieria radiosa</i> (Seebach) (40–45 cm, 73 cm, and 75 cm below top; Fig. 14: 9), <i>Dumortieria</i> cf. <i>radiosa</i> (Seebach) (40–45 cm, 70 cm, and 75 cm below top); other fossils: <i>Chlamys textoria</i> (Schlotheim), <i>Pseudomytiloides</i> sp., belemnites; grey, poorly bedded, argillaceous marl with shell microdebris and abundant ammonites (pyrite casts and marcasite-veneered imprints), abundant belemnites, and small phosphorite nodules; ammonoids: <i>Cotteswoldia mactra</i> (Dumortier) (Fig. 15: 3), <i>Dumortieria</i> cf. <i>moorei</i> (Lycett), <i>Dumortieria costula</i> (Reinecke), <i>Paradumortieria</i> cf. <i>tectiforme</i> Elmi & Caloo-Fortier, <i>Dumortieria</i>	cf. <i>externicostata</i> (Branco), <i>Pleydellia</i> cf. <i>subcompta</i> (Branco) (transitional form to <i>C. mactra</i>), <i>Pleurolytoceras wrighti</i> (Buckman); other fossils: rhynchonellid brachiopode, belemnites; grey, well bedded, argillaceous marl rich in shell microdebris of <i>Bositra suessi</i> , with scattered small branching burrows (<i>Chondrites</i>), scarce nubeculariid foraminifera, small pyrite nodules and pyrite ammonite casts; <i>Bositra suessi</i> pavement 32 cm below top; <i>Pleydellia subcompta</i> (Branco) (35 cm below top; Fig. 15: 12), <i>Cotteswoldia aalensis</i> (Zieten) (5 cm, 22 cm, 25 cm, 30 cm, and 35 cm below top), <i>Cotteswoldia distans</i> (Buckman) (35 cm below top), <i>Cotteswoldia mactra</i> (Dumortier) (40 cm below top), <i>Dumortieria</i> cf. <i>moorei</i> (Lycett) (40 cm below top), <i>Dumortieria costula</i> (Reinecke) (30 cm below top; Fig. 15: 8), <i>Dumortieria externicostata</i> (Branco) (30 cm below top; Fig. 15: 7), <i>Pleurolytoceras wrighti</i> (Buckman) (25 cm below top), <i>Pleurolytoceras hircinum</i> (Schlotheim) (35 cm below top), other fossils: <i>Bositra suessi</i> (Oppel), belemnites;
Bed 25: 2 cm	grey, well bedded, calcareous claystone with scattered small branching burrows (<i>Chondrites</i>), minor shell microdebris, very few nubeculariid foraminifera, and very few echinoderm bioclasts; abundant small pyrite casts of ammonites, especially near the basis of the bed; ammonoids: <i>Pleydellia subcompta</i> (Branco), <i>Pleydellia distans</i> (Buckman) (Fig. 15: 9), <i>Cotteswoldia aalensis</i> (Zieten) (Fig. 15: 6), <i>Pseudolioceras beyrichi</i> (Schloenbach), <i>Pleurolytoceras hircinum</i> (Schlotheim) (Fig. 15: 2), <i>Pleurolytoceras wrighti</i> (Buckman) (Fig. 15: 1), other fossils: belemnites; grey, well bedded, calcareous claystone rich in shell microdebris of <i>Bositra suessi</i> and nubeculariid foraminifera; with scattered small pyrite nodules and pyrite ammonite casts; at the top accumulation of small pyritic ammonites (embedded in various orientation); <i>Bositra suessi</i> pavement 50 cm below top; ammonoids: <i>Pleydellia subcompta</i> (Branco) (1 cm below top), <i>Pleydellia costulata</i> (Zieten) (1 cm below top; Fig. 15: 13), <i>Cotteswoldia aalensis</i> (Zieten) (1 cm below top), <i>Pseudolioceras beyrichi</i> (Schloenbach) (Fig. 15: 2), <i>Pleurolytoceras hircinum</i> (Schlotheim) (Fig. 15: 2), <i>Pleurolytoceras wrighti</i> (Buckman) (Fig. 15: 1), other fossils: belemnites;	grey (unweathered) to yellowish-brown (weathered), well bedded, calcareous claystone with scattered small branching burrows (<i>Chondrites</i>), minor shell microdebris, very few nubeculariid foraminifera, and very few echinoderm bioclasts; abundant small pyrite casts of ammonites, especially near the basis of the bed; ammonoids: <i>Pleydellia subcompta</i> (Branco), <i>Pleydellia distans</i> (Buckman) (Fig. 15: 9), <i>Cotteswoldia aalensis</i> (Zieten) (Fig. 15: 6), <i>Pseudolioceras beyrichi</i> (Schloenbach), <i>Pleurolytoceras hircinum</i> (Schlotheim) (Fig. 15: 2), <i>Pleurolytoceras wrighti</i> (Buckman) (Fig. 15: 1), other fossils: belemnites;
Bed 26: 50 cm	grey, well bedded, argillaceous marl rich in shell microdebris of <i>Bositra suessi</i> , with scattered small branching burrows (<i>Chondrites</i>), scarce nubeculariid foraminifera, small pyrite nodules and pyrite ammonite casts; <i>Bositra suessi</i> pavement 32 cm below top; <i>Pleydellia subcompta</i> (Branco) (35 cm below top; Fig. 15: 12), <i>Cotteswoldia aalensis</i> (Zieten) (5 cm, 22 cm, 25 cm, 30 cm, and 35 cm below top), <i>Cotteswoldia distans</i> (Buckman) (35 cm below top), <i>Cotteswoldia mactra</i> (Dumortier) (40 cm below top), <i>Dumortieria</i> cf. <i>moorei</i> (Lycett) (40 cm below top), <i>Dumortieria costula</i> (Reinecke) (30 cm below top; Fig. 15: 8), <i>Dumortieria externicostata</i> (Branco) (30 cm below top; Fig. 15: 7), <i>Pleurolytoceras wrighti</i> (Buckman) (25 cm below top), <i>Pleurolytoceras hircinum</i> (Schlotheim) (35 cm below top), other fossils: <i>Bositra suessi</i> (Oppel), belemnites;	grey (unweathered) to yellowish-brown (weathered), well bedded, calcareous claystone with scattered small branching burrows (<i>Chondrites</i>), minor shell microdebris, very few nubeculariid foraminifera, and very few echinoderm bioclasts; abundant small pyrite casts of ammonites, especially near the basis of the bed; ammonoids: <i>Pleydellia subcompta</i> (Branco), <i>Pleydellia distans</i> (Buckman) (Fig. 15: 9), <i>Cotteswoldia aalensis</i> (Zieten) (Fig. 15: 6), <i>Pseudolioceras beyrichi</i> (Schloenbach), <i>Pleurolytoceras hircinum</i> (Schlotheim) (Fig. 15: 2), <i>Pleurolytoceras wrighti</i> (Buckman) (Fig. 15: 1), other fossils: belemnites;
Bed 27: 5–10 cm	grey (unweathered) to yellowish-brown (weathered), well bedded, calcareous claystone with scattered small branching burrows (<i>Chondrites</i>), minor shell microdebris, very few nubeculariid foraminifera, and very few echinoderm bioclasts; abundant small pyrite casts of ammonites, especially near the basis of the bed; ammonoids: <i>Pleydellia subcompta</i> (Branco), <i>Pleydellia distans</i> (Buckman) (Fig. 15: 9), <i>Cotteswoldia aalensis</i> (Zieten) (Fig. 15: 6), <i>Pseudolioceras beyrichi</i> (Schloenbach), <i>Pleurolytoceras hircinum</i> (Schlotheim) (Fig. 15: 2), <i>Pleurolytoceras wrighti</i> (Buckman) (Fig. 15: 1), other fossils: belemnites;	grey (unweathered) to yellowish-brown (weathered), well bedded, calcareous claystone with scattered small branching burrows (<i>Chondrites</i>), minor shell microdebris, very few nubeculariid foraminifera, and very few echinoderm bioclasts; abundant small pyrite casts of ammonites, especially near the basis of the bed; ammonoids: <i>Pleydellia subcompta</i> (Branco), <i>Pleydellia distans</i> (Buckman) (Fig. 15: 9), <i>Cotteswoldia aalensis</i> (Zieten) (Fig. 15: 6), <i>Pseudolioceras beyrichi</i> (Schloenbach), <i>Pleurolytoceras hircinum</i> (Schlotheim) (Fig. 15: 2), <i>Pleurolytoceras wrighti</i> (Buckman) (Fig. 15: 1), other fossils: belemnites;
Bed 28: 80–85 cm	grey, well bedded, calcareous claystone rich in shell microdebris of <i>Bositra suessi</i> and nubeculariid foraminifera; with scattered small pyrite nodules and pyrite ammonite casts; at the top accumulation of small pyritic ammonites (embedded in various orientation); <i>Bositra suessi</i> pavement 50 cm below top; ammonoids: <i>Pleydellia subcompta</i> (Branco) (1 cm below top), <i>Pleydellia costulata</i> (Zieten) (1 cm below top; Fig. 15: 13), <i>Cotteswoldia aalensis</i> (Zieten) (1 cm below top), <i>Pseudolioceras beyrichi</i> (Schloenbach) (Fig. 15: 2), <i>Pleurolytoceras hircinum</i> (Schlotheim) (Fig. 15: 2), <i>Pleurolytoceras wrighti</i> (Buckman) (Fig. 15: 1), other fossils: belemnites;	grey, well bedded, calcareous claystone rich in shell microdebris of <i>Bositra suessi</i> and nubeculariid foraminifera; with scattered small pyrite nodules and pyrite ammonite casts; at the top accumulation of small pyritic ammonites (embedded in various orientation); <i>Bositra suessi</i> pavement 50 cm below top; ammonoids: <i>Pleydellia subcompta</i> (Branco) (1 cm below top), <i>Pleydellia costulata</i> (Zieten) (1 cm below top; Fig. 15: 13), <i>Cotteswoldia aalensis</i> (Zieten) (1 cm below top), <i>Pseudolioceras beyrichi</i> (Schloenbach) (Fig. 15: 2), <i>Pleurolytoceras hircinum</i> (Schlotheim) (Fig. 15: 2), <i>Pleurolytoceras wrighti</i> (Buckman) (Fig. 15: 1), other fossils: belemnites;

	<i>richi</i> (Schloenbach) (1 cm below top; Fig. 15: 4), <i>Pleurolytoceras hircinum</i> (Schlotheim) (1 cm below top), <i>Pleurolytoceras wrighti</i> (Buckman) (1 cm and 25 cm below top); other fossils: <i>Toarctocera</i> sp., <i>Bositra suessi</i> (Oppel), <i>Palaeonucula</i> sp., <i>Chladocrinus</i> sp., belemnites;
Bed 29: 10–12 cm	grey, poorly bedded, calcareous marlstone with abundant nubeculariid foraminifera;
Bed 30: 30 cm	grey, well bedded, marl to calcareous claystone rich in shell microdebris of <i>Bositra suessi</i> (Oppel) and nubeculariid foraminifera;

Opalinuston Formation:

Bed 31: 2 cm	grey (unweathered) to brownish-grey (weathered), poorly bedded calcareous claystone with abundant, partially aligned belemnites of the <i>Hastites</i> group;
Bed 32: 80 cm	grey, well bedded, calcareous claystone rich in shell microdebris of <i>Bositra suessi</i> (Oppel); at 50 cm below top rich in nubeculariid foraminifera;
Bed 33: 2–3 cm	grey (unweathered) to brownish-grey (weathered), poorly bedded calcareous claystone with few small phosphorite nodules, abundant belemnites and compressed ammonoids; one shell fragment of <i>Lytoceras</i> with a stromatolitic crust at the top inside of the body chamber; ammonoids: <i>Cotteswoldia lotharingica</i> (Branco) (Fig. 15: 15), <i>Pleydellia buckmani</i> Maubeuge (Fig. 15: 16), <i>Pleydellia</i> cf. <i>falcifer</i> Maubeuge (Fig. 15: 17), <i>Pleurolytoceras torulosum</i> (Schübler in Zieten) (Fig. 15: 14); other fossils: <i>Acrocoelites</i> sp., <i>Hastites subclavatus</i> (Voltz), <i>Thecocystatus mactrus</i> (Goldfuss), <i>Palaeonucula hammeri</i> (De france), <i>Nicanella voltzii</i> (Hoeninghaus in Roemer), <i>Chlamys textoria</i> (Schlotheim), <i>Pseudomytiloides</i> sp., <i>Sphenodus</i> sp. (tooth 4 mm);
Bed 34: >50 cm	grey (unweathered) to brownish-grey (weathered), well bedded clay;

Carbonate and organic carbon contents

The Amaltheenton Formation is characterized by low CaCO_3 contents (2.5–3.3 wt%) as well as low C_{org} contents (0.8–1.0 wt%) (Table 1, Fig. 4).

The Posidonienschiefere Formation, however, shows a sudden and strong increase in CaCO_3 to 94 wt% at its basis, followed by consistently high values (73–98 wt%) in the lower part of the formation (i.e. limestone and argillaceous limestone), with only the Falciferum Shale showing a lower value (45 wt%). Higher parts of Posidonienschiefere exhibit marl equivalent values around 50–65 wt% CaCO_3 , with only two intercalations of reduced CaCO_3 content (35 wt%) in the upper third (Table 1, Fig. 4). C_{org} contents of the Posidonienschiefere vary between 0.3 and 2.0 wt% in limestone beds, and higher values up to 5.3 wt% in less CaCO_3 -rich lithologies. The highest value (7.5 wt%) was measured in the Falciferum Shale. However, C_{org} contents calculated for the carbonate-free rock fraction demonstrate a different trend: Very high contents characterize Laibstein I and II near basis of formation (i.e., bed 7 and 8, with up to 17.6 wt%), while fish scale debris bed 9 shows a slightly lower value (7.4 wt%). It follows a further maximum in the interval Falciferum Shale to Monotis Bed (up to 14.1 wt%). Higher parts of the formation finally show fluctuating C_{org} contents (4.4–14.0 wt%), with two minima in top parts (1.5 and 1.8 wt%) (Table 1, Fig. 4).

CaCO_3 contents at the basis of the Jurensismergel Formation correspond to calcareous marl (65–71 wt%) and marl (44–53 wt%), then decrease to marls (37–62 wt%) and argillaceous marls (17–34 wt%). Near the top of the formation, one last bed of calcareous marl (66 wt%) is found. Increased C_{org} values (3.0 and 4.3 wt%) were found near basis (bed 18, "Belemnite Battlefield", "Toarcensis Shale"), followed by low values of 1–2 wt% in middle and upper parts of the formation. Only two horizons, basis of bed 24 and bed 25, show slightly increased C_{org} contents (2.5 and 2.8 wt%). Finally, the Opalinuston Formation revealed CaCO_3 contents only slightly lower than top parts of the Jurensismergel, and C_{org} as low as in the Amaltheenton (Table 1, Fig. 4).

Discussion

Lithostratigraphy

The assignment of beds to specific formations of the Schwarzwjura Group follows the definitions given in Bloos et al. (2005), Mönnig et al. (2015), and Nitsch et al. (2015), with only minor modifications.

1. The lower part of section, i.e. beds 1–6, represent the top 9 m of the Amaltheenton Formation (Figs 2A, 5), which shows a total thickness of 36 m at this location (Fig. 3). The formation is characterized by monotonous bluish-grey claystones with disseminated pyrite, low CaCO_3 and low C_{org} contents.
2. The Posidonienschiefere Formation (Figs 2B, 4), with a total thickness of 1.85–1.90 m, is characterized by bituminous marls and limestones rich in fossils. The basis is drawn with the first bituminous and calcareous bed, i.e. "Laibstein I". The erosive discontinuity

Table 1. Carbon (C_{tot} , C_{org} , C_{carb}), total sulphur (S_{tot}), and total nitrogen (N_{tot}) contents of sedimentary rocks of the Ludwigskanal section.

Sample number	Formation	Bed number	Section from—to [cm]	Lithology	Remarks	C_{tot} mean [wt %]	C_{org} mean [wt %]	C_{carb} mean [wt %]	$CaCO_3$ calculated [wt %]	C_{org} carbonate-free [wt %]	N_{tot} mean [wt %]	S_{tot} mean [wt %]	S_{tot} carbonate-free [wt %]
Lud 72	Opalinuston	34	639	calcareous clay-stone		3.23	0.33	2.90	24.2	0.44	0.035	0.013	0.02
Lud 1	Opalinuston	34	629	clay		0.37	0.35	0.02	0.2	0.35	0.057	0.016	0.02
Lud 2	Opalinuston	33	618	argillaceous limestone	stromatolitic crust	9.66	0.30	9.36	78.0	1.36	0.019	0.040	0.18
Lud 3	Opalinuston	33	617–619	calcareous clay-stone	matrix of belemnite accumulation	2.60	0.60	2.00	16.7	0.72	0.047	0.009	0.01
Lud 4	Opalinuston	32	607	calcareous clay-stone		2.70	0.42	2.28	19.0	0.52	0.039	0.011	0.01
Lud 73	Opalinuston	32	602	calcareous clay-stone		3.25	0.78	2.47	20.6	0.98	0.047	0.011	0.01
Lud 74	Opalinuston	32	567	calcareous clay-stone		3.33	0.55	2.78	23.2	0.72	0.041	0.014	0.02
Lud 75	Opalinuston	32	557	calcareous clay-stone	rich in nubeculariid foraminifera	2.93	0.66	2.27	18.9	0.81	0.046	0.010	0.01
Lud 76	Jurensismergel	30	533	calcareous clay-stone	rich in nubeculariid foraminifera	3.61	0.74	2.87	23.9	0.97	0.048	0.020	0.03
Lud 5	Jurensismergel	30	515	calcareous clay-stone	rich in nubeculariid foraminifera	3.16	0.68	2.48	20.7	0.86	0.046	0.014	0.02
Lud 6	Jurensismergel	29	495 to 505	calcareous marl		8.24	0.28	7.96	66.3	0.83	0.024	0.012	0.04
Lud 7	Jurensismergel	28	475 to 480	calcareous clay-stone	rich in nubeculariid foraminifera	3.39	1.07	2.32	19.3	1.33	0.061	0.015	0.02
Lud 8	Jurensismergel	28	465 to 470	calcareous clay-stone		3.20	0.43	2.77	23.1	0.6	0.05	0.03	0.04
Lud 9	Jurensismergel	28	455 to 460	calcareous clay-stone		3.49	0.52	2.97	24.7	0.7	0.04	0.02	0.02
Lud 10	Jurensismergel	28	445 to 450	calcareous clay-stone	rich in nubeculariid foraminifera	3.60	1.18	2.42	20.2	1.5	0.07	0.04	0.06
Lud 11	Jurensismergel	28	435 to 440	calcareous clay-stone	rich in nubeculariid foraminifera	4.01	1.35	2.66	22.2	1.7	0.07	0.06	0.07
Lud 12	Jurensismergel	28	425 to 430	calcareous clay-stone	rich in nubeculariid foraminifera	3.11	1.12	1.99	16.6	1.3	0.06	0.04	0.05
Lud 13	Jurensismergel	28	415 to 420	calcareous clay-stone		2.88	1.18	1.70	14.2	1.4	0.07	0.03	0.04
Lud 14	Jurensismergel	27	405 to 410	calcareous clay-stone	"Yellow Bed"	3.62	1.07	2.55	21.2	1.4	0.07	0.05	0.07
Lud 15	Jurensismergel	26	395 to 400	calcareous clay-stone		3.31	0.85	2.46	20.5	1.1	0.05	0.05	0.06
Lud 16	Jurensismergel	26	385 to 390	calcareous clay-stone		4.14	1.17	2.97	24.7	1.6	0.06	0.05	0.06
Lud 17	Jurensismergel	26	375 to 380	argillaceous marl		4.57	1.29	3.28	27.3	1.8	0.07	0.12	0.17
Lud 18	Jurensismergel	26	365 to 370	argillaceous marl		4.34	0.92	3.42	28.5	1.3	0.05	0.05	0.07
Lud 19	Jurensismergel	25	355 to 360	bituminous marl	matrix of "Mac-tra Bed"	10.26	2.83	7.43	61.9	7.4	0.09	0.61	1.60
Lud 20	Jurensismergel	24	345 to 350	argillaceous marl		4.82	1.01	3.81	31.7	1.5	0.06	0.16	0.23
Lud 21	Jurensismergel	24	335 to 340	argillaceous marl		5.02	1.36	3.66	30.5	2.0	0.07	0.80	1.15
Lud 22	Jurensismergel	24	325 to 330	argillaceous marl		5.09	1.09	4.00	33.3	1.6	0.07	0.94	1.41
Lud 23	Jurensismergel	24	315 to 320	calcareous clay-stone	rich in nubeculariid foraminifera	3.60	1.03	2.57	21.4	1.3	0.07	0.52	0.67
Lud 24	Jurensismergel	24	305 to 310	calcareous clay-stone	rich in nubeculariid foraminifera	3.53	1.04	2.49	20.7	1.3	0.07	0.60	0.75
Lud 25	Jurensismergel	24	295 to 300	argillaceous marl	rich in nubeculariid foraminifera	4.75	0.94	3.81	31.7	1.4	0.06	0.51	0.75
Lud 26	Jurensismergel	24	285 to 290	marl	rich in nubeculariid foraminifera	6.22	0.90	5.32	44.3	1.6	0.05	0.66	1.18
Lud 27	Jurensismergel	24	275 to 280	argillaceous marl	rich in nubeculariid foraminifera	5.89	1.78	4.11	34.2	2.7	0.08	1.45	2.20
Lud 28	Jurensismergel	24	265 to 270	poorly bituminous, argillaceous marl	rich in nubeculariid foraminifera	5.83	2.54	3.29	27.4	3.5	0.08	1.53	2.11
Lud 29	Jurensismergel	23	255 to 260	marl	rich in nubeculariid foraminifera	5.41	1.09	4.32	36.0	1.7	0.05	0.18	0.28
Lud 30	Jurensismergel	23	245 to 250	marl		5.65	1.06	4.59	38.2	1.7	0.04	0.25	0.40

Sample number	Formation	Bed number	Section from-to [cm]	Lithology	Remarks	C _{tot} mean [wt %]	C _{org} mean [wt %]	C _{carb} mean [wt %]	CaCO ₃ calculated [wt %]	C _{org} carbonate-free [wt %]	N _{tot} mean [wt %]	S _{tot} mean [wt %]	S _{tot} carbonate-free [wt %]
Lud 31	Jurensismergel	23	235 to 240	marl	rich in nubeculariid foraminifera	5.30	0.88	4.42	36.8	1.4	0.04	0.25	0.39
Lud 32	Jurensismergel	23	225 to 230	argillaceous marl	rich in nubeculariid foraminifera	4.59	1.04	3.55	29.6	1.5	0.07	0.10	0.15
Lud 33	Jurensismergel	22	220 to 225	argillaceous marl	matrix of belemnite accumulation	4.24	1.03	3.18	26.5	1.4	0.06	0.16	0.21
Lud 34	Jurensismergel	21	205 to 220	bituminous marl	"Toarcensis Shale"	8.49	3.00	5.49	45.7	5.5	0.10	1.23	2.26
Lud 35	Jurensismergel	20	198 to 205	marl	matrix of "Main Phosphorite Bed"	5.96	0.73	5.23	43.6	1.3	0.04	0.69	1.21
Lud 36	Jurensismergel	19	195 to 198	poorly bituminous, calcareous marl	"Belemnite Battlefield"	9.87	1.30	8.57	71.4	4.5	0.04	0.69	2.41
Lud 37	Jurensismergel	19	192 to 195	bituminous marl	"Belemnite Battlefield"	10.62	4.30	6.32	52.7	9.1	0.12	0.99	2.10
Lud 38	Jurensismergel	18	187 to 192	poorly bituminous, calcareous marl		9.58	1.75	7.83	65.2	5.0	0.06	0.99	2.84
Lud 39	Posidonienschiefner	17	185 to 187	poorly bituminous marl	"Fucoid Bed"	8.69	1.88	6.81	56.7	4.3	0.06	1.09	2.52
Lud 40	Posidonienschiefner	16	180	bituminous, calcareous marl	"Variabilis Shale"	11.69	3.57	8.12	67.7	11.0	0.11	0.66	2.05
Lud 41	Posidonienschiefner	16	179	bituminous, calcareous marl	"Variabilis Shale"	11.44	3.40	8.04	67.0	10.3	0.10	0.83	2.50
Lud 42	Posidonienschiefner	16	175	bituminous, calcareous marl	"Variabilis Shale"	12.68	4.79	7.89	65.7	14.0	0.15	0.75	2.18
Lud 43	Posidonienschiefner	16	165	poorly bituminous, argillaceous marl	"Variabilis Shale"	4.93	1.04	3.89	32.4	1.5	0.05	0.10	0.15
Lud 44	Posidonienschiefner	16	155	bituminous marl	"Variabilis Shale"	11.63	4.70	6.93	57.7	11.1	0.14	0.72	1.69
Lud 45	Posidonienschiefner	16	145	poorly bituminous marl	"Variabilis Shale"	5.70	1.08	4.62	38.5	1.8	0.05	1.03	1.68
Lud 46	Posidonienschiefner	16	135	bituminous marl	"Variabilis Shale"	11.63	5.34	6.29	52.4	11.2	0.16	1.27	2.66
Lud 47	Posidonienschiefner	16	125	bituminous marl	"Variabilis Shale"	10.23	3.81	6.42	53.5	8.2	0.11	0.64	1.38
Lud 48	Posidonienschiefner	15	115	bituminous marl	"Bifrons Shale"	11.29	5.01	6.28	52.3	10.5	0.14	1.41	2.95
Lud 49	Posidonienschiefner	15	105	bituminous marl	"Bifrons Shale"	10.26	3.80	6.46	53.8	8.2	0.11	1.05	2.28
Lud 50	Posidonienschiefner	15	95	bituminous marl	"Bifrons Shale"	10.82	4.02	6.80	56.7	9.3	0.13	1.39	3.20
Lud 51	Posidonienschiefner	15	85	bituminous marl	"Bifrons Shale"	9.67	2.88	6.79	56.6	6.6	0.10	1.25	2.89
Lud 52	Posidonienschiefner	15	76	bituminous marl	"Bifrons Shale"	11.58	4.58	7.00	58.3	11.0	0.14	1.14	2.74
Lud 53	Posidonienschiefner	14	66 to 75	poorly bituminous limestone	"Monotis Bed"	12.02	0.31	11.71	97.6	12.8	0.02	0.05	2.11
Lud 54	Posidonienschiefner	13	65 to 66	poorly bituminous, argillaceous limestone		12.04	2.44	9.60	80.0	12.2	0.09	0.60	3.00
Lud 55	Posidonienschiefner	12	40 to 65	poorly bituminous limestone	"Dactylioceras Bed"	12.12	0.80	11.32	94.3	14.1	0.03	0.24	4.22
Lud 56	Posidonienschiefner	11	37 to 40	poorly bituminous, argillaceous limestone		12.31	2.17	10.14	84.5	14.0	0.07	0.18	1.13
Lud 57	Posidonienschiefner	10	27 to 37	bituminous marl	"Falciferum Shale"	12.84	7.47	5.37	44.7	13.5	0.21	2.18	3.94
Lud 58	Posidonienschiefner	9	22 to 27	poorly bituminous, argillaceous limestone	"Fish Scale Bed"	11.89	1.29	10.60	88.3	11.1	0.05	0.28	2.38
Lud 59	Posidonienschiefner	8	17 to 22	poorly bituminous, argillaceous limestone	"Laibstein II" (top)	11.63	1.97	9.66	80.5	10.1	0.06	0.77	3.92
Lud 60	Posidonienschiefner	8	12 to 17	poorly bituminous limestone	"Laibstein II" (centre)	12.01	0.56	11.45	95.4	12.2	0.02	0.09	1.92
Lud 61	Posidonienschiefner	8	7 to 12	poorly bituminous, argillaceous limestone	"Laibstein II" (bottom)	11.64	1.75	9.89	82.4	10.0	0.06	0.59	3.35
Lud 62	Posidonienschiefner	7	0 to 7	poorly bituminous, calcareous marl	lateral to "Laibstein I"	10.75	1.99	8.76	73.0	7.4	0.07	1.32	4.88
Lud 63	Posidonienschiefner	7	5 to 7	poorly bituminous, argillaceous limestone	"Laibstein I" (top)	11.57	1.02	10.55	87.9	8.4	0.04	0.68	5.59
Lud 64	Posidonienschiefner	7	2 to 5	poorly bituminous limestone	"Laibstein I" (centre)	12.33	1.03	11.30	94.2	17.7	0.03	0.33	5.67
Lud 65	Posidonienschiefner	7	0 to 2	poorly bituminous, argillaceous limestone	"Laibstein I" (bottom)	12.02	1.07	10.95	91.2	12.2	0.05	0.38	4.35

Sample number	Formation	Bed number	Section from-to [cm]	Lithology	Remarks	C_{tot} mean [wt %]	C_{org} mean [wt %]	C_{carb} mean [wt %]	$CaCO_3$ calculated [wt %]	C_{org} carbonate-free [wt %]	N_{tot} mean [wt %]	S_{tot} mean [wt %]	S_{tot} carbonate-free [wt %]
Lud 66	Amaltheenton	5	-15	claystone		1.23	0.88	0.35	2.9	0.9	0.06	2.00	2.06
Lud 67	Amaltheenton	5	-40	claystone		1.11	0.82	0.29	2.4	0.8	0.05	2.05	2.10
Lud 68	Amaltheenton	5	-230	claystone		1.33	0.94	0.39	3.2	1.0	0.06	0.73	0.76
Lud 69	Amaltheenton	5	-300	claystone		1.31	0.98	0.33	2.7	1.0	0.06	0.64	0.66
Lud 70	Amaltheenton	4	-800 to -810	calcareous clay-stone	matrix of "Delta-Fossil Bed"	2.16	0.78	1.38	11.5	0.9	0.05	0.56	0.63
Lud 71	Amaltheenton	1	-930	claystone		1.24	0.84	0.40	3.3	0.9	0.06	2.48	2.57

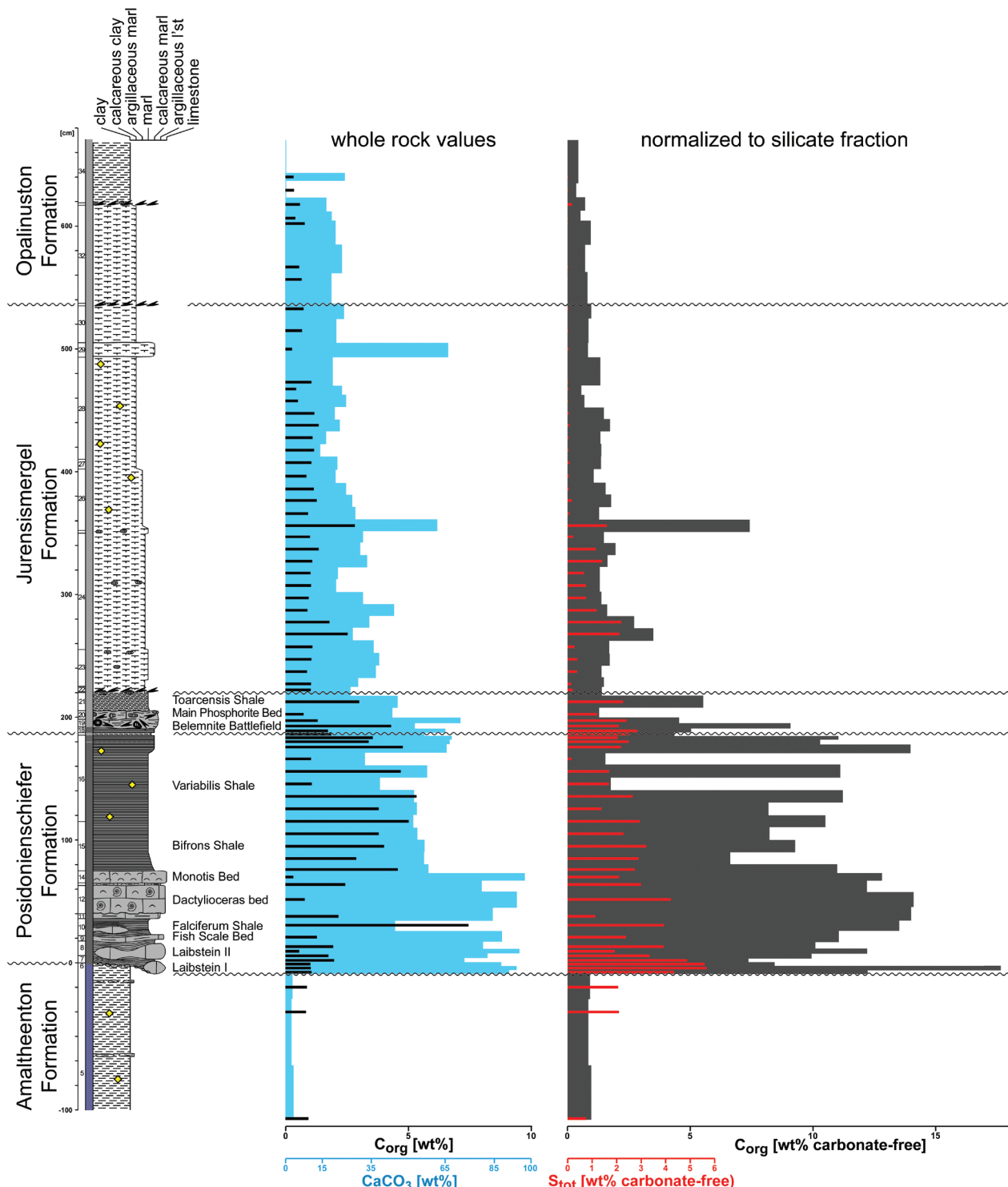


Figure 4. Lithology and lithostratigraphy of the Ludwigskanal section (top Amaltheenton to basis Opalinuston Formation) with $CaCO_3$ and organic carbon contents. For legend see Fig. 7.

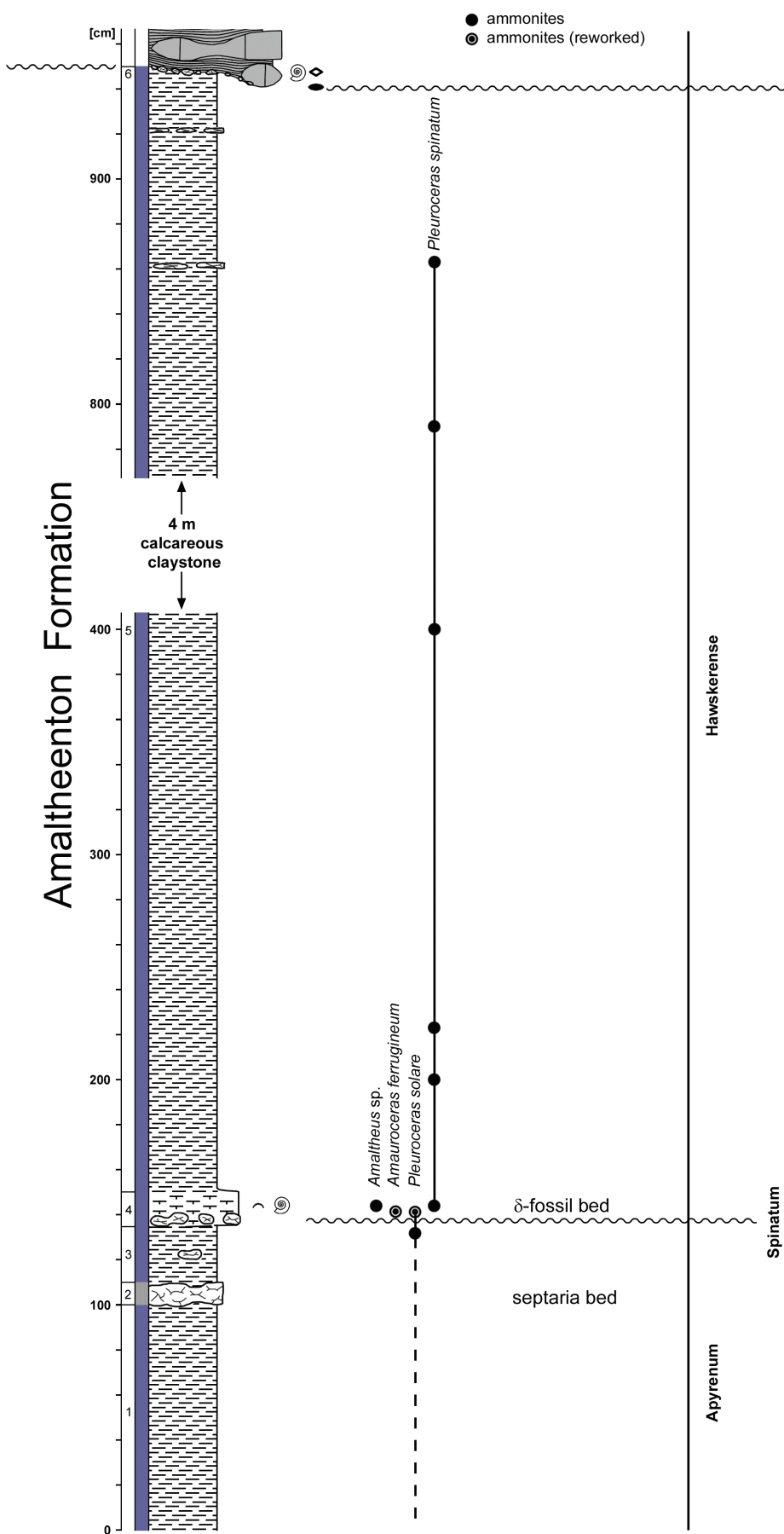


Figure 5. Litho- and biostratigraphy of the upper Amaltheenton Formation, Upper Pliensbachian, exposed at the Ludwigskanal. For legend see Fig. 7.

- at its basis is indicated by reworked concretions of the Amaltheenton. Accordingly, the basal alternation of marls, bituminous marls and *Chondrites*-rich beds, as seen in the Swabian Posidonienschiefer (Urlachs 1977a; Riegraf et al. 1984; Riegraf 1985a; Bloos et al. 2005), is absent in this region. While the total rock C_{org} contents are clearly lower than in the Swabian sections (mean C_{org} = 2.45 wt% at Ludwigskanal versus 6.77 wt% at Dotternhausen, for top Semicelatum to Bifrons Zone), C_{org} contents of the carbonate-free fraction are almost identical (mean C_{org} carbonate-free = 11.18 wt% at Ludwigskanal versus 12.22 wt% at Dotternhausen; Frimmel 2003; Frimmel et al. 2004). Therefore, the comparatively low C_{org} values at Ludwigskanal section reflect a “dilution effect” by increased carbonate contents.
3. The Jurensismergel Formation (Figs 2B, 4), with a total thickness of 3.50 m, is formed by highly fossiliferous marls with phosphorite (lower part) or pyrite nodules (higher part). Major parts of the formation show abundant nubeculariid foraminifera as a significant component of the sediment. Increased C_{org} contents were only detected near the basis (“Belemnite Battlefield”, “Toarcensis Shale”) and in bed 25, a condensed bed in the middle of the formation. Carbonate contents are generally lower (predominantly argillaceous marls; Table 1), if compared to sections of the Swabian Alb (e.g. Göppingen-Ursenwang and Aselfingen: marls and argillaceous limestone beds: Bruder 1968, his tab 4.).

The lower boundary of the Jurensismergel has previously been drawn at the top of the “Belemnite Battlefield”: Urlachs (1971: p. 70f) argued that earlier publications (von Gübel 1891: p. 359; Reuter 1927: p. 56) assigned this belemnite accumulation to the Posidonienschiefer, and that its components are reworked from the Posidonienschiefer below. However, the phosphorite nodules with borings (Fig. 2D) are not derived from bituminous shales below, and correlations with sections in the Swabian Alb (Figs 7, 9) indicate an erosive discontinuity at the basis of the marl bed 18 below the “Belemnite Battlefield” (see discussion of sequence stratigraphy below). Therefore, the “Fucoid Bed” (bed 17) forms, in our view, the top of the Posidonienschiefer Formation, and the poorly bituminous marls of bed 18 form the basis of a new stratigraphic sequence, i.e., the basis of the Jurensismergel Formation.

4. The basis of the comparatively thick Opalinuston Formation (Figs 2B, 4) should be drawn with the lithological change from marl (Jurensismergel) to claystone (Opalinuston). While this change appears gradual in the northern Franconian Alb (e.g., Mistelgau; Schulbert 2001a, b), the Ludwigskanal section still shows a clear calcareous marl bed 308–318 cm above the basis of the Jurensismergel. A calcareous marl bed has also been found in a similar position in the neighbouring section Pölling and likewise assigned to the

Jurensismergel (Arp 2010). Therefore, the change from marl to claystone occurs above this bed, and the belemnite accumulation of bed 31, marking a 3rd order sequence boundary (see sequence stratigraphic discussion below) could be taken as the lithostratigraphic lower boundary of the Opalinuston Formation. This suggested boundary definition coincides with change from pyritic to phosphoritic or compressed preservation of ammonoids in this region.

Biostratigraphy

The biostratigraphic subdivision of the investigated section follows the standard scheme by Dean et al. (1961), with revisions for the Lower Toarcian by Howarth (1973) and Riegraf et al. (1984: p. 19), and for the Upper Toarcian by Knitter and Ohmert (1983), Ohmert et al. (1996), Elmi et al. (1997), Cresta et al. (2001), and Schulbert (2001a) (Fig. 8). As a principal, the lower boundaries of subzones are drawn in the present paper by the first appearance datum (FAD) of the corresponding index species, with the exception of the Hawskerense Subzone (last appearance datum LAD of *Pleuroceras solare*: Dean et al. 1961). The distribution of each of the ammonite genera and species along the investigated section is given in Figs 5 and 6.

(i) Upper Pliensbachian (>9 m)

The first *Pleuroceras solare* of the investigated section has been found 5 cm below the “Delta-Fossil Bed” (bed 4), indicating the Apyrenum Subzone of the Spinatum Zone. Abundant specimens of this species were found enclosed within reworked concretions of the “Delta-Fossil Bed” (bed 4), together with rare *Amauroceras ferrugineum* (Fig. 10: 1, 2). Few of the *Pleuroceras solare* specimens already show minor tubercles, corresponding to var. *solitarium* (Fig. 10: 2).

The marl matrix of the “Delta-Fossil Bed” (bed 4) enclosing the reworked concretions already yielded compressed *Pleuroceras spinatum* with clear tubercles, while *P. solare* is absent. This suggests that the conglomeratic bed represents the base of the Hawskerense Subzone (sensu Dean et al. 1961: “lower boundary [...] drawn immediately above the highest *Pleuroceras solare*”; equivalent to “Upper Spinatum Zone” sensu Hoffmann et al. 2007). Besides, a juvenile *Amaltheus* sp. (possibly a *Pseudoomaltheus*) was recovered.

The following top 8 m claystones of the Amaltheenton (bed 5) contain siderite concretions with typical morphotypes of *Pleuroceras spinatum* (strong ribs with clear tubercles, whorl section square; Fig. 10: 3, 4). However, neither *Pleuroceras hawskerense* nor *Pleuroceras buckmani*, characteristic for the top parts of the Hawskerense Subzone (see e.g. Jordan 1960), were found at the Ludwigskanal/Dörlbach, although they are known from the very top of the Amaltheenton in this region (Zeiss and Schirmer 1965; Arp 1989).

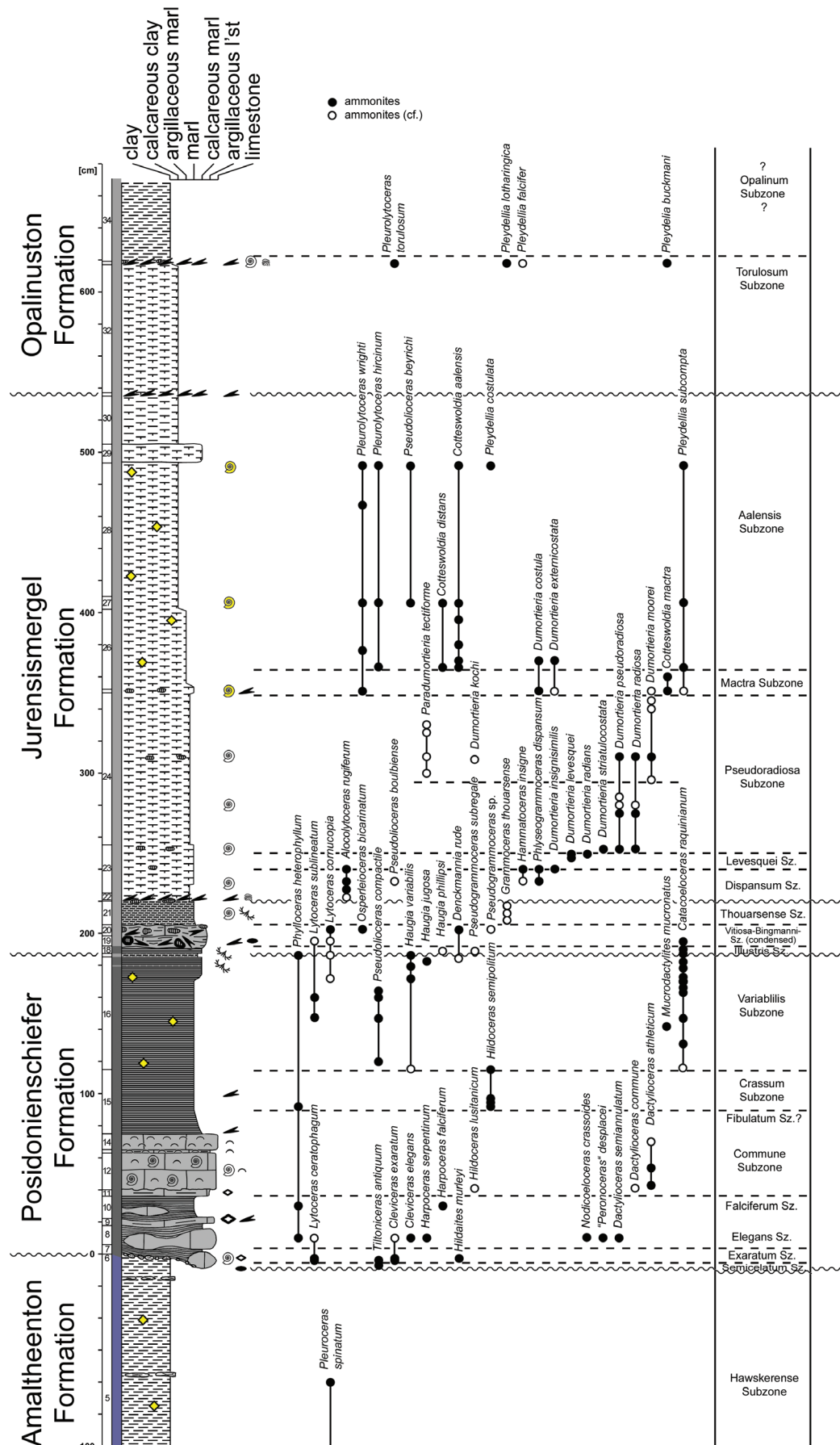


Figure 6. Litho- and biostratigraphy of the Posidonienschiefer, Jurensismergel, and basal Opalinuston Formation, Toarcian, exposed at the Ludwigskanal near Dörlbach. For legend see Fig. 7.

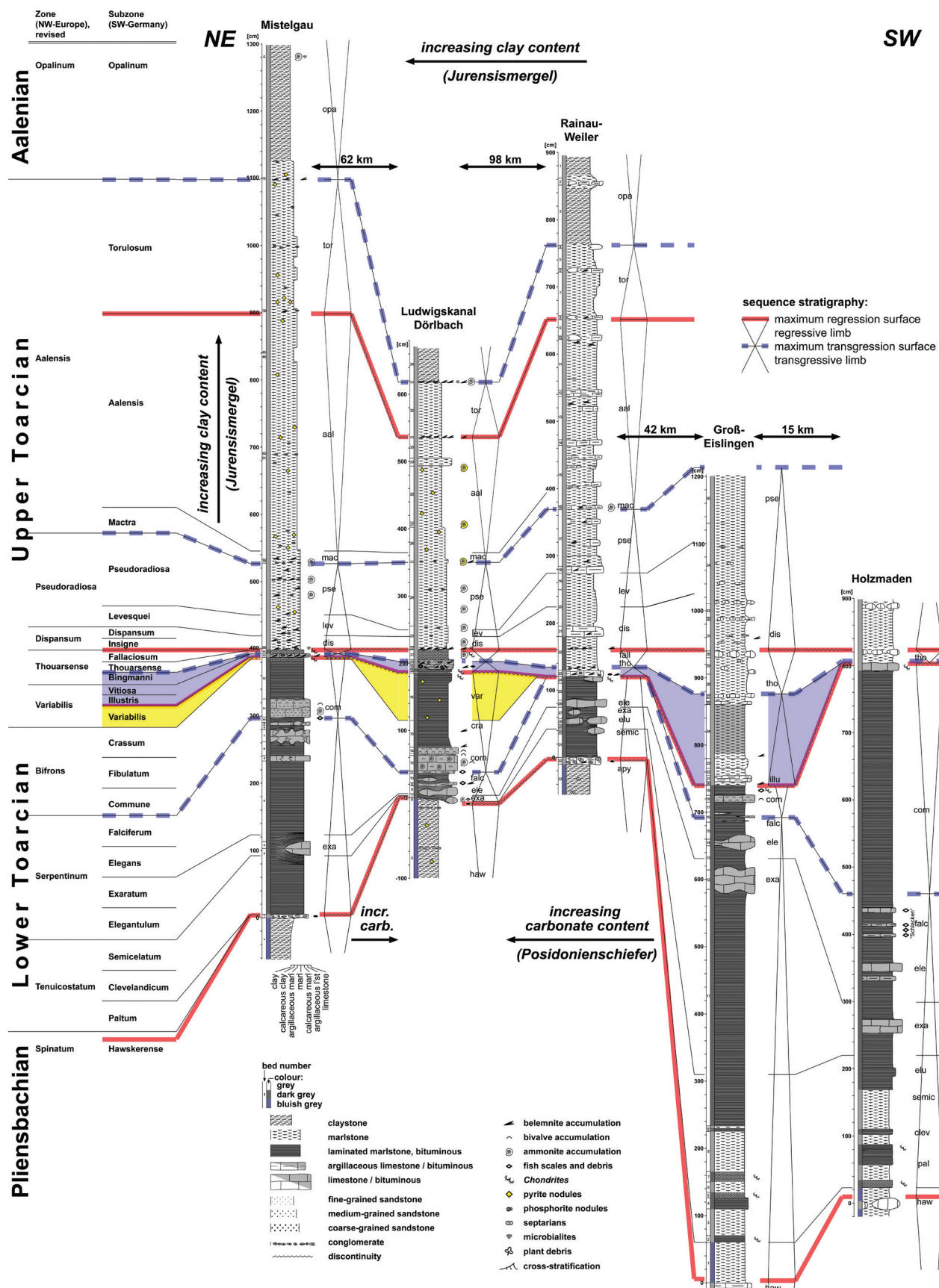


Figure 7. Correlation of the investigated section Ludwigskanal/Dörnbach with sections from the northern Franconian Alb (Mistelgau: Krumbeck 1932c; Schulbert 2001a, b; Arp and Gropengießer 2015; Basis Mactra Subzone drawn with the "Dumortieria bed I"; Basis Aalensis Subzone defined by FAD of *P. subcompta*) and Swabian Alb (Rainau-Weiler: Etzold et al. 1989; Gross-Eislingen: Wiedemann 1966; Holzmaden: Hauff 1921; Riegraf 1985a; Urlichs 1977a), with suggested T-R cycles.

(ii) Lower Toarcian (1.15–1.20 m)

Posidonienschiefer Formation starts with a clear discontinuity and Amaltheenton-derived intraclasts within the shell-debris-rich "Laibstein I" (bed 7). These laminated limestone concretions revealed a layer with several *Tiltoniceras antiquum* 2–3 cm above their basis (Fig. 10: 5, 6), representing the latest interval of the Semicelatum Subzone (Antiquum Horizon; Page 2003, 2004). This finding confirms previous rare reports on *Tiltoniceras antiquum* (syn.: *T. schroederi*: Krumbeck 1932a; Kolb 1964; *T. antiquum*: Kraus 1983: his fig. on p. 415), which – together with "*Lytoceras siemensi*" (most of them belong to *L. ceratophagum*: see Riegraf 1985b) – have initially lead to the assumption that the Laibstein concretions are representing the Tenuicostatum Zone (e.g., Urlichs 1971). However, no dactylioceratid ammonoids of the tenuicostatum group have been reported from the working area. Likewise, in middle and upper parts of the "Laibstein I"-bed abundant *Cleviceras exaratum* (Fig. 10: 10), *Lytoceras ceratophagum* (Fig. 10: 7), and *Hildaites murleyi* (Fig. 10: 8, 9) clearly indicate the Exaratum Subzone of the Falciferum Zone. Rare reports of *Eleganticeras* (Weißmüller 2017: his fig. 187) suggest that the Elegans Zone might be present, too, condensed within the "Laibstein I" (bed 7). Nonetheless, the Laibstein I bed largely represents the Exaratum Subzone, as previously shown by Riegraf (1985b) and Arp (1989).

The following "Laibstein II" (bed 8), with the abundant holoplanktic gastropod *Coelodiscus minutus*, comprises an ammonoid assemblage typical of the Elegans Subzone: *Cleviceras exaratum* (Fig. 11: 6), *Harpoceras serpentinum* (Fig. 11: 1), and a number of dactylioceratids (*Dactylioceras anguinum*, *D. semiannulatum*, *Nodicoeloceras crassoides*, "*Peronoceras*" *desplacei*; Fig. 11: 2–4, 7). *Phylloceras heterophyllum* (Fig. 11: 5), which is absent in "Laibstein I", has also been found in this limestone concretion bed (Kolb 1964; Arp 1989; Weißmüller 2017).

Higher parts of the Falciferum Zone are less well documented at the Ludwigskanal section as well as in the whole region. One compressed specimen of *Harpoceras falciferum* (Fig. 2C) has been found within the "Falciferum Shale" (bed 10), indicating that these bituminous marlstones above the "Fish Scale Bed" (bed 9) belong to the Falciferum Subzone.

The lower bedding plane of "Dactylioceras Bed" (bed 12) and the fish-scale-rich argillaceous limestone layer at its base (bed 11) exhibit poorly preserved specimen of *Dactylioceras commune* (Fig. 12: 1), marking the basis of the Bifrons Zone. The lowermost part of "Dactylioceras Bed" (bed 12) also revealed a poorly preserved *Hildoceras cf. lusitanicum* (Fig. 12: 2), consistent with basis of the Bifrons Zone. In addition, *Frechiella subcarinata* has been reported for this bed 5.5 km ESE of the Ludwigskanal section (Krumbeck 1932a; Weiß and Freitag 1991). No indication of the Ovatum Horizon (Howarth 1992; Page 2003) was found. Within the "Dactylioceras" to "Monotis Bed", however, *Dactylioceras athleticum* (Fig. 12: 3) is

most abundant. Therefore, the complete event bed (Arp and Gropengießer 2016) as well as the fish-scale-rich layer below, belongs to the Commune Subzone.

Between 18 and 38 cm above the basis of the "Bifrons Shale" (bed 15), the occurrence of compressed *Hildoceras semipolitum* (Fig. 12: 4, 5) defines the Semipolitum Horizon at the top of the Bifrons Zone, as known from France and the Mediterranean (Guex 1975; Gabilly 1976a; Elmi et al. 1994, 1997). *Hildoceras semipolitum* has also been recovered from the condensed Variabilis Zone immediately below the "Belemnite Battlefield" of Mistelgau, together with *Haugia jugosa* and *Denckmannia tumefacta* (Simonsen 2013). Associated ammonoids are *Pseudolioceras cf. lythensis* and *Phylloceras heterophyllum*. Neither *Hildoceras bifrons*, *Catacoeloceras crassum* nor representatives of the genus *Peronoceras* were found in this bed at Dörlbach. However, a poorly preserved *H. cf. bifrons* 5 cm above the Monotis Bed in the neighbouring section Alt-dorf-Hirschbühl Bach and findings noted in Kolb (1964: p. 131) and Urlichs (1971: p. 70) suggest that the Fibulatum Subzone (see Dean et al. 1961: p. 482) is present.

(iii) Upper Toarcian (5.04 m)

The first appearance of *Haugia* sp. at the basis of bed 16 ("Variabilis Shale"), i.e. one compressed fragment at 40 cm above the "Monotis Bed", indicated the lower boundary of the Variabilis Subzone, Upper Toarcian. Only a minor overlap of this genus with *Hildoceras* was observed at the Ludwigskanal/Dörlbach. Pyritized and compressed *Catacoeloceras raquinianum* (Fig. 13: 2, 3), *Pseudolioceras compactile* (Fig. 12: 10, 11), and *Lytoceras sublineatum* (Fig. 13: 1) are abundant in this zone, while compressed *Haugia variabilis* (Fig. 12: 8) concentrate in the top 15 cm. *Phylloceras heterophyllum*, *Mucrodactylites mucronatus* (Fig. 12: 6, 7), and *Lytoceras cf. cornucopia* are present, too.

One compressed *Haugia jugosa* 3 cm below top (Fig. 12: 9) and one compressed *Denckmannia rude* 1 cm below top of bed 16 are consistent with the Jugosa Horizon (Elmi et al. 1997) at the top of the Variabilis Subzone. A finding of *Haugia ogerieni* from Berg by Krumbeck (1943), which is a coarse ribbed variety of *Haugia jugosa* according to Lacroix (2011), may further support this interpretation. The following "Fucoid Bed" (bed 17), containing *Haugia variabilis*, *Catacoeloceras raquinianum*, *Phylloceras heterophyllum*, and *Lytoceras cf. cornucopia* may also belong to this horizon.

A change in the ammonoid assemblage, however, is evident for bed 18, i.e., the 5 cm calcareous marl below the "Belemnite Battlefield": *Pseudogrammoceras subregale* (Pinna) (Fig. 13: 4) and *Haugia cf. phillipsi* (Simpson) (Fig. 13: 5) point to the Illustris Subzone (Gabilly 1976a: p. 126), with *Catacoeloceras raquinianum* still abundant. Likewise, Krumbeck (1943: p. 298) reported a *Haugia cf. illustris* from shales just below the Belemnite Battlefield of the Teufelsgraben.

The “Belemnite Battlefield” (bed 19) is rather poor in ammonoids. *Catacoeloceras raquinianum* (d’Orbigny) has been recovered at the lower bedding plane (Fig. 13: 6), and deformed phosphoritic casts of *Lytoceras cf. cornucopia* occur within the bed. One fragmentary *Pseudogrammoceras* sp. is poorly preserved. This rather unspecific assemblage is, nonetheless, consistent with the view of Urlichs (1971) that the Belemnite Battlefield still belongs to the (upper) Variabilis Zone, with no elements of the Thouarsense Zone. However, no direct evidence of the Vittiosa Subzone was found at Dörlbach.

The following “Main Phosphorite Bed” (bed 20) has been assigned by Krumbeck (1943: p. 305) to the Thouarsense Zone because of findings of *Grammoceras thouarsense* in the neighbouring section Hausheim. At the Ludwigskanal/Dörlbach, this bed yielded a number of *Lytoceras cornucopia* (Fig. 13: 8) specimens, one coarsely ribbed *Pseudogrammoceras* sp., one *Osperleioceras bicarinatum* (Fig. 13: 7), and one phosphoritic cast of *Denckmannia rude* (Fig. 13: 9). While *D. rude* is restricted to the Variabilis Zone (Becaud et al. 2005; Lacroix 2011: p. 235), *O. bicarinatum* ranges from the Semipolitum Horizon to the Bingmanni Horizon (Lacroix 2011: p. 113). The “Main Phosphorite Bed” (bed 20), therefore, represents a condensation horizon comprising the top of Variabilis and the basis of Thouarsense Zone.

Numerous, compressed *Grammoceras cf. thouarsense* (Fig. 14: 1) occur as a monospecific assemblage in the overlying “Toarcensis Shale” (bed 21), which consequently represents the Thouarsense Subzone. Neither lytoceratids nor any other ammonite genus was found in this bed. Indication of the Fallaciolum Subzone is absent at the Ludwigskanal/Dörlbach, but phosphoritic casts of *Pseudogrammoceras gr. fallaciolum* were mentioned by Krumbeck (1943: p. 305) from a belemnite-rich marl at the neighbouring section Hausheim (4.4 km SE of Dörlbach).

The “belemnite accumulation” of bed 22 yielded, except for *Alocolytoceras cf. rugiferum*, no determinable ammonoids. The range of *A. rugiferum* is not well constrained, but shows a maximum abundance in the Dispansum Zone in northern and southwestern Germany (Wunstorf 1904; Ernst 1923; Knitter and Riegraf 1984). Therefore, this bed is considered as erosive basis of the Dispansum Zone, and may contain reworked components of the Fallaciolum Subzone, as the ones described by Krumbeck (1943).

First *Phlyseogrammoceras dispansum* (Fig. 14: 5, 8), however, have been found 5 cm above the “belemnite accumulation bed 22”, in bed 23. This ammonoid extends up to 18 cm above basis of bed 23 and is associated with abundant *Alocolytoceras rugiferum* (Fig. 14: 2, 4) and rare *Pseudolioceras cf. boulbiense* (Fig. 14: 3). 10 and 15 cm above basis of bed 23, *Hammatoceras insigne* (Fig. 14: 10, 12) has been detected, clearly overlapping with the range of *Phlyseogrammoceras dispansum* in this section, so that the Dispansum Zone cannot be subdivided at the Ludwigskanal/Dörlbach.

At 11 cm below top of bed 23, first *Dumortieria* occur, specifically *Dumortieria insignisimilis* (Fig. 14: 6, 7), cor-

responding to the basis of the Levesquei Subzone (“Dumortieri Horizon”: Elmi et al. 1997; “Insignisimilis Zonule”: Page 2003). The index fossil *Dumortieria levesquei* (Fig. 14: 11, 13) was detected slightly above (i.e., 6 and 9 cm below top of bed 23), together with *Dumortieria radians*.

The top 4 cm of bed 23 finally show an ammonite accumulation with *Dumortieria pseudoradiosa* (Fig. 14: 14), *D. radiosa*, and *D. striatulocostata*, marking the onset of the Pseudoradiosa Subzone. The first appearance of *Dumortieria moorei* (Fig. 15: 10), which descends from *D. radiosa*, is delayed relative to *D. pseudoradiosa*, and falls into the upper part of the Pseudoradiosa Subzone. The (chrono)species also shows an overlap with its successor *Cotteswoldia mactra*, in accordance with data from sections from France (Rulleau 2007: p. 32). Consequently, the Moorei Subzone sensu Dean et al. (1961) in England is, in our view, not equivalent to the Pseudoradiosa Subzone sensu Gabilly 1976a and Elmi et al. 1997 (Fig. 8). However, the Moorei Subzone sensu Knitter and Ohmert (1983) in SW Germany (defined by the FAD of *Dumortieria pseudoradiosa*) is identical to the Pseudoradiosa Subzone used in the present paper. Moreover, top parts of the Pseudoradiosa Subzone at the Ludwigskanal/Dörlbach yielded *Paradumortieria cf. tectiforme* (Fig. 15: 5), forming the transition to the subsequent *Cotteswoldia aalensis* group.

Bed 25 clearly forms a minor condensation with the enrichment of phosphorite nodules, ammonites and belemnites. *Cotteswoldia mactra* (Fig. 15: 3) obtained from this bed indicates the basis of the Mactra Subzone, Aalensis Zone, still occurring together with the latest *D. cf. moorei*. This lowermost part of the Aalenis Zone, which is a comparatively short interval of only 20 cm thickness, is characterized by the persistent occurrence of coarse-ribbed *Dumortieria*, specifically *D. costula* und *D. externicostata*, which appear to be absent (or rare) in the upper part of the section. Also, first *Pleurolytoceras wrighti* were found in this bed.

With a minor overlap with *Cotteswoldia mactra*, *Cotteswoldia aalensis* (Fig. 15: 6), *C. distans* (Fig. 15: 9), *Pleydellia subcompta* (Fig. 15: 12) and *Pleurolytoceras hircinum* (Fig. 15: 2) occur from 15 cm above the basis of bed 26 to the top of bed 28, i.e. an ammonoid accumulation just below the calcareous marlstone bed 29. This ammonoid assemblage is characteristic for the Aalensis Subzone. From the following 120 cm of the section (beds 29 to 32), no ammonoids were recovered (lack of collection). However, according to the section Pölling 6.3 km SSE of Dörlbach (Arp 2010), the marlstone bed (equivalent to bed 29) and 30 cm marls above (equivalent to bed 30) still belong to the Aalensis Subzone, and the basis of the Torulosum Subzone is drawn at a belemnite accumulation of bed 31. Bed 33, a condensed horizon with phosphorite nodules, enrichment of belemnites, ammonites, and bivalves provided compressed specimens of *Pleydellia buckmani* (Fig. 15: 16), *P. cf. falcifer* (Fig. 15: 17), *P. lotharingica* (Fig. 15: 15), and *Pleurolytoceras torulosum* (Fig. 15: 14). The bed clearly belongs to the youngest ammonite subzone of the Lower Jurassic, i.e., the Torulosum Subzone.

Stage	Zone (NW-Europe) ¹⁾	Subzone (Great Britain) ¹⁾	Horizon (Yorkshire, Scotland) ²⁾	Subzone (SW-Germany) ³⁾	Subzone (France) ⁴⁾	Horizon (France) ⁴⁾	Zone (NW-Europe), revised ⁴⁾
Aal.	Opalinum		< not defined >	Opalinum			Opalinum
				Torulosum	Pseudo-lotharingicum	Buckmani Pseudolotharingicum	Aalensis
	Levesquei	Aalensis		Aalensis	Mactra	Celtica Mactra	
		Moorei		Mactra		Tectiforme	
	Levesquei			Moorei	Pseudoradiosa	Pseudoradiosa	
				Levesquei	Levesquei	Munieri Dumontieri	
	Dispansum			Dispansum	Gruneri	Gruneri	
				Insigne	Insigne	Pachu Cappuccinum	Dispansum
	Thouarsense	Struckmanni		Fallaciosum	Fallaciosum	Fallaciosum	
		Striatulum			Fascigerum	Fascigerum	Thouarsense
	Variabilis			Thouarsense	Thouarsense	Thouarsense Doerntense	
		<not defined>		Bingmanni	Bingmanni	Bingmanni	Variabilis
	Bifrons	Braunianus/ Crassum		Vitiosa	Vitiosa	Vitiosa	
		Crassum-Bifrons		Illistris	Illistris	Phillipsi Illistris	
Lower Toarcian	Fibulatum	Vortex		Variabilis	Variabilis	Jugosa Navis	
		Braunianus					
		Turriculatum					
	Commune	Athleticum	Commune			Lusitanicum	
		Commune				Sublevisoni	
		Ovatum				Tethysi Sublevisoni	
	Falcifer	Falciferum	Semicelatum	Falciferum	Falciferum	Douvillei	
		Pseudoserpentinum				Pseudoserpentinum	Serpentinum
	Exaratum	Elegans	Elegantulum	Elegans	Elegantulum	Strangewaysi	
		Exaratum		Exaratum			
	Tenuicostatum	Elegantulum	Clevelandicum	Elegantulum		Elegantulum	
	Semicelatum	Antiquum	Semicelatum	Antiquum	Semicelatum	Semicelatum	
		Semicelatum		Semicelatum			Tenuicostatum
	Clevelandicum	Tenuicostatum		Tenuicostatum			
		Clevelandicum		Clevelandicum			Crosbeyi
	Paltum	Crosbeyi					
		Paltum		Paltum	Paltus	Paltum	
Pliensb.	Spinatum	Hawskerense	Hawskerense	Hawskerense	Hawskerense	Hawskerense	
		Elabratum				Lotta	
	Apyrenum	Solare	Apyrenum	Solare	Apyrenum	Solare	
		Transiens		Transiens		Transiens	
		Salebrosum				Salebrosum	

Figure 8. Ammonite zones, subzones, and horizons for the NW-European Toarcian according to different authors. 1) Dean et al. 1961; Howarth 1978. 2) Page 2003, 2004. 3) Knitter and Ohmert 1983; Riegraf et al. 1984; Riegraf 1985a; Ohmert et al. 1996; Cresta et al. 2001. 4) Gabilly 1976a; Elmi et al. 1997). Note that *Pleydellia (Walkericeras) lugdunensis* Elmi & Rulleau, 1997 is considered by Di Cencio and Weis (2020) as junior synonym of *P. (W.) pseudolotharingicum* Maubeuge, 1950, so that the subzone and horizon is termed accordingly.

(iv) Lower Aalenian (>0.5 m)

No *Leioceras opalinum* has been found in the Ludwigskanal/Dörlbach section. However, compressed *Leioceras opalinum* found in a drill core (highway viaduct Pilsach, unpublished observations) immediately above the equivalent of bed 33 suggests that the Toarcian-Aalenian boundary is located at the basis of bed 34.

Sequence stratigraphy

Sequence stratigraphic interpretations require correlation and comparison of sections across the shelf with respect to discontinuities, facies trends, geometry and stacking patterns (e.g., Catuneanu et al. 2011). In the present paper, the definition of sequences as “transgressive-regressive cycles”

(T-R cycles) follows Embry and Johannessen (1992), with “sequence boundaries” at maximum regression surfaces (mrs; for further discussion see Catuneanu et al. 2011 and Simmons 2012). However, it remains difficult to distinguish stratigraphic gaps at maximum regression surfaces (with reworked fauna in the following transgressive “ravinement surface”; Nummedal and Swift 1987) from condensation or non-deposition of maximum flooding surfaces (mfs) in sections distant from siliciclastic sediment influx.

This also applies to the South German Toarcian succession, because of low sedimentation rates and high distance to deltaic siliciclastic influx, no evident subaerial exposure surfaces, and (with respect to the Upper Toarcian) a limited number of sections with both, detailed sedimentological plus biostratigraphic observations. The following sequence stratigraphic interpretations, therefore, remain preliminary (Figs 7, 9).

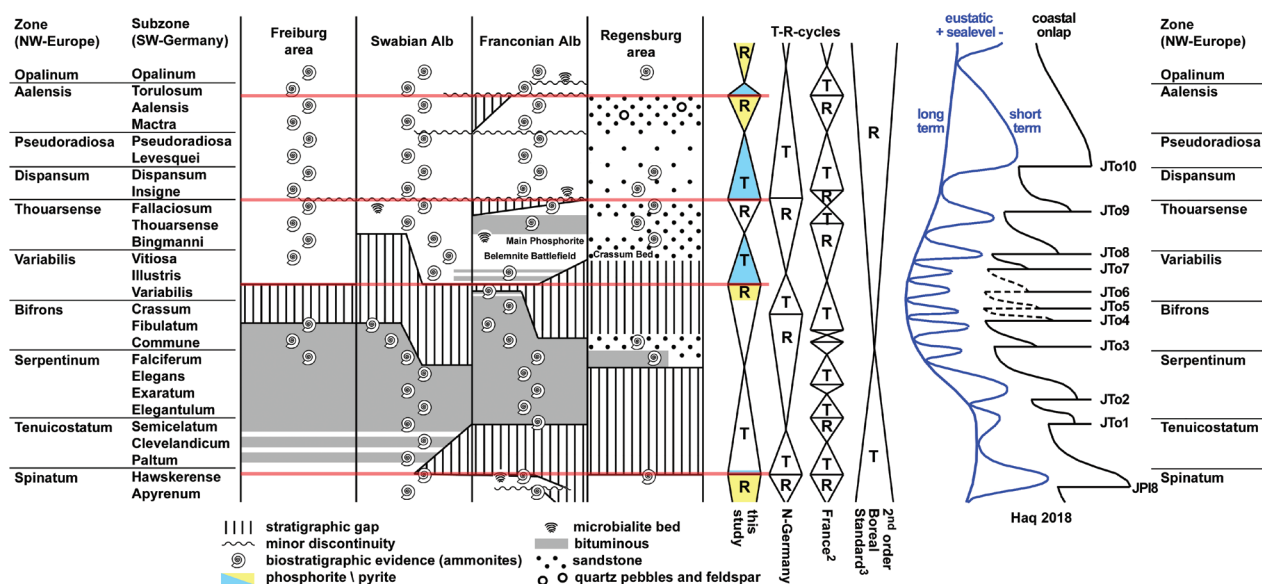


Figure 9. Sequence stratigraphic interpretation of the Toarcian succession in the Franconian Alb (including Ludwigskanal/Dörlbach section) and adjacent areas. Sedimentary succession and ammonite biostratigraphic evidence according to Pompeckj (1901), Krumbeck (1932b, 1943), Putzer (1939), Baumberger et al. (1969), Meyer and Baumberger (1998) (Regensburg area), Brockert (1959), Fischer (1964), Wiedemann (1966), Urlichs (1977a), Riegraf et al. (1984), Riegraf (1985a), Etzold et al. (1989) (Swabian Alb), Ohmert (1976), Knitter and Ohmert (1983), Ohmert et al. (1996) (Freiburg area), T-R cycles: 1 = third order sequences N-Germany (Zimmermann et al. 2015), 2 = third order sequences France (de Graciansky et al. 1998); 3 = second order sequences Boreal standard (de Graciansky et al. 1998; Jacquin et al. 1998). Eustatic sea level and coastal onlap according to Haq (2018). Note that the definition of sequence boundaries in Haq (2018) differs from the concept of T-R-sequences, with the latter bounded by maximum regression surfaces (Embry and Johannessen 1992; see also Simmons 2012).

A sequence stratigraphic framework, however, has been developed for the Toarcian of Northern Germany, based on a comprehensive analysis of drillings (sedimentology and gamma ray logs) covering the transition from marine to fluvio-deltaic deposits of the NE-German Basin to fully marine deposits of the NW-German Basin (Zimmermann et al. 2015). Nonetheless, the biostratigraphic calibration of the drillings relies on a combination of microfossil records and comparatively rare ammonite records, with limited resolution at the subzone level. Furthermore, a sequence stratigraphic interpretation was given by Röhl and Schmid-Röhl (2005) for the Lower Toarcian in Southern Germany, specifically based on the biostratigraphically and sedimentologically well investigated sections Dotternhausen (Swabian Alb) and Schesslitz (Franconian Alb).

For the Upper Toarcian of Southern Germany, no such detailed analysis exists, but important information can be derived from proximal sections near Regensburg, where minor coarse siliciclastic influx during regressive phases intercalate between fine-grained open-marine sediments with ammonoids (Fig. 9). Furthermore, sequence stratigraphic interpretations based on well dated drillings and outcrops exist for the Toarcian of France (de Graciansky et al. 1998), including Quercy (Cubaynes et al. 1984; Lezin et al. 1997) and the type region of the Toarcian (Galbrun et al. 1994). Indeed, the most recent interpretation of the Toarcian eustatic sealevel curve by Haq (2018) is largely based on

European sections from France, United Kingdom, Poland, and Switzerland, with additional data from sections in Argentina, Tibet, and the Arabian Platform (partially with tentative correlations).

The total duration of the Toarcian is about 8.5 Ma (Gradstein et al. 2012: from 182.7 to 174.1 Ma, i.e. 8.6 Ma; Boulila et al. 2014: 8.3 Ma), while the duration of each of the ammonite zones is to date under discussion (Gradstein et al. 2012; Boulila et al. 2014; Rübsam and Al-Husseini 2020). In the following, vertical thickness and facies trends as well as discontinuities of the Ludwigskanal/Dörlbach section are discussed in comparison with neighbouring sections (Fig. 7) and areas to reveal T-R cycles for the top Pliensbachian to basis Aalenian succession in Southern Germany (Fig. 9).

(i) Amaltheenton Formation

Only two stratigraphic gaps in the otherwise monotonous claystones of the Amaltheenton are evident: The first gap is located within higher parts of the formation. Here, the “Delta-Fossil Bed” (Fig. 5) forms a distinct intraformational discontinuity at the basis of the Hawskerense Subzone. This discontinuity is also evident in neighbouring sections farther north (Buttenheim: Hoffmann et al. 2007) and south, where the section Sulzkirchen exhibits a clear erosional relief with compensation of the gap by sediment of the Hawskerense Subzone (Keupp and Arp 1990).

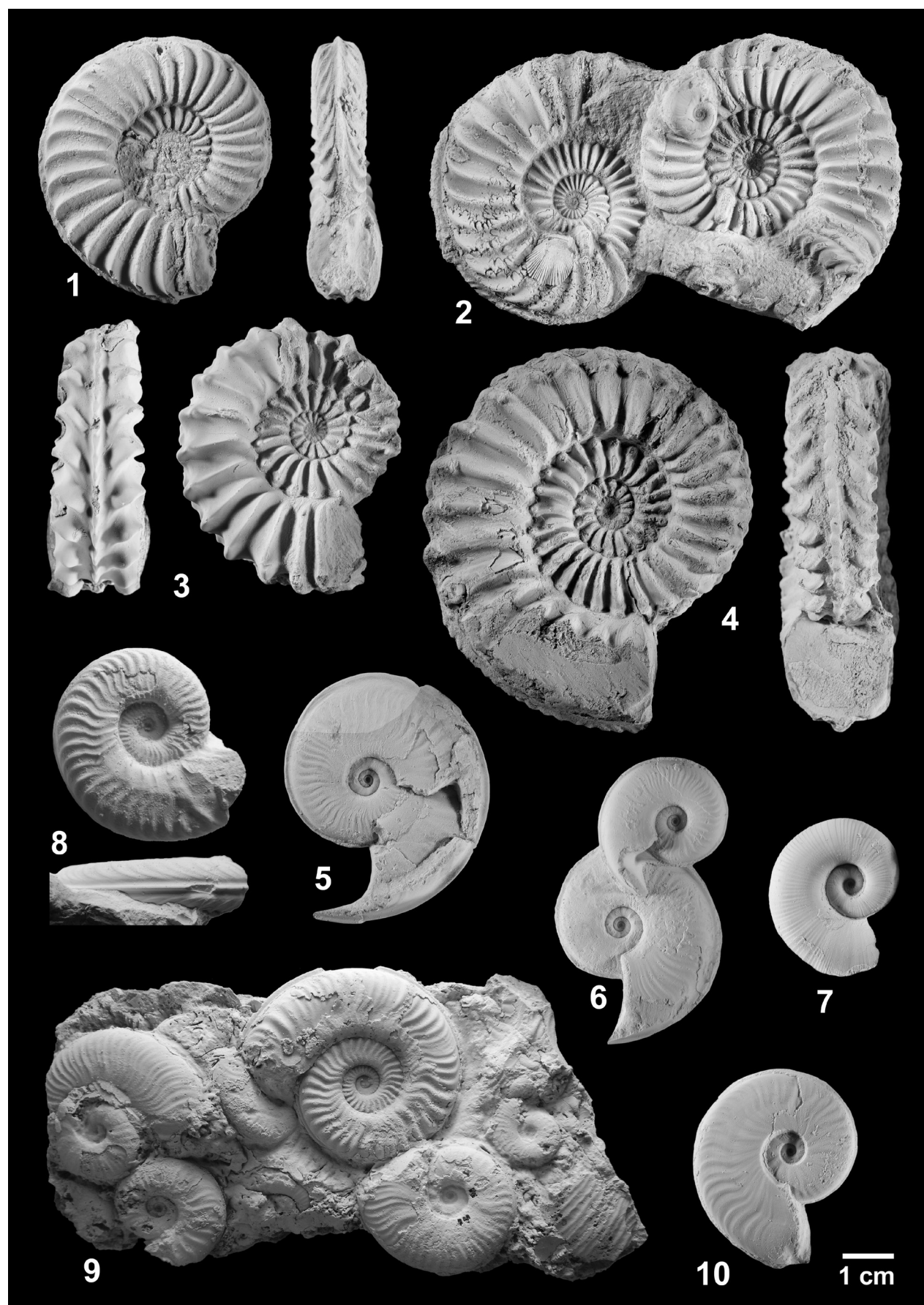


Figure 10. 1. *Pleuroceras solare* (Phillips), reworked concretion in bed 4, basis of Hawskerense Subzone, Amaltheenton Formation. GZG.INV.70496: d = 53 mm, di = 39 mm, u = 22 mm, wh = 17 mm, wb = 15 mm, rb/2 = 15. 2. Two specimens of *Pleuroceras solare* var. *solitarium* (Simpson), together with a juvenile *Amauroceras ferrugineum* (Simpson), reworked concretion in bed 4, basis of Hawskerense Subzone, Amaltheenton Formation. GZG.INV.70497a: d = 54 mm, di = 39 mm, u = 21 mm, wh = 17 mm, wb = 15 mm, rb/2 = 15; GZG.INV.70497b: d = 56 mm, di = 40 mm, u = 24 mm, wh = 18 mm, wb = 14 mm, rb/2 = 15; GZG.INV.70497c: d = 11 mm, di = 7 mm, u = 3 mm, wh = 5 mm, wb = 3 mm, rb/2 = 28. 3. *Pleuroceras spinatum* (Bruguière), 2 m below top of bed 5, Hawskerense Subzone, Amaltheenton Formation. GZG.INV.70498: d = 54 mm, di = 37 mm, u = 23 mm, wh = 19 mm, wb = 18 mm, rb/2 = 11. 4. *Pleuroceras spinatum* (Bruguière), 50 cm above basis of bed 5, Hawskerense Subzone, Amaltheenton Formation. GZG.INV.70499: d = 76 mm, di = 58 mm, u = 36 mm, wh = 24 mm, wb = 24 mm, rb/2 = 14. 5. *Tiltoniceras antiquum* (Wright), 1–2 cm above basis of bed 7, Semicelatum Subzone, Posidonienschiefer Formation. Minor part (bright area) of the body chamber restored. GZG.INV.45641a: d = 48 mm, di = 33 mm, u = 12 mm, wh = 20 mm, wb = 12 mm, rb/2 = 22. 6. *Tiltoniceras antiquum* (Wright), 1–2 cm above basis of bed 7, Semicelatum Subzone, Posidonienschiefer Formation. GZG.INV.45641b: d = 38 mm, di = 26 mm, u = 9 mm, wh = 17 mm, wb = 9 mm, rb/2 = (33); GZG.INV.45641c: d = 27 mm, di = 18 mm, u = 6.5 mm, wh = 11 mm, wb = 7 mm, rb/2 = (30). 7. *Lytoceras ceratophagum* (Quenstedt), middle part of bed 7, Exaratum Subzone, Posidonienschiefer Formation. GZG.INV.70500: d = 29 mm, di = 18 mm, u = 9 mm, wh = 12 mm, wb = 11 mm, rb/2 = 46. 8. *Hildaites murleyi* (Moxon), bed 7, Exaratum Subzone, Posidonienschiefer Formation. GZG.INV.70501: d = 41 mm, di = 27 mm, u = 14 mm, wh = 16 mm, wb = 12 mm, rb/2 = 21; (leg. Arno Garbe). 9. *Hildaites murleyi* (Moxon), together with juvenile *Cleviceras exaratum* (Young and Bird), bed 7, Exaratum Subzone, Posidonienschiefer Formation. GZG.INV.70502: d = 44 mm, di = 32 mm, u = 17 mm, wh = 15.5 mm, wb = 10 mm, rb/2 = 24; (leg. Arno Garbe). 10. *Cleviceras exaratum* (Young and Bird), middle part of bed 7, Exaratum Subzone, Posidonienschiefer Formation. GZG.INV.70503: d = 39 mm, di = 27 mm, u = 10 mm, wh = 17 mm, wb = 8 mm, rb/2 = 24.

The second gap is developed at the top of the Amaltheenton, where reworked nodules indicate an erosion at the Ludwigskanal (Fig. 5). In neighbouring sections, these nodules are commonly accumulated to form the so-called "Bollernkalk" (Bandel and Knitter 1983; Böhm and Brachert 1993), which shows a non-bituminous bioclastic micrite matrix with minor phosphorite. This conglomeratic bed is probably still Upper Pliensbachian in age (Riegraf 1985a: his fig. 17) and coincides with the formation of an erosional relief including the "Altdorf High" and a coast-parallel strip devoid of Amaltheenton sediments, compensated by later sediments of the Posidonienschiefer (Knitter 1983: p. 240; Arp et al. 2014). Strikingly, the Spinatum Zone in the Franconian Alb shows a considerably higher thickness compared to sections of the Swabian Alb. In turn, the carbonate contents of the Spinatum Zone sediments increase towards the Swabian Alb ("Costatenkalke": alternation of marls and concretionary limestone beds; Quenstedt 1858: p. 164; Urlich 1977a, b).

Based on these observations, sediments of the Spinatum Zone in the Franconian Alb are considered to reflect a regression with prograding siliciclastics from NE, and a corresponding maximum regression surface in top parts of the Hawskerense Subzone (Fig. 9). This is in accordance with delta progradation and regression seen in N-Germany (Zimmermann et al. 2015) and a sequence boundary near the top of the Spinatum Zone (JPI8 sensu Haq 2018). Hence, the reduced thickness and increasing carbonate content towards the SW (Swabian Alb) mirrors the greater distance to the source of siliciclastics from NE (see Paul et al. 2008: fig. 5). An additional, minor, intermittent regression (with changes in bottom currents) might be seen in the erosional discontinuity at basis of the Hawskerense Subzone, while the coast-parallel lack of

the total Amaltheenton mirrors a coast-parallel current intensification during the Pliensbachian-Toarcian transition (Fig. 9). Röhl and Schmid-Röhl (2005), however, suggest that the sequence boundary at the Pliensbachian-Toarcian transition in Southern Germany is located within the Tenuicostatum Zone, which might correspond to the medium sequence boundary JTo1 sensu Haq (2018). No decision can be made on that from the present data of the condensed Ludwigskanal section. In any case, the Upper Pliensbachian is generally known as a period of low sealevel, reflecting a cold climate interval with polar ice caps (Price 1999), glendonites (Teichert and Lippold 2013), and cool-water faunal elements (Arp and Seppelt 2012). Nonetheless, no evidence of subaerial exposure was found to date at basin margin sections (Regensburg area). However, these oolitic and laminated iron ores are poorly investigated with respect to sedimentology and geochemistry.

(ii) Posidonienschiefer Formation

The Posidonienschiefer shows a very low thickness, combined with high carbonate contents. C_{org} contents normalized to the silicate sediment fraction show that the T-OAE clearly peaks in the Exaratum Subzone (Fig. 4). A second maximum is developed in the Falciferum-Commune Subzones. Strikingly, first Posidonienschiefer beds (Laibstein I and II) show endo- and epibenthic bivalves (*Nicanella* sp., *Pleuromya* sp., *Goniomya rhombifera*, *Camptonectes subulatus*), which are absent farther up the section, suggesting a delayed overstepping of anoxic bottom waters on the Altdorf High. Ammonite zones and subzones are densely spaced, however, with only one clear stratigraphic gap at the basis of the formation (Fig. 6). Here, the

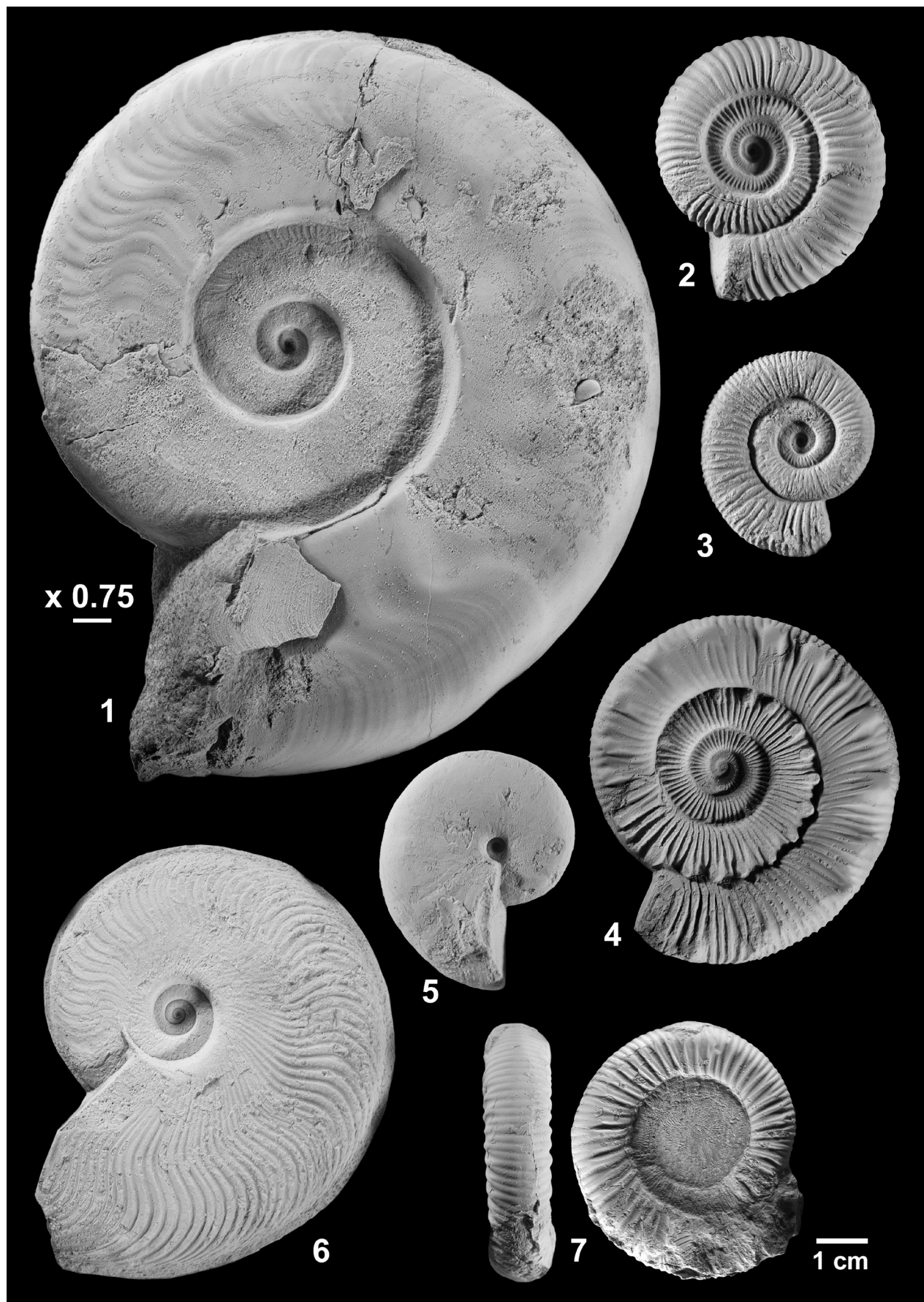


Figure 11. 1. *Harpoceras serpentinum* (Schlotheim), bed 8, Elegans Subzone, Posidonienschiefere Formation. GZG.INV.70504: d = 197 mm, di = 144 mm, u = 80 mm, wh = 70 mm, wb = 40 mm, rb/2 = n.a.; (leg. Matthias Weißmüller). 2. *Dactylioceras sp. forma aegra circumdata* (Martin 1858) Hölder 1956, bed 8, Elegans Subzone, Posidonienschiefere Formation. GZG.INV.70505a: d = 53 mm, di = 40.5 mm, u = 22 mm, wh = 13.5 mm, wb = 15 mm, rb/2 = 30. 3. *Dactylioceras anguinum* (Reinecke), bed 8, Elegans Subzone, Posidonienschiefere Formation. GZG.INV.70505b: d = 40 mm, di = 30 mm, u = 14.5 mm, wh = 11 mm, wb = (11 mm), rb/2 = 31. 4. “*Peronoceras*” *desplacei* (d’Orbigny), bed 8, Elegans Subzone, Posidonienschiefere Formation. GZG.INV.70506: d = 68 mm, di = 53 mm, u = 38 mm (56%), wh = 16 mm (24%), wb = 16 mm, rb/2 = 41. 5. *Phylloceras heterophyllum* (Sowerby), bed 8, Elegans Subzone, Posidonienschiefere Formation. GZG.INV.70507: d = 44 mm, di = 29 mm, u = 4.5 mm, wh = 24 mm, wb = 12 mm, rb/2 = n.a. 6. *Cleviceras elegans* (Sowerby), bed 8, Elegans Subzone, Posidonienschiefere Formation. GZG.INV.70508: d = 86 mm, di = 53 mm, u = 15 mm, wh = 43 mm, wb = 19 mm, rb/2 = 49. 7. *Dactylioceras semiannulatum* Howarth, bed 8, Elegans Subzone, Posidonienschiefere Formation. GZG.INV.70509: d = 49 mm, di = 39 mm, u = 26 mm, wh = 12 mm, wb = 13 mm, rb/2 = 30.

Posidonienschiefere Formation unconformably overlies the Hawskerense Subzone, with a stratigraphic gap comprising the Paltum- to midth of Semicelatum Subzone (Riegraf 1985a, b).

All other ammonite subzones from top of the Semicelatum to the Crassum Subzone are present in the bituminous and laminated sediments of the Ludwigskanal/Dörlbach area (Fig. 6), although minor sedimentary gaps below the ammonite subzone resolution may be developed. The laminated bituminous marls continue into the lower Variabilis Zone with non-bituminous intercalations, fucoid beds, and scattered re-occurrence of benthic fauna (*Grammatodon* sp.). The fish scale-rich beds in the Falciferum Zone and at the basis of the Bifrons Zone, however, may reflect considerable sedimentological condensation, while the Dactylioceras-Monotis bed itself is an exceptional event bed with an erosional basis, possibly formed by a tsunami (Arp and Gropengießer 2015).

Towards the basin margin (Regensburg area), bituminous shales of the Falciferum Zone are overlain by prograding sandstones containing *Dactylioceras commune* and *D. athlecticum* (Pompeckj 1901; Putzer 1939; Krumbeck 1932b), followed by a discontinuity comprising the Fibulatum and Crassum Subzones (Fig. 9). Note that the “Crassum Bed” in this area does not contain *Catacoeloceras crassum*, but the younger species *Catacoeloceras raquinianum*, and is an equivalent of the “Belemnite Battlefield” (see below). In the Posidonienschiefere of Swabian Alb a number of fish scale-rich beds (“Schlacken”) at top of Falciferum Zone (Riegraf et al. 1984; Riegraf 1985a) reflect a sedimentological condensation. Contrary to the Franconian Alb, bituminous sedimentation in the Swabian Posidonienschiefere ends with the Fibulatum Subzone.

Consequently, the sequence stratigraphic interpretation is as follows (Fig. 9): The transgression in the lower half of the Posidonienschiefere is documented by the successive onlap of subzones from SW to NE (Riegraf et al. 1984: p. 26, fig. 7; Riegraf 1985a: p. 55, fig. 27), delayed onset of sedimentation on the Altdorf High and basin margin (Regensburg area), and delayed benthos elimination on the Altdorf High. Minor sediment condensation (fish scale rich beds) at the Falciferum-Commune Subzone transition (bed 11; Fig. 6) may correspond to a maximum flooding surface, probably equivalent to fish-scale-rich in-

tercalations (“Schlacken”; Hauff 1921; Riegraf et al. 1984: p. 16 ff) in a similar lithostratigraphic position in the Swabian Posidonienschiefere (Fig. 7). Hence, higher Bifrons and Variabilis Subzone reflect regression with increasing siliciclastic influx, associated with pyrite preservation of ammonites (only Variabilis Subzone), and temporary re-oxygenation of the seafloor.

This interpretation is similar to the 3rd order T-R cycle previously proposed for the Swabian and Franconian Posidonienschiefere by Röhl and Schmid-Röhl (2005) (Fig. 9). The only addition to be made is, that the regressive system tract of the cycle extends into the lower Variabilis Zone. In N-Germany, this T-R cycle appears slightly shifted, with a maximum flooding surface already in top parts of the Tenucostatum Zone (mfs Toa 1), followed by regression and maximum regression surface in top parts of the Bifrons Zone (mrs Toa 1) (Zimmermann et al. 2015). A possible explanation for this minor shift is the higher subsidence as well as higher sediment supply in North-German Basin at that time.

Considerable differences exist with respect to the proposed 3rd order sequences in France. De Graciansky et al. (1998) suggest four 3rd order sequences for the Lower Toarcian, and a fifth sequence for the Fibulatum to Thouarsense Subzone. None of these T-R cycles appear recognizable in Germany, and may refer to minor superimposed changes (4th order sequences) only seen in areas of high sedimentation rate. Strikingly, there is also a continuous sedimentation from the higher Bifrons throughout the complete Variabilis Zone, in contrast to the erosive Intra-Variabilis-Discontinuity in S-Germany (Fig. 9).

(iii) Jurensismergel

Similar to the previous formation, the thickness of the Jurensismergel Formation is low (5 m). Ammonite zones and subzones are densely spaced and condensed at the phosphoritic and (slightly) bituminous basis of the formation (Fig. 6). Similar to the section Mistelgau (Schulbert 2001a, b), an increasing subzone thickness, decreasing carbonate content, and change from phosphoritic to pyritic ammonite preservation is observed towards the top of the formation (Fig. 7). A trend of increasing clay content is also recognizable from SW to NE, when compared to the increasingly

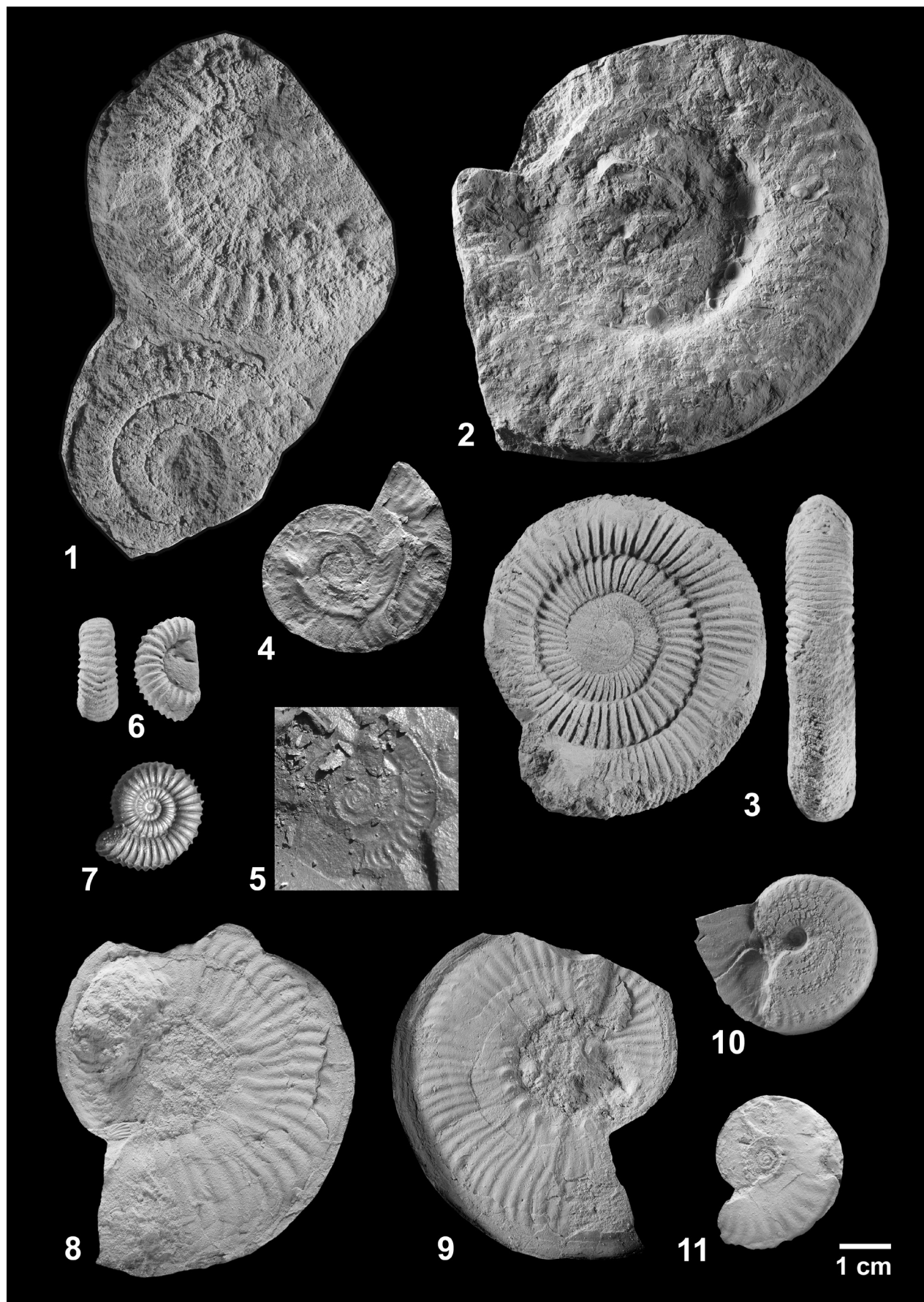


Figure 12. 1. *Dactylioceras cf. commune* (Sowerby), lower bedding plane of bed 12, Commune Subzone, Posidonienschiefer Formation. GZG.INV.70510a: d = 61 mm, di = 49 mm, u = 34 mm, wh = 14 mm, wb = n.a., rb/2 = (24); GZG.INV.70510b: d = 45 mm, di = 35 mm, u = 27 mm, wh = 10 mm, wb = n.a., rb/2 = (25). 2. *Hildoceras cf. lusitanicum* Meister, lower bedding plane of bed 12, Commune Subzone, Posidonienschiefer Formation. GZG.INV.70511: d = 92, di = (68 mm), u = 43 mm, wh = 26 mm, wb = (12 mm), rb/2 = (27). 3. *Dactylioceras athleticum* (Simpson), middle part of bed 12, Commune Subzone, Posidonienschiefer Formation. GZG.INV.70512: d = 64 mm, di = 51 mm, u = 38 mm, wh = 13.5 mm, wb = 13.5 mm, rb/2 = 37. 4. *Hildoceras semipolitum* Buckman, 18 cm below top of bed 15, Crassum Subzone, Posidonienschiefer Formation. GZG.INV.70513: d = 40 mm, di = 28 mm, u = 12 mm, wh = 16.5 mm, wb = n.a., rb/2 = (23). 5. *Hildoceras semipolitum* Buckman, 18 cm below top of bed 15, Crassum Subzone, Posidonienschiefer Formation. Field image: d = (30 mm), di = (23 mm), u = 11 mm, wh = 10 mm, wb = n.a., rb/2 = (24). 6. *Mucrodactylites mucronatus* (d'Orbigny), 43 cm below top of bed 16, Variabilis Subzone, Posidonienschiefer Formation. GZG.INV.70514: d = 20 mm, di = (15 mm), u = 9 mm, wh = 6.5 mm, wb = 8 mm, rb/2 = 17. 7. *Mucrodactylites mucronatus* (d'Orbigny), bed 16 ex situ, Variabilis Subzone, Posidonienschiefer Formation. leg. Volker Münzner: d = 22 mm, di = 16.5, u = 10 mm, wh = 6 mm, wb = 6 mm, rb/2 = 18. 8. *Haugia variabilis* (d'Orbigny), 13 cm below top of bed 16, Variabilis Subzone, Posidonienschiefer Formation. GZG.INV.45642: d = 67 mm, di = 44 mm, u = 20 mm, wh = 27 mm, wb = n.a., rb/2 = 27. 9. *Haugia jugosa* (Sowerby), 3 cm below top of bed 16, Variabilis Subzone, Posidonienschiefer Formation. GZG.INV.70515: d = 71 mm, di = 46 mm, u = 19 mm, wh = 30 mm, wb = n.a., rb/2 = 34. 10. *Pseudolioceras compactile* (Simpson), 37 cm below top of bed 16, Crassum Subzone, Posidonienschiefer Formation. GZG.INV.70516: d = 32 mm, di = 19 mm, u = 4.5 mm, wh = 17 mm, wb = 7 mm, rb/2 = 21. 11. *Pseudolioceras compactile* (Simpson), 32 cm below top of bed 16, Crassum Subzone, Posidonienschiefer Formation. GZG.INV.70517: d = 30 mm, di = 20 mm, u = 5 mm, wh = 15 mm, wb = n.a., rb/2 = 15.

carbonate-rich sections in the Swabian Alb (Fig. 7). This points to a general progradation of deltas in N-Germany at that time, affecting the Franconian realm, with the Swabian area more proximal to the warm Tethyan Ocean.

The erosive basis of the Jurensismergel Formation, forming a sequence boundary, has early been recognized in the Swabian Alb, with an apparent transgression beginning with the Variabilis Zone (Stier 1922; Fischer 1964: p. 99; Bruder 1968: p. 150; Riegraf 1985a: his fig. 18; Etzold et al. 1989: p. 44 f.). Indeed, a continuous sequence of ammonite subzones across the Posidonienschiefer-Jurensismergel boundary is only developed in the Wutach area SW of the Swabian Alb (Straub 1946: p. 56; Riegraf 1985a: p. 31). At the Ludwigskanal/Dörlbach, however, a continuous sedimentation across the Bifrons-Variabilis Zone boundary is evident, and a major stratigraphic gap appears developed at the “Belemnite Battlefield”, i.e. the top of the Variabilis Zone (Figs 6, 7). These contracting observations require a detailed look on the actual biostratigraphic evidence, i.e. ammonite records:

At the Ludwigskanal/Dörlbach, the Semipolitum Subzone is overlain by a Variabilis Subzone, characterized by abundant *Catacoeloceras raquinianum*, *Pseudolioceras compactile*, and *Mucrodactylites mucronatus* (Fig. 6). The Illustris Subzone follows after a thin, but evident fucoid bed, and grades in the “Belemnite Battlefield” containing reworked as well as autochthonous ammonite fossils of the higher Variabilis Zone (e.g., Urlichs 1971). On the other hand, the oldest ammonite assemblages of the channel-like occurrences of the Variabilis Zone in the Swabian Jurensismergel already comprise representatives of the Illustris (*Haugia illustris*, Holzheim-Ursenwang: Stolz 1911 in Straub 1946: p. 27; *Pseudogrammoceras doerntense*, Groß-Eislingen: Wiedemann 1966: p. 104) and Vitiosa Subzones (*Haugia vitiosa*, Jebenhausen: Urlichs 1977a; *Haugia cf. vitiosa*, Weilheim: Knitter and Riegraf 1984: p. 75, their fig. 4). These ammonites co-occur with *Haugia variabilis*

and *Haugia navis*, but – contrary to Ludwigskanal/Dörlbach – *Catacoeloceras*, *Pseudolioceras* and *Collina* are absent. The same applies to sections of the Freiburg area, with the Illustris and Vitiosa Subzone erosive on top of a partially eroded Posidonienschiefer (Ohmert 1976; Knitter and Ohmert 1983).

Therefore, we suggest that the erosive basis of the Jurensismergel Formation and sequence boundary lies within the Variabilis Zone, specifically at the basis of the Illustris Subzone (Figs 7, 9). While no Intra-Variabilis-Zone mrs (maximum regression surface) is seen in N-German sections (Zimmermann et al. 2015), an equivalent mrs and sequence boundary at the basis of the Illustris Subzone was identified in the Toarcian type area in western France (Galbrun et al. 1994: their fig. 5).

Consequently, the “Belemnite Battlefield” with its fossil accumulation and phosphorite nodules rather represents a transgressive sediment, and indeed grades in basin margin sections into a cephalopod-rich sandstone bed (“Crassum Bed” with *Dactylotheutis irregularis*, *Catacoeloceras raquinianum*, *Haugia* sp., *Mucrodactylites mucronatus* and *Pseudolioceras compactile*: Meyer and Baumberger 1998: p. 40–41, fig. 10; “nodule bed a” with *Catacoeloceras raquinianum*, *Mucrodactylites mucronatus*, *Hildoceras cf. bifrons*: Krumbeck 1943: p. 332). At Dörlbach and other sections of the Franconian Alb (e.g. Mistelgau, Fig. 7), the “Belemnite Battlefield” is overlain by the “Main Phosphorite Bed” and the bituminous “Toarcensis Shale” (Krumbeck 1943), with a time-equivalent calcareous sandstone bed in basin margin sections (“Grammoceras limestone”: Putzer 1939; “nodule bed b” with *Pseudogrammoceras aff. subquadratum*; “nodule bed c” with *G. thouarsense*, *P. cf. saemanni*, *P. fallaciosum*: Krumbeck 1943: p. 332). These cephalopod-rich beds indicate flooding and highstand conditions at the basin margin.

In the Swabian Alb, submarine “swells” (i.e., remaining topographic highs after erosion within Variabilis Zone;

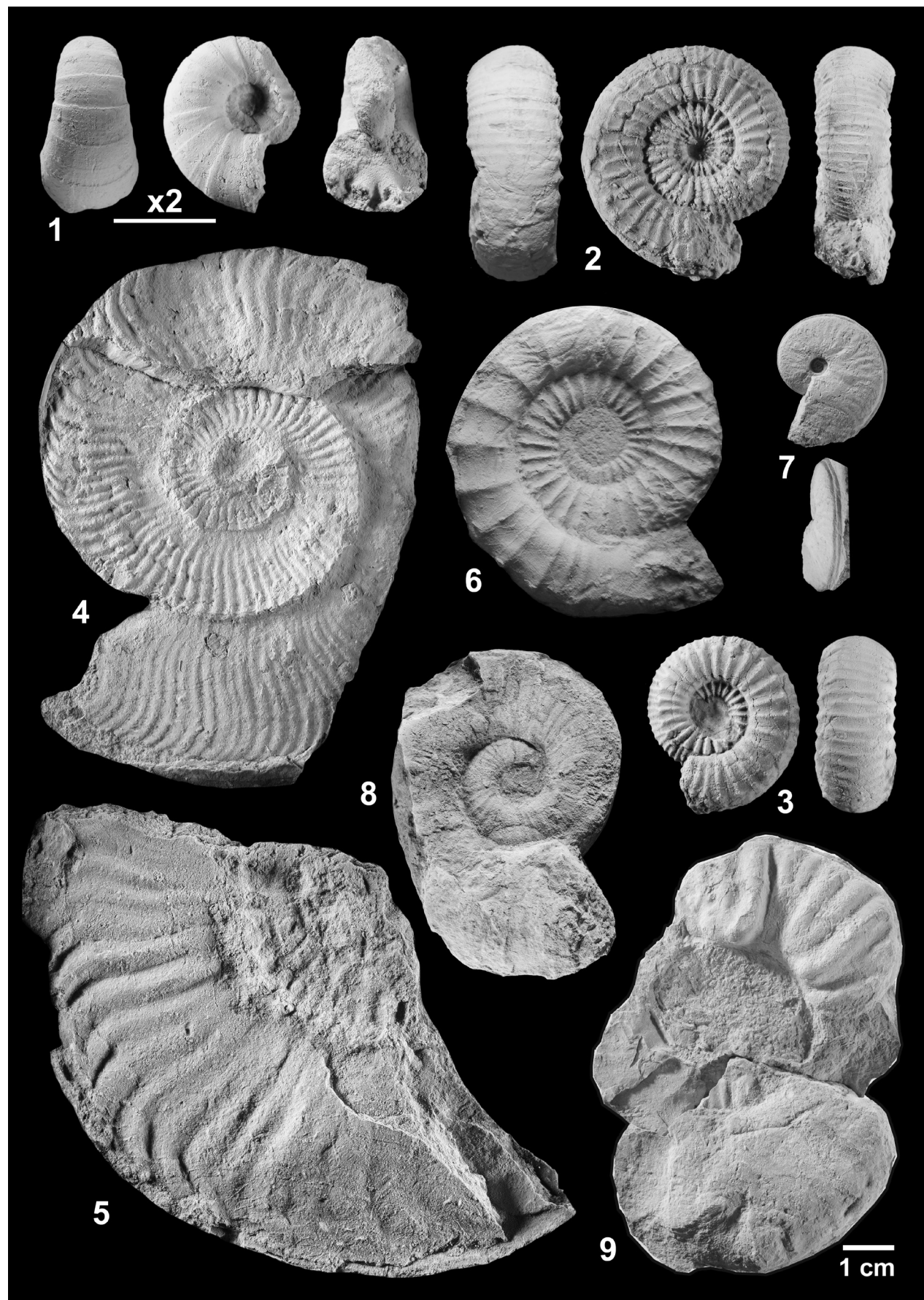


Figure 13. 1. *Lytoceras sublineatum* (Oppel), 38 cm below top of bed 16, Variabilis Subzone, Posidonienschifer Formation. The telescope-like, shallow constrictions in this juvenile specimen are reminiscent of *Pleurolytoceras propehircinum* Krumbeck of the Aalensis Subzone, but the high wb/wh ratio points to *Lytoceras sublineatum* (Oppel). GZG.INV.70518: d = 17 mm, di = 10.5 mm, u = 5 mm, wh = 7.5 mm, wb = 10 mm, rb/2 = 10. 2. *Catacoeloceras raquinianum* (d'Orbigny), 19 cm below top of bed 16, Variabilis Subzone, Posidonienschifer Formation. GZG.INV.70519: d = 45 mm, di = 35 mm, u = 21 mm, wh = 12.5 mm, wb = 16 mm, rb/2 = 18. 3. *Catacoeloceras raquinianum* (d'Orbigny), 13 cm below top of bed 16, Variabilis Subzone, Posidonienschifer Formation. GZG.INV.70520: d = 35 mm, di = 26 mm, u = 14 mm, wh = 11.5 mm, wb = 15 mm, rb/2 = 13. 4. *Pseudogrammoceras subregale* (Pinna), 4 cm below top of bed 18, Illustris Subzone, Jurensismergel Formation. GZG.INV.70521; d = 107 mm, di = 77 mm, u = 46 mm, wh = 34 mm, wb = n.a., rb/2 = (48). 5. *Haugia* cf. *phillipsi* (Simpson), 3 cm below top of bed 18, Illustris Subzone, Jurensismergel Formation. GZG.INV.70522; d = (125 mm), di = n.a., u = n.a., wh = 46 mm, wb = n.a., rb/2 = (22). 6. *Catacoeloceras raquinianum* (d'Orbigny), basis of bed 19, Variabilis Subzone, Posidonienschifer Formation. GZG.INV.70523: d = 62 mm, di = 49 mm, u = 31 mm, wh = 15 mm, wb = (16 mm), rb/2 = 13. 7. *Osperleioceras bicarinatum* (Zieten), phosphorite nodule in bed 20, condensed transition Variabilis-Thouarsense Zone, Jurensismergel Formation. GZG.INV.70524: d = 25 mm, di = 15 mm, u = 3.5 mm, wh = 14 mm, wb = 6 mm, rb/2 = (18). 8. *Lytoceras cornucopia* (Young & Bird), marl matrix of bed 20, condensed transition Variabilis-Thouarsense Zone, Jurensismergel Formation. GZG.INV.70525: d = 66 mm, di = 46 mm, u = 23 mm, wh = 27 mm, wb = (28 mm), rb/2 = n.a. 9. *Denckmannia rude* (Simpson), phosphorite nodule in bed 20, condensed transition Variabilis-Thouarsense Zone, Jurensismergel Formation. GZG.INV.70526: d = 86 mm, di = 58 mm, u = 32 mm, wh = 32 mm, wb = (26 mm), rb/2 = n.a.

Stier 1922; Etzold et al. 1989), show aphotic microbialites in the Toarcensis Zone (e.g., Aalen-Weidenfeld: Dietl and Etzold 1977; Keupp and Arp 1990; Ohmden: Arp and Heyng 2013), indicating highly reduced sedimentation (Keupp and Arp 1990). These condensed deposits may represent a maximum flooding, while the Fallaciosum Subzone shows a very discontinuous distribution of sediments, in the Swabian as well as in the Franconian Alb. High sealevel, however is still indicated by the sporadic occurrence of *P. fallaciosum* at the basin margin ("nodule bed c", see above).

A clear and significant discontinuity is developed at the basis of the Dispansum Zone in the Franconian Alb. This erosive sequence boundary, commonly associated with a belemnite accumulation and aphotic microbialites (Dörlbach, Mistelgau: Fig. 7) is also recognizable in the Swabian Alb (Bad Boll: Wiedemann 1966: p. 91, Taf. 9; Bruder 1968: p. 15f.; middle part of bed 22 Rainau-Weiler, and KB4 Reutehau: Etzold et al. 1989). In N-Germany, the basis of the Dispansum Zone is a significant erosive surface (Heidorn 1928; Hoffmann 1968a: p. 465: "Zeta-Konglomerat") and coincides with the mrs Toa 2 proposed by Zimmermann et al. (2015). Likewise, the Fallaciosum-Insigne Subzone boundary represents a mrs and sequence boundary in SW-France (Cubaynes et al. 1984: their fig. 18). The widespread erosion of the Fallaciosum Subzone in the Franconian Alb explains the scarcity of *Lytoceras jureense* findings in this area, as this species is most common in this subzone.

Subsequently, condensation and phosphorites characterize the transgressive sediments of the Dispansum Zone at the Ludwigskanal/Dörlbach and elsewhere in the Franconian Alb, while in the following Pseudoradiosa Subzone with several beds of compressed *Dumortieria* accumulations may reflect further deepening. A flooding at the basin margin area might be indicated by findings of Pompeckj (1901: p. 143), who noted the occurrence of *Phlyseogrammoceras* cf. *dispansum*, *Hammatoceras insignis* and *Dumortieria dumortieri* (syn.: *D. insignisimilis*) from the Regensburg area.

The condensed bed 25 (i.e., basis of Mactra Subzone; Fig. 7) at Dörlbach, with abundant ammonites, belemnites and phosphorite, may correspond to maximum flooding. The same horizon has also been described from Mistelgau (Dumortieria bed I: Schulbert 2001a) and Rainau-Weiler (Etzold et al. 1989: p. 49, their bed 16 with abundant phosphoritic *Dumortieria* and belemnites) (Fig. 6). By contrast, Galbrun et al. (1994: their fig. 5) infer a possible mrs and sequence boundary at the Pseudoradiosa/Aalensis Zone boundary from sections in western France.

Finally, the increasingly thick marls with pyritic ammonites of the Aalensis Subzone could reflect the regressive system tract of this 3rd order cycle, with increasing clay supply from N. Indeed, at the basin margin (Regensburg area) quartz-pebble and feldspar-containing calcareous sandstones document this regressive interval (Putzer 1939: p. 93, 107) (Fig. 9). Consistent with this interpretation, the sedimentary succession in Quercy/France appears regressive for the Mactra to Aalensis Subzone, followed by a discontinuity and sequence boundary (Lezin et al. 1997).

(iv) Opalinuston

While basal parts of this formation, i.e., the Torulosum Subzone, still show a low thickness, discontinuities, phosphorite, and some carbonate, major parts are composed of a thick monotonous series of claystones. Discontinuities within the formation and lateral facies trends are poorly documented. However, the sections Grossenbuch (middle Franconian Alb) and Wittelshofen (southern Franconian Alb) described by Krumbeck (1943) demonstrate that the Aalensis-Torulosum Subzone boundary is associated with erosion, locally removing the complete Aalensis Subzone.

Therefore, the belemnite accumulation (bed 31) at the Aalensis-Torulosum Subzone boundary of the Ludwigskanal/Dörlbach section (Fig. 6), although unspectacular at first glance, can be interpreted as a mrs and sequence

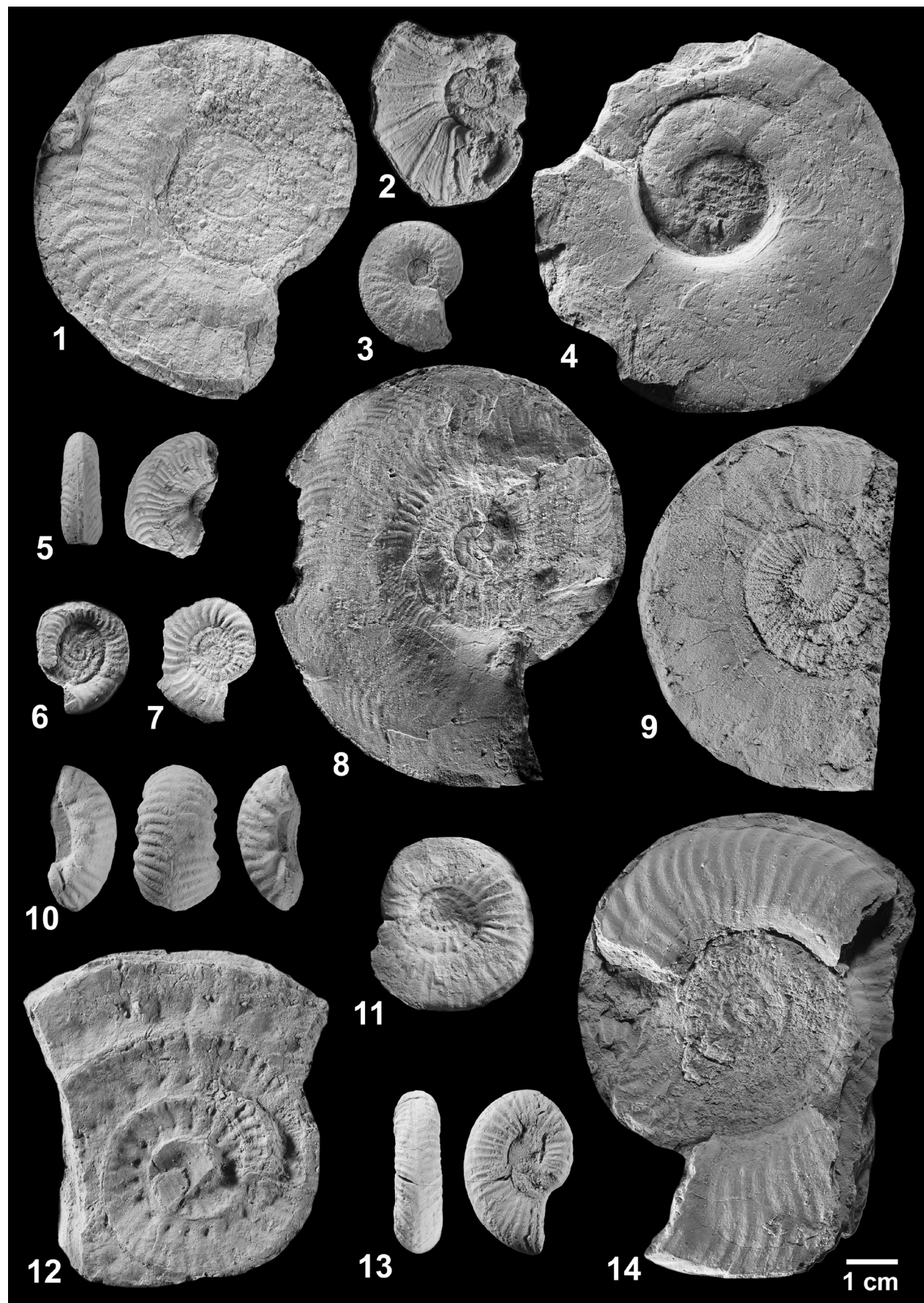


Figure 14. 1. *Grammoceras thouarsense* (d'Orbigny), 10 cm below top of bed 21, Thouarsense Subzone, Jurensismergel Formation. GZG. INV.70527: d = 72 mm, di = 50 mm, u = 25 mm, wh = 27 mm, wb = n.a., rb/2 = (25). 2. *Alocolytoceras rugiferum* (Pompeckj), 20–25 cm below top of bed 23, Dispansum Subzone, Jurensismergel Formation. GZG. INV.70528: d = (39 mm), di = (27 mm), u = 12 mm, wh = 16 mm, wb = n.a., rb/2 = (42). 3. *Pseudolioceras cf. boulbiense* (Young and Bird), 12–20 cm below top of bed 23, Dispansum Subzone, Jurensismergel Formation. GZG. INV.70529: d = 26 mm, di = 17 mm, u = 5.5 mm, wh = 13 mm, wb = n.a., rb/2 = 13. 4. *Alocolytoceras rugiferum* (Pompeckj), 20–25 cm below top of bed 23, Dispansum Subzone, Jurensismergel Formation. GZG. INV.70530: d = 76 mm, di = 56 mm, u = 21 mm, wh = 31 mm, wb = n.a., rb/2 = n.a. 5. *Phlyseogrammoceras dispansum* (Lycett), 12–20 cm below top of bed 23, Dispansum Subzone, Jurensismergel Formation. GZG. INV.70531: d = (30 mm), di = n.a., u = (9 mm), wh = 12 mm, wb = 9 mm, rb/2 = n.a. 6. *Dumortieria insignisimilis* (Brauns), 11 cm below top of bed 23, basis of Levesquei Subzone, Jurensismergel Formation. GZG. INV.70532: d = 22 mm, di = 17 mm, u = 12 mm, wh = 6 mm, wb = n.a., rb/2 = 20. 7. *Dumortieria insignisimilis* (Brauns), 11 cm below top of bed 23, basis of Levesquei Subzone, Jurensismergel Formation. GZG. INV.70533: d = 25 mm, di = 17 mm, u = 10.5 mm, wh = 8.5 mm, wb = n.a., rb/2 = 18. 8. *Phlyseogrammoceras dispansum* (Lycett), 20–25 cm below top of bed 23, Dispansum Subzone, Jurensismergel Formation. GZG. INV.70534: d = 83 mm, di = 61 mm, u = 27 mm, wh = 31 mm, wb = n.a., rb/2 = (45). 9. *Dumortieria radiosua* (Seebach), 75 cm below top of bed 24, Pseudoradiosa Subzone, Jurensismergel Formation. GZG. INV.70535: d = 73 mm, di = (54 mm), u = 30 mm, wh = 23 mm, wb = n.a., rb/2 = n.a. 10. *Hammatoeceras insigne* (Schübeler in Zieten), 15 cm below top of bed 23, Dispansum Subzone, Jurensismergel Formation. GZG. INV.70536: d = (56 mm), di = (42 mm), u = 26 mm, wh = (16 mm), wb = n.a., rb/2 = (28). 11. *Dumortieria levesquei* (d'Orbigny), 6 cm below top of bed 23, Levesquei Subzone, Jurensismergel Formation. GZG. INV.70537a: d = 34 mm, di = 24 mm, u = 13 mm, wh = 12 mm, wb = n.a., rb/2 = 18. 12. *Hammatoeceras insigne* (Schübeler in Zieten), 15 cm below top of bed 23, Dispansum Subzone, Jurensismergel Formation. GZG. INV.70538: d = 29 mm, di = (22 mm), u = (10 mm), wh = 10 mm, wb = 17 mm, rb/2 = (16). 13. *Dumortieria levesquei* (d'Orbigny), 9 cm below top of bed 23, Levesquei Subzone, Jurensismergel Formation. GZG. INV.70539: d = 32 mm, di = (23 mm), u = (13 mm), wh = 11 mm, wb = 10 mm, rb/2 = 21. 14. *Dumortieria pseudoradiosa* (Branco), 4 cm below top of bed 23, Levesquei Subzone, Jurensismergel Formation. GZG. INV.70537c: d = 92 mm, di = 70 mm, u = 41 mm, wh = 28 mm, wb = n.a., rb/2 = 32.

boundary (Fig. 7). Indeed, time-equivalent discontinuities have been described from N-Germany (e.g., Schlewecke, Dörnten: Ernst 1923; Heidorn 1928) and Quercy (Lezin et al. 1997). At the latter region, the discontinuity is associated with a lack of the *Pseudolotharingicum* (syn.: *Lugdunensis*) Horizon (Lezin et al. 1997), which also has not yet been detected in the Franconian Alb.

In the Ludwigskanal/Dörlbach section (Figs 6, 7), marls of bed 32 could reflect a subsequent sealevel rise, with condensed sediments, phosphorites, and the fossil accumulation in bed 33 representing a mfs, possibly equivalent to mfs Aal 1 in N-Germany (Zimmermann et al. 2015).

The monotonous and about 50 m thick claystone succession of the Opalinum Subzone, with only the lowermost 0.5 m exposed in the Ludwigskanal/Dörlbach section, reflects a progradation of siliciclastic influx from North, finally leading to shallow water conditions during deposition of the Upper Aalenian Eisensandstein Formation.

Conclusions

- The 16 m thick Ludwigskanal/Dörlbach section exposed upper parts of the Schwarjura Group, from top parts of the Amaltheenton (>9 m), through the Posidonienschifer (1.8–1.9 m) and Jurensismergel (3.5 m) to basal parts of the Opalinuston (>1.3 m). All formation boundaries are erosional discontinuities. Carbonate contents are low in the Amaltheenton, high in lower and middle parts of the Posidonienschifer, followed by a successive decline to basal parts of the Opalinuston, with a last calcareous marl bed near the top of the Jurensismergel. The Posidonienschifer shows increased

organic carbon contents, which are, nonetheless, significantly lower than in other N- and SW-German sections due to the “dilution effect” by high carbonate contents. However, normalized to the sediment silicate fraction, organic carbon contents show a clear first maximum in the Exaratum Subzone and high values in the Falciferum and Bifrons Zone, similar to SW-German reference sections. Highly fluctuating values characterize the Variabilis and Thouarsense Zone, while low organic carbon contents were found in the Dispansum and younger zones, with one single spike at the basis of the Aalensis Zone (Mactra Subzone).

- Despite of the low thickness of the formations and a number of sedimentological gaps and condensation, all ammonite zones and subzones from the top of the Pliensbachian to the top of the Toarcian are present, with the following exceptions: Paltum and Clevelandicum (sedimentary gap), Vitiosa and Bingmanni (probably present, but no definite ammonite proof), and Fallaciosum Subzone (sedimentary gap). The erosive basis of the Torulosum Subzone may explain the lack of evidence for the *Pseudolotharingicum* (syn.: *Lugdunensis*) Horizon at the top of the Aalensis Subzone. The basis of the Aalenian is drawn in analogy to a neighbouring drill section that yielded *Leioceras opalinum*. Three subzones and horizons were detected for the first time in the investigated area: The Semipolitum Horizon, the Illustris Subzone, and the Dumortieri Horizon. The standard zone index ammonite *Harporoceras falciferum*, previously mentioned only by Urlich (1971: p. 69), is figured for the first time for the Franconian Alb.

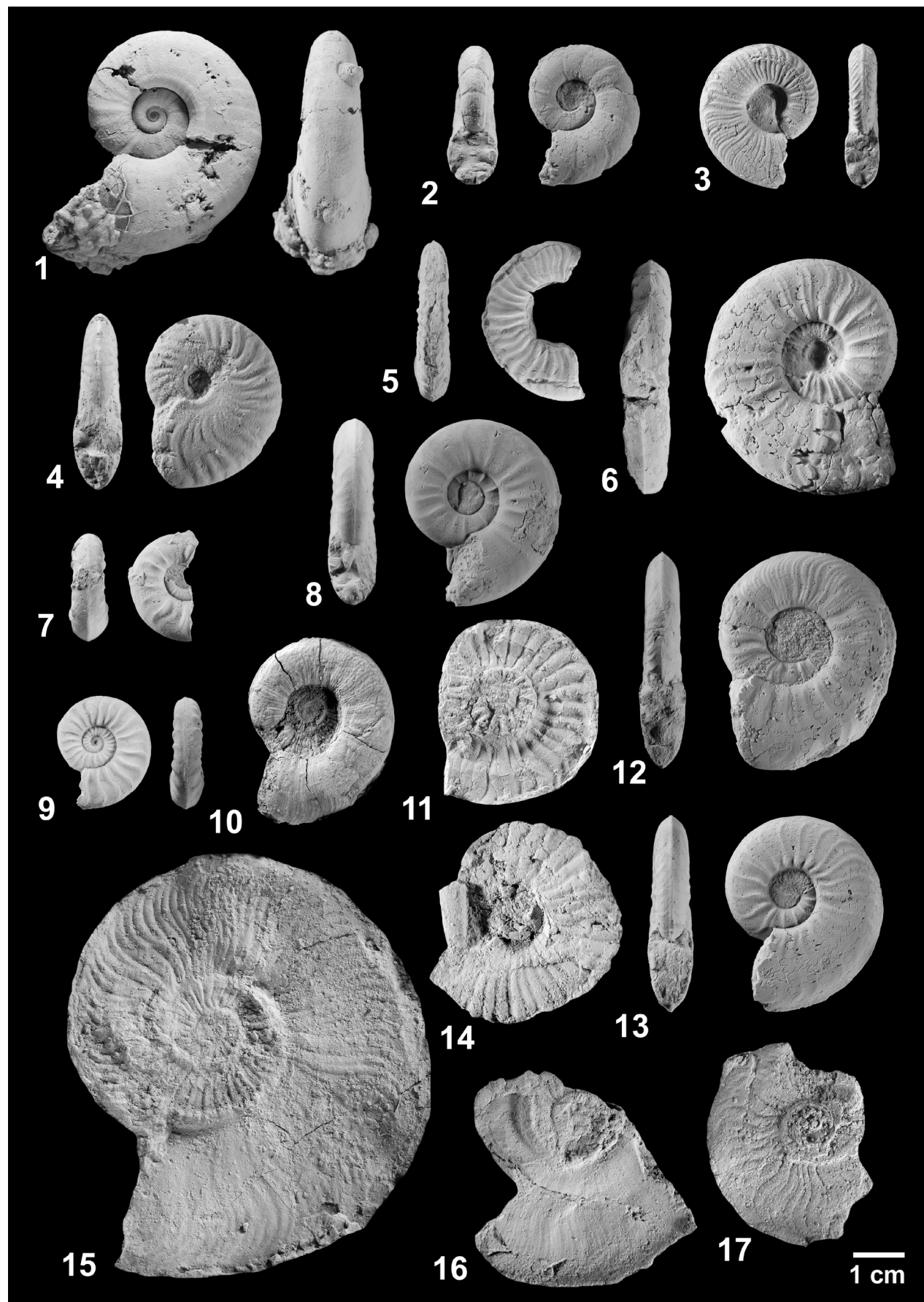


Figure 15. 1. *Pleurolytoceras wrighti* (Buckman), bed 27, Aalensis Subzone, Jurensismergel Formation. This species has previously been assigned to *Pachylytoceras* Buckman 1905, which is a junior subjective synonym of *Pleurolytoceras* Hyatt 1900 (Hoffmann 2010, 2015). GZG.INV.70540: d = 44 mm, di = 27 mm, u = 14 mm, wh = 19 mm, wb = 15.5 mm, rb/2 = 19. 2. *Pleurolytoceras hircinum* (Schlotheim), bed 27, Aalensis Subzone, Jurensismergel Formation. GZG.INV.70541: d = 27 mm, di = 18 mm, u = 10 mm, wh = 10.5 mm, wb = 10 mm, constr/2 = 6. 3. *Cotteswoldia mactra* (Dumontier), bed 25, Mactra Subzone, Jurensismergel Formation. GZG.INV.70542: d = 29 mm, di = 20 mm, u = 10 mm, wh = 11 mm, wb = 7 mm, rb/2 = 35. 4. *Pseudolioceras beyrichi* (Schloenbach), 1 cm below top of bed 28, Aalensis Subzone, Jurensismergel Formation. GZG.INV.45644: d = 34 mm, di = 21 mm, u = 6 mm, wh = 17.5 mm, wb = 10 mm, rb/2 = 15; (leg. Sebastian Demmel). 5. *Paradumortieria cf. tectiforme* Elmi and Caloo-Fortier, 45 cm below top of bed 24, Pseudoradiosa Subzone, Jurensismergel Formation. GZG.INV.70543: d = 32 mm, di = 23 mm, u = 13 mm, wh = 11 mm, wb = 7.5 mm; rb/2 = 20. 6. *Cotteswoldia aalensis* (Zieten), bed 27, Aalensis Subzone, Jurensismergel Formation. GZG.INV.70544: d = 46 mm, di = 31 mm, u = 16 mm, wh = 18 mm, wb = 9.5 mm, rb/2 = 19. 7. *Dumortieria externicostata* (Branco), 30 cm below top of bed 26, Aalensis Subzone, Jurensismergel Formation. GZG.INV.70545: d = 21 mm, di = 14 mm, u = 7.5 mm, wh = 8 mm, wb = 8 mm, rb/2 = 10. 8. *Dumortieria costula* (Reinecke), 30 cm below top of bed 26, Aalensis Subzone, Jurensismergel Formation. GZG.INV.70546: d = 36 mm, di = 26 mm, u = 12 mm, wh = 14 mm, wb = 9.5 mm, rb/2 = 11. 9. *Pleydellia distans* (Buckman), bed 27, Aalensis Subzone, Jurensismergel Formation. GZG.INV.70547: d = 22 mm, di = 15 mm, u = 8 mm, wh = 8 mm, wb = 6.5 mm, rb/2 = 11. 10. *Dumortieria moorei* (Lycett), 40 cm below top of bed 24, Pseudoradiosa Subzone, Jurensismergel Formation. GZG.INV.70548: d = 38 mm, di = 27 mm, u = 15 mm, wh = 13 mm, wb = (7 mm), rb/2 = 62. 11. *Dumortieria cf. kochi* Benecke, 40 cm below top of bed 24, Pseudoradiosa Subzone, Jurensismergel Formation. GZG.INV.70549: d = 37 mm, di = (27 mm), u = 14 mm, wh = 13 mm, wb = n.a., rb/2 = 17. 12. *Pleydellia subcompta* (Branco), 35 cm below top of bed 26, basis of Aalensis Subzone, Jurensismergel Formation. GZG.INV.70550: d = 44 mm, di = 29 mm, u = 16 mm, wh = 17 mm, wb = 9 mm, rb/2 = 30. 13. *Pleydellia costulata* (Zieten), 1 cm below bed 28, Aalensis Subzone, Jurensismergel Formation. GZG.INV.70551: d = 39 mm, di = 26 mm, u = 11.5 mm, wh = 16.5 mm, wb = 9 mm, rb/2 = 12. 14. *Pleurolytoceras torulosum* (Schübler in Zieten), bed 33, Torulosum Subzone, Opalinuston Formation. This species has previously been assigned to *Pachylytoceras* Buckman 1905, which is a junior subjective synonym of *Pleurolytoceras* Hyatt 1900 (Hoffmann 2010, 2015). GZG.INV.70552a: d = 40 mm, di = (29 mm), u = 12 mm, wh = 16 mm, wb = n.a., cstr/2 = 20. 15. *Cotteswoldia lotharingica* (Branco), bed 33, Torulosum Subzone, Opalinuston Formation. GZG.INV.70553: d = 84 mm; di = 60 mm, u = 32 mm, wh = 28 mm, wb = n.a., rb/2 = (48). 16. *Pleydellia buckmani* Maubeuge, bed 33, Torulosum Subzone, Opalinuston Formation. GZG.INV.70554: d = (55 mm), di = n.a., u = 18 mm, wh = 26 mm, wb = n.a., rb/2 = n.a. 17. *Pleydellia cf. falcifer* Maubeuge, bed 33, Torulosum Subzone, Opalinuston Formation. GZG.INV.70552b: d = 40 mm, di = (27 mm), u = 12 mm, wh = 17 mm, wb = n.a., rb/2 = 20.

- The sequence stratigraphic standard Boreal 2nd order cycle (de Graciansky et al. 1998), with a transgression during the Lower Toarcian, maximum flooding at the basis of the Bifrons Zone, and a regressive succession in the remaining Toarcian to Aalenian, is clearly developed in Southern Germany. Superimposed to that, three 3rd order T-R cycles are recognized at the Ludwigskanal/Dörlbach and adjacent sections, with a maximum regression near the basis of the Toarcian (i.e., within the lower Tenuicostatum Zon of Swabian Alb), within the Variabilis Zone (i.e., at the basis of the Illustris Subzone), at the basis of the Dispansum Zone, and less prominent at the basis of the Torulosum Zone. In turn, maximum flooding surfaces are developed at the basis of the Commune Subzone, basis of the Thouarsense Subzone, basis of Mactra Subzone, and basis of Opalinum Zone. While transgressive sediments of the Franconian Toarcian commonly show phosphorites (similar to other epicontinental marine deposits: Loutit et al. 1988; Glenn et al. 1994: p. 767; Glenn and Garrison 2003: p. 524), regressive sediments frequently show pyrite preservation of fossils, especially ammonites. The extraordinary “Belemnite Battlefield” near the basis of the Jurensismergel is considered as transgressive sediment, consistent with the previous formation model by Urlichs (1971) of winnowing by a coast-parallel seawater current.
- The litho-, bio-, and sequence stratigraphic framework of the Ludwigskanal section may serve as a basis for further isotope and biogeochemical studies on the Toarcian Oceanic Anoxic Event, and its recovery phase, in this seawater current-affected part of the NW-European Epicontinental Seaway.

Acknowledgements

We are grateful for the permission by the water management office Nürnberg, Rainer Ketterle, to investigate and sample at the construction site of the Ludwigskanal cutting. Thin sections were prepared by Axel Hackmann, geochemical analyses were performed with the help of Birgit Röhrling and Wolfgang Dröse, and fieldwork was supported by Christian Strobl, Barbara Seuß, and Georg Maier. We thank Matthias Weissmüller, Arno Garbe, Martin Görlich, Sebastian Demmel, Volker Münzner, and Gernot Smolle for their generous donation of ammonites. Difficult ammonite preparations were preformed by Klaus Weiß and Stephan Seppelt. Photographs of the ammonites were taken by Max Hundertmark. Günter Schweigert and Ingmar Werneburg are gratefully acknowledged for access to original ammonite specimens hosted at the Stuttgart State Museum of Natural History and the Paleontological Collection of the University of Tübingen IGPT, respectively. We thank the engineering office Dr. Ing. Johann Spotka for the report on the landfill exploratory drilling Dörlbach

D2. The manuscript significantly benefited from discussions with René Hoffmann. Charlotte Kniest helped with the acquisition of rare papers. We thank Eckhard Mönnig and Matthias Franz (Göttingen) for their constructive and helpful reviews of the manuscript.

References

- Arp G (1989) Neue Profile des Unteren Toarciums aus dem Alt-dorf-Neumarkter Raum. *Geologische Blätter für Nordost-Bayern* 39: 99–116.
- Arp G (2010) Ammonitenfauna und Stratigraphie des Grenzbereichs Jurensismergel/Opalinuston-Formation bei Neumarkt i.d. Opf. (oberstes Toarcium, Fränkische Alb). *Zitteliana A* 50: 25–54.
- Arp G, Heyng AM (2013) Jurassic Fossil Lagerstätten of Southern Germany. In: Reitner J, Reich M (Eds) *Palaeobiology and Geobiology of Fossil Lagerstätten through Earth History. A Joint Conference of the "Paläontologische Gesellschaft" and the "Palaeontological Society of China"*, Göttingen. Field Guide to Excursions, Göttingen, 1–16.
- Arp G, Gropengießer S (2016) The Monotis-Dactylioceras Bed in the Posidonienschiefer Formation (Toarcian, southern Germany): condensed section, tempestite, or tsunami-generated deposit? *Paläontologische Zeitschrift* 90: 271–286. <https://doi.org/10.1007/s12542-015-0271-7>
- Arp G, Seppelt S (2012) The bipolar bivalve *Oxytoma (Palmoxytoma) cygnipes* (Young and Bird, 1822) in the Upper Pliensbachian of Germany. *Paläontologische Zeitschrift* 86: 43–57. <https://doi.org/10.1007/s12542-011-0113-1>
- Arp G, Aiglstorfer M, Havlik P, Krause T, Schulbert C, Seppelt S (2014) New exposure of the Ludwigskanal section near Dörlbach – a key section for the Lower Jurassic in the Franconian Alb, Southern Germany. *Zeitschrift der Deutschen Gesellschaft für Geowissenschaften* 165: 163–177. <https://doi.org/10.1127/1860-1804/2014/0054>
- Bandel K, Knitter H (1983) Litho- und biofazielle Untersuchung eines Posidonienschieferprofils in Oberfranken. *Geologische Blätter für Nordost-Bayern* 32: 95–129.
- Bauberger W, Cramer P, Tillmann H (1969) Erläuterungen zur Geologischen Karte von Bayern 1:25000, Blatt Nr. 6938 Regensburg [mit Beiträgen von Bader, K., Berger, K., Buchner, A., Claus, G., Hauner, U., Stroh, A. und Wittmann, O.]. Bayerisches Geologisches Landesamt, München, 414 pp. [+ 1 map]
- Becaud M, Rulleau L, Elmi S (2005) The ammonite fauna renewal at the boundary middle-late Toarcian: new data and consequences. *Bulletin de la Société Géologique de France* 176(1): 23–35. <https://doi.org/10.2113/176.1.23>
- Beyschlag (1841) Über die geognostische Stellung der Gebirgsschichten, welche beim Bau des Ludwigskanales aufgedeckt oder durchschnitten wurden. Amtlicher Bericht über die 18. Versammlung der Naturforscher und Ärzte zu Erlangen im September 1840: 101–108.
- Bloos G, Dietl G, Schweigert G (2005) Der Jura Süddeutschlands in der Stratigraphischen Tabelle von Deutschland 2002. *Newsletters on Stratigraphy* 41: 263–277. <https://doi.org/10.1127/0078-0421/2005/0041-0263>
- Böhme F, Brachert TC (1993) Deepwater Stromatolites and *Frutexites* Maslov from the Early and Middle Jurassic of S-Germany and Austria. *Facies* 28: 145–168. <https://doi.org/10.1007/BF02539734>
- Boulila S, Galbrun B, Huret E, Hinnov LA, Rouget I, Gardin S, Bartolini A (2014) Astronomical calibration of the Toarcian Stage: implications for sequence stratigraphy and duration of the early Toarcian OAE. *Earth and Planetary Science Letters* 386: 98–111. <https://doi.org/10.1016/j.epsl.2013.10.047>
- Brachmann H (1991) Die Ammonitenfauna der "Dörntener Schichten" (Ober-Toarcium) von der Typikalität bei Dörnten (N Harzvorland). *Arbeitskreis Paläontologie Hannover* 19(3/4): 88–115.
- Brockert M (1959) Zur Ammonitenfauna und Stratigraphie des Lias zeta in Baden-Württemberg. Dissertation Eberhard Karls Universität, Tübingen, 155 pp.
- Bruder HJ (1968) Ökologische, geochemische und sedimentologische Untersuchungen im Lias zeta (Oberes Toarcium) Schwabens, mit Berücksichtigung des obersten Lias epsilon. Arbeiten aus dem Geologisch-Paläontologischen Institut der Technischen Hochschule Stuttgart, Neue Folge 56: 1–65.
- Buckman SS (1919–1921) Type Ammonites III. Wheldon and Wesley, London, 64 pp. [+ pls 131–266b]
- Catuneanu O, Galloway WE, Kendall CGSC, Miall AD, Posamentier HW, Strasser A, Tucker ME (2011) Sequence stratigraphy: Methodology and Nomenclature. *Newsletters on Stratigraphy* 44: 173–245. <https://doi.org/10.1127/0078-0421/2011/0011>
- Cresta S, Goy A, Ureta S, Arias C, Barrón E, Bernad J, Canales ML, García-Joral F, García-Romero E, Gialanella PR, Gómez JJ, González JA, Herrero C, Martínez G, Osete ML, Perilli N, Villalaín JJ (2001) The Global Boundary Stratotype Section and Point (GSSP) of the Toarcian-Aalenian Boundary (Lower-Middle Jurassic). *Episodes* 24: 166–175. <https://doi.org/10.18814/epiiugs/2001/v24i3/003>
- Cubaynes R, Boutet C, Delfaud J, Faure P (1984) La megasequence d'ouverture du Lias quercynois (Bordure sud-ouest du Massif Central français). *Bull. Centres Rech. Explor.-Prod Elf-Aquitaine* 8(2): 333–370.
- de Graciansky PC, Dardeau G, Dommergues JL, Durlet C, Marchand D, Dumont T, Hesselbo SP, Jacquin T, Goggin V, Meister C, Mouterde R, Rey J, Vail PR (1998) Ammonite biostratigraphic correlation and Early Jurassic sequence stratigraphy in France: comparisons with some U.K. sections. In: de Graciansky PC, Hardenbol J, Jacquin T, Vail PR (Eds) *Mesozoic and Cenozoic Sequence Stratigraphy of European Basins*, SEPM, Tulsa, 583–622. <https://doi.org/10.2110/pec.98.02.0583>
- Dean WT, Donovan DT, Howarth MK (1961) The Liassic ammonite zones and subzones of the north-west European Province. *Bulletin of the British Museum (Natural History) Geology Series* 4: 435–505.
- Di Cencio A, Weis R (2020) Revision of upper Toarcian ammonites (Lytoceratidae, Graphoceratidae and Hammatoceratidae) from the Minette ironstones, southern Luxembourg. *Ferrantia* 83: 5–103.
- Dietl G, Etzold A (1977) The Aalenian at the type locality. *Stuttgarter Beiträge zur Naturkunde B* 30: 1–13.
- Elmi S, Gabilly J, Mouterde R, Rulleau L, Rocha RB (1994) L'étage Toarcien de l'Europe et de la Téthys; divisions et corrélations. *Geobios Mémoire Spécial* 17: 149–159. [https://doi.org/10.1016/S0016-6995\(94\)80135-5](https://doi.org/10.1016/S0016-6995(94)80135-5)

- Elmi S, Rulleau L, Gabilly J, Mouterde R (1997) Toarcien. In: Cariou E, Hantzpergue P (Coord.) Biostratigraphie du Jurassique ouest-européen et méditerranéen. Bulletin du Centre de Recherches Elf Exploration et Production, Mémoire 17: 25–36.
- Embry AF, Johannessen EP (1992) T-R sequence stratigraphy, facies analysis and reservoir distribution in the uppermost Triassic-Lower Jurassic succession, western Sverdrup Basin, Arctic Canada. In: Vorren TO, Bergsager E, Dahl-Stamnes OA, Holter E, Johannessen B, Lie E, Lund TB (Eds) Arctic Geology and Petroleum Potential, vol. 2 (Special Publication). Norwegian Petroleum Society (NPF), 121–146. <https://doi.org/10.1016/B978-0-444-88943-0.50013-7>
- Ernst W (1923–1924) Zur Stratigraphie und Fauna des Lias Zeta im nordwestlichen Deutschland. Palaeontographica 65(1923): 1–96, plates 1–6; 66(1924): 97–222, plates 7–14.
- Etzold A, Ohmert W, Balle T (1989) Toarcium und unterstes Aalenium im Gebiet der oberen Jagst nordöstlich Aalen. Jahreshefte des geologischen Landesamtes Baden-Württemberg 31: 23–68.
- Fischer W (1964) Die *jurensis*-Schichten (Oberes Toarcien) im Vorland der Schwäbischen Alb. Neues Jahrbuch für Geologie und Paläontologie, Abhandlungen 120: 81–106.
- Freudenberger W, Schwerd K [Eds] (1996) Erläuterungen zur Geologischen Karte von Bayern 1 : 500 000. 4th edn. Bayerisches Geologisches Landesamt, München, 329 pp. [+ 1 map]
- Frimmel A (2003) Hochauflösende Untersuchungen von Biomarkern an epikontinentalen Schwarzschiefern des Unteren Toarciums (Posidonienschiefer, Lias ε) von SW-Deutschland. Dissertation Eberhard-Karls-Universität Tübingen, 108 pp.
- Frimmel A, Oschmann W, Schwark L (2004) Chemostratigraphy of the Posidonia Black Shale, SW Germany. I. Influence of sea-level variation on organic facies evolution. Chemical Geology 206: 199–230. <https://doi.org/10.1016/j.chemgeo.2003.12.007>
- Gabilly J (1976a) Le Toarcien à Thouars et dans le centre-ouest de la France. Les Stratotypes français 3: 217 pp. [+ 29 pls]
- Gabilly J (1976b) Évolution et systématique des Phymatoceratinae et des Grammoceratinae (Hildocerataceae Ammonitina) de la région de Thouars, stratotype du Toarcien. Mémoires de la Société Géologique de France, Nouvelle Série 124: 1–196. [+ 36 pls]
- Galácz A, Császár G, Géczy B, Kovács Z (2010) Ammonite stratigraphy of a Toarcian (Lower Jurassic) section on Nagy-Pisznice Hill (Gerecse Mts, Hungary). Central European Geology 53(4): 311–342. <https://doi.org/10.1556/CEuGeol.53.2010.4.1>
- Galbrun B, Baudin F, Bassoullet JP, Depeche F, Emmanuel L, Lachkar G, Renard M, Riveline J, Gabilly J, Hantzpergue P, Manivit H, Ruget C (1994) Stratigraphie intégrée du Toarcien stratotypique (coupes de Thouars et Airvault, Deux-Sèvres, France). Geobios Mémoire Spécial 17: 575–595. [https://doi.org/10.1016/S0016-6995\(94\)80222-X](https://doi.org/10.1016/S0016-6995(94)80222-X)
- Géczy B (1966) Upper Liassic Dactylioceratids of Úrkút. Acta Geologica Academiae Scientiarum Hungaricae 10: 427–443.
- Glenn CR, Garrison RE (2003) Phosphorites. In: Middleton GV, Church MJ, Coniglio M, Hardie LA, Longstaffe FJ (Eds) Encyclopedia of Sediments and Sedimentary Rocks, Kluwer, Dordrecht, 519–526.
- Glenn CR, Föllmi KB, Riggs SR, Baturin GN, Grimm KA, Trappe J, Abed AM, Galli-Olivier C, Garrison RE, Ilyin AV, Jehl C, Rohrlich V, Sadqaah RMY, Schidlowski M, Sheldon RE, Siegmund H (1994) Phosphorus and phosphorites: sedimentology and environments of formation. Eclogae geologicae Helvetiae 87: 747–788.
- Gradstein FM, Ogg JG, Schmitz K, Ogg G (2012) The Geologic Time Scale 2012. Vol. 2. Elsevier, Amsterdam, 1144 pp.
- Gründel J, Nützel A (2015) Gastropoden aus dem oberen Pliensbachium (Amaltheenton-Formation) NE Bayerns (Umgebung von Stauf/Dörlbach/Altdorf) (Franken, Süddeutschland). Zitteliana A 55: 45–76.
- Guex J (1973) Aperçu biostratigraphique sur le Toarcien inférieur du Moyen-Atlas marocain et discussion sur la zonation de ce sous-étage dans les séries méditerranéennes. Eclogae Geologicae Helveticae 66: 493–523.
- Guex J (1975) Description biostratigraphique du Toarcien supérieur de la bordure sud des Causses (France). Eclogae geologicae Helveticae 68: 97–129.
- Haq BU (2018) Jurassic sea-level variations: a reappraisal. GSA Today 28(1): 4–10. <https://doi.org/10.1130/GSATG359A.1>
- Hauff B (1921) Untersuchung der Fossilfundstätten von Holzmaden im Posidonienschiefer des Oberen Lias Württembergs. Palaeontographica 64: 1–42. [+ 21 pls]
- Heidorn F (1928) Paläogeographisch-tektonische Untersuchungen im Lias Zeta von Nordwestdeutschland. Neues Jahrbuch für Mineralogie, Geologie und Paläontologie, Beilage-Bände 59(Abt. B): 117–244.
- Hofbauer G (2001) Die Diskussion um die Entstehung der Süddeutschen Schichtstufenlandschaft: Eine historisch-methodologische Skizze mit einem Modell zur fluviatil gesteuerten Schichtstufen-Morphogenese. Natur und Mensch, Jahresmitteilungen der Naturhistorischen Gesellschaft Nürnberg eV, Jubiläumsausgabe 200: 85–108.
- Hoffmann K (1968a) Die Stratigraphie und Paläogeographie der bituminösen Fazies des nordwestdeutschen Oberlias (Toarcium). Geologisches Jahrbuch, Beihefte 58: 443–498.
- Hoffmann K (1968b) Neue Ammonitenfunde aus dem tieferen Unter-Toarcium (Lias ε) des nördlichen Harzvorlandes und ihre feinstratigraphische Bedeutung. Geologisches Jahrbuch 85: 1–32.
- Hoffmann R (2010) New insights on the phylogeny of the Lytoceratoidea (Ammonitina) from the septal lobe and its functional interpretation. Revue de Paléobiologie 29: 1–156.
- Hoffmann R (2015) Part L, Revised, Volume 3B, Chapter 3: Systematic Descriptions of the Lytoceratoidea. Treatise Online 70: 1–34. [Lawrence, Kansas]
- Hoffmann R, Keupp H, Grädl H (2007) Zur Korrelation der Lias-Tongruben von Unterstürming und Buttenheim (Frankenalb). Jahresberichte und Mitteilungen des oberrheinischen geologischen Vereins, Neue Folge 89: 37–48. <https://doi.org/10.1127/jmogv/89/2007/37>
- Howarth MK (1958) A monograph of the ammonites of the Liassic family Amaltheidae in Britain. Monograph of the Palaeontographical Society, 111: i–xvi, 1–26, pls 1–4; 112: xv–xxxvii, 27–53, pls 5–10.
- Howarth MK (1962) The Jet Rock Series and the Alum Shale Series of the Yorkshire coast. Proceedings of the Yorkshire Geological Society 33: 381–422. <https://doi.org/10.1144/pygs.33.4.381>
- Howarth MK (1973) The stratigraphy and ammonite fauna of the Upper Liassic Grey Shales of the Yorkshire coast. Bulletin of the British Museum (Natural History), Geology Series 24: 235–277.
- Howarth MK (1978) The stratigraphy and ammonite fauna of the Upper Lias of Northamptonshire. Bulletin of the British Museum (Natural History), Geology Series 29: 235–288.

- Howarth MK (1992) The ammonite family Hildoceratidae in the Lower Jurassic of Britain. Monograph of the Paleontographical Society 586: 1–106, pls 1–16; 590: 107–200, pls 17–38.
- Howarth MK (2013) Chapter 4: Psiloceratoidea, Eodoceratoidea, Hildoceratoidea. In: Selden PA (Ed.) Treatise Online 57 (Part L Revised) Mollusca 4, vol. 3B, Triassic and Jurassic Ammonoidea, Lawrence, Kansas (University of Kansas), 1–139. <https://doi.org/10.17161/to.v0i0.4441>
- Jacquin T, Dardeau C, Durlet C, de Graciansky PC, Hantzpergue P (1998) An overview of 2nd-order transgressive/regressive facies cycles in Western Europe. In: de Graciansky PC, Hardenbol J, Jacquin T, Vail P (Eds) Mesozoic and Cenozoic Sequence Stratigraphy of European Basin. SEPM Special Publication 60: 445–467. <https://doi.org/10.2110/pec.98.02.0445>
- Jattiot R, Fara E, Brayard A, Vennin E (2016) Revised stratigraphic range of the Toarcian ammonite genus *Porpoceras* Buckman, 1911. *Geodiversitas* 38: 505–513. <https://doi.org/10.5252/g2016n4a3>
- Jenkyns HC (1988) The early Toarcian (Jurassic) anoxic event: Stratigraphic, sedimentary, and geochemical evidence. *American Journal of Science* 288: 101–151. <https://doi.org/10.2475/ajs.288.2.101>
- Jordan R (1960) Paläontologische und stratigraphische Untersuchungen im Lias delta (Domerium) Nordwestdeutschlands. Dissertation Eberhard-Karls-Universität, Tübingen, 178 pp. [+ 9 pls]
- Keupp H, Arp G (1990) Aphotische Stromatolithe aus dem süddeutschen Jura (Lias, Dogger). Berliner Geowissenschaftliche Abhandlungen A 124: 3–33.
- Knitter H, Ohmert W (1983) Das Toarcium an der Schwärze bei Badenweiler (Oberrheingebiet S Freiburg). *Jahreshefte des geologischen Landesamtes Baden-Württemberg* 25: 233–281.
- Knitter H, Riegraf W (1984) Biostratigraphie (Cephalopoden, Ostracoden) des Oberen Toarcium von Blumberg-Achdorf/Wutach und Weilheim/Teck (Baden-Württemberg). *Jahreshefte des geologischen Landesamtes Baden-Württemberg* 26: 57–97.
- Knitter H (1983) Biostratigraphische Untersuchungen mit Ostracoden im Toarcien Süddeutschlands. *Facies* 8: 213–262. <https://doi.org/10.1007/BF02536743>
- Kolb H (1964) Der Lias ε im Gebiet zwischen Altdorf und Neumarkt. *Geologische Blätter für Nordost-Bayern* 14: 129–144.
- Kottek A (1963) Die Ammonitenabfolge des griechischen Toarcium. *Annales Géologiques des Pays Helléniques*, première série 17: 1–157. [+ 17 pls]
- Kovács Z (2011) Lower Toarcian Ammonitida fauna and biostratigraphy of the Gerecse Mountains (Hungary). *Fragmenta Palaeontologica Hungarica* 29: 1–48.
- Kraus W (1983) Paläontologische Notizen aus Mittelfranken. *Mineralien Magazin* 7(9): 414–416.
- Krumbeck L (1932a) Über den Lias von Kalchreuth bei Erlangen, besonders γ und ε. *Centralblatt für Mineralogie, Geologie und Paläontologie*, Abteilung B (Geologie und Paläontologie) 1932: 43–64, 73–90.
- Krumbeck L (1932b) Über den Fallaciosus-Horizont im Lias Mittel-ζ von Irnbach bei Regensburg. *Centralblatt für Mineralogie, Geologie und Paläontologie*, Abt. B Geologie und Paläontologie 1932: 499–518.
- Krumbeck L (1932c) Über die Höckerfazies im Lias ε Nordbayerns. *Fortschritte der Geologie und Paläontologie* 35: 245–259.
- Krumbeck L (1943–1944) Zur Stratigraphie und Faunenkunde des Lias ζ in Nordbayern. *Zeitschrift der Deutschen Geologischen Gesellschaft* 95(1943): 279–340; 96(1944): 1–74.
- Kursawe U (1995) 300 Jahre Fossiliensammeln in Altdorf. *Geologische Blätter für Nordost-Bayern* 45: 271–288.
- Kursawe U (1996) Bauder'scher Marmor – Vom Ausgangsgestein zum „kostbaren Ammonitenmarmor“. *Geologische Blätter für Nordost-Bayern* 46: 53–70.
- Lacroix P (2011) Les Hildoceratidae du Lias Moyen et Supérieur des domaines NW Européen et Téthysien. Une histoire de Famille. Dédale Editions, St-Just-la-Pendue, 354 pp. [+ 152 pls]
- Lezin C, Cubaynes R, Fauré P, Pelissié T, Rey J (1997) Le Toarcien supérieur-Aalénien dans la région de Villefranche-du-Rouergue (sud-ouest de la France). Biostratigraphie et évolution sédimentaire. *Géologie de la France* 4: 3–14.
- Loutit TS, Hardenbol J, Vail PR, Baum GR (1988) Condensed sections, the key to age determination and correlation of continental margin sequences. In: Wilgus CK, Hastings BS, Kendall CGSC, Posamentier HW, Ross CA, Van Wagoner JC (Eds) Sea-Level Changes—An Integrated Approach. SEPM Special Publication 42: 183–213. <https://doi.org/10.2110/pec.88.01.0183>
- Mäuser M (2001) Altdorf bei Nürnberg. In: Weidert WK (Ed.) Klassische Fundstellen der Paläontologie 4: 97–110. [Korb (Goldschnecke Verlag)]
- Mayr H (1995) Über Medusenhäupter, marine Palmen und Liliensteine. *Jahresbericht der Freunde der Bayerischen Staatssammlung für Paläontologie und historische Geologie* 23(1994): 18–31.
- Meyer RKF, Bauberger W (1998) Erläuterungen zur Geologische Karte von Bayern 1:25000, Blatt Nr. 6739 Bruck i. d. OPf. [mit Beiträgen von Apel, R., Bader, K., Gregor, H.J., Poschlod, K., Dobner, A., Eckbauer, M., Schmidt, F., Förster, H. und Schneider, G.]. Bayerisches Geologisches Landesamt, München, 164 pp. [+ 1 map]
- Meyer RKF, Schmidt-Kaler H (1996) Jura. In: Freudenberger W, Schwerd K (Eds) Erläuterungen zur Geologischen Karte von Bayern 1 : 500 000. 4th edn., München (Bayerisches Geologisches Landesamt), 90–111.
- Mönnig E, Nitsch E, Arp G (2015) Posidonienschiefen-Formation. In: LithoLex [Online-Datenbank]. Hannover: BGR. Last updated 19.10.2015 [cited 14.04.2020]. Record No. 4012098. <https://litholex.bgr.de>
- Nitsch E, Arp G, Mönnig E (2015) Jurensismergel-Formation. In: LithoLex [Online-Datenbank]. Hannover: BGR. Last updated 19.10.2015 [cited 14.04.2020]. Record No. 4012084. <https://litholex.bgr.de>
- Nummedal D, Swift DJP (1987) Transgressive stratigraphy at sequence-bounding unconformities: some principles derived from Holocene and Cretaceous examples. In: Nummedal D, Pilkey OH, Howard JD (Eds) Sealevel fluctuation and coastal evolution. SEPM Special Publication 41: 241–260. <https://doi.org/10.2110/pec.87.41.0241>
- Ohmert W (1976) Das Toarcium-Profil von Ballrechten (Oberrheingebiet südlich Freiburg). *Jahreshefte des geologischen Landesamtes Baden-Württemberg* 18: 79–103.
- Ohmert W, Wonik T, Rolf C, Martin M, Höhndorf A, Wetzel A, Allia V, Riegraf W, Baldanza A, Mattioli E, Bucefalo Palliani R, de Kaenel E, Bergen JA, Goy A, Ureta S, Arias C, Canales ML, Garcia Joral F, Herrero C, Martinez G, Perilli N (1996) Die Grenzziehung Unter-, Mitteljura (Toarcium, Aalenium) bei Wittnau und Fuentelsaz. Beispiele interdisziplinärer geowissenschaftlicher Zusammenarbeit. *Informationen Geologisches Landesamt Baden-Württemberg* 8: 52 pp.

- Page KN (2003) The Lower Jurassic of Europe: its subdivision and correlation. Geological Survey of Denmark and Greenland Bulletin 1: 23–59. <https://doi.org/10.34194/geusb.v1.4646>
- Page KN (2004) A sequence of biohorizons for the Subboreal Province Lower Toarcian in northern Britain and their correlation with a Submediterranean Standard. *Rivista Italiana di Paleontologia e Stratigrafia* 110(1): 109–114.
- Paul J, Wemmer K, Ahrendt H (2008) Provenance of siliciclastic sediments (Permian to Jurassic) in the Central European Basin. *Z. dt. Ges. Geowiss.* 159: 641–650. <https://doi.org/10.1127/1860-1804/2008/0159-0641>
- Peterek A, Schröder B (2010) Geomorphologic evolution of the cuesta landscapes around the Northern Franconian Alb – review and synthesis. *Zeitschrift für Geomorphologie* 54: 305–345. <https://doi.org/10.1127/0372-8854/2010/0054-0037>
- Pinna G, Levi-Setti F (1971) I Dactylioceratidae della Provincia Mediterranea (Cephalopoda Ammonoidea). *Memorie della Società Italiana di Scienze Naturali Museo Civico di Storia Naturale di Milano* 19: 49–136. [+ 12 pls]
- Pompeckj JF (1901) Der Jura zwischen Regensburg und Regenstauf. *Geognostische Jahreshefte* 14: 139–220.
- Price GD (1999) The evidence and implications of polar ice during the Mesozoic. *Earth-Science Reviews* 48: 183–210. [https://doi.org/10.1016/S0012-8252\(99\)00048-3](https://doi.org/10.1016/S0012-8252(99)00048-3)
- Putzer H (1939) Der Jura am Keilberg bei Regensburg. *Neues Jahrbuch für Mineralogie, Geologie und Paläontologie, Beilage-Bände* 82(Abt. B): 90–154.
- Quenstedt FA (1845–1849) Cephalopoden. *Petrefactenkunde Deutschlands*, 1. Abt. 1845: 1–104, Taf. 1–6; 1846: 105–184, Taf. 7–12; 1847: 185–264, Taf. 13–18; 1848: 265–472, Taf. 19–30; 1849: 473–580, Taf. 31–36; Tübingen (Fues).
- Quenstedt FA (1851–1852, 1865–1866, 1882–1885a) Handbuch der Petrefactenkunde. 1. Aufl.: 792 pp., 62 pls; 2nd edn.: 982 pp., 86 pls; 3rd edn.: 1239 pp., 100 pls; Tübingen (Laupp).
- Quenstedt FA (1856–1858) Der Jura. 1856: 1–576, Taf. 1–72; 1857: 577–824, Taf. 73–100; 1858: 825–843; Tübingen (Laupp).
- Quenstedt FA (1872–1875) Petrefactenkunde Deutschlands. III. Echinodermen (Echiniden). Text und Atlas, 720 pp., Taf. 62–89; Tübingen (Fues).
- Quenstedt FA (1876) Petrefactenkunde Deutschlands. IV. Die Echinodermen (Asteriden und Encriniden nebst Cysti- und Blastoideen). Text und Atlas, 720 S., Taf. 90–114; Tübingen (Fues).
- Quenstedt FA (1881–1884) Petrefactenkunde Deutschlands. Erste Abteilung, 7: Gasteropoden. 1881: 1–192, Taf. 185–190; 1882: 193–320, Taf. 191–196; 1882: 321–464, Taf. 197–202; 1883: 465–592, Taf. 203–208; 1884: 593–736, Taf. 209–214; 1884: 737–867, Taf. 215–218; Leipzig (Fues).
- Quenstedt FA (1882–1885b) Die Ammoniten des Schwäbischen Jura. 1. Band. Der Schwarze Jura (Lias). 1882: 1–48; 1883: 49–56; 1884: 97–240; 1885b: 241–440; Stuttgart (Schweizerbart).
- Reuter L (1927) Geologische Darstellung des schwäbisch-fränkischen Juras, seines triasischen Vorlandes und des südlich angrenzenden Molasse-Gebietes. In: Schuster M (Ed.) *Abriß der Geologie von Bayern r. d. Rh.*, Abt. IV: 1–132, München (Oldenburg and Piloty).
- Riegraf W, Werner G, Lörcher F (1984) Der Posidonienschifer – Biostratigraphie, Fauna und Fazies des südwestdeutschen Untertoarciums (Lias epsilon). Enke, Stuttgart, 195 pp.
- Riegraf W (1985a) Mikrofauna, Biostratigraphie und Fazies im Unteren Toarcium Südwestdeutschlands und Vergleiche mit benachbarten Gebieten. *Tübinger Mikropaläontologische Mitteilungen* 3: 1–232.
- Riegraf W (1985b) Biostratigraphie, Fauna und Mikropaläontologie des Untertoarcium-Profiles von Unterstürmig (Oberfranken, Süddeutschland). *Geologische Blätter für Nordost-Bayern* 34/35: 241–272.
- Röhl HJ, Schmid-Röhl A (2005) Lower Toarcian (Upper Liassic) Black Shales of the Central European Epicontinental Basin: A Sequence Stratigraphic Case Study from the SW German Posidonia Shale. In: Harris NB (Ed.) *The Deposition of Organic-Carbon-Rich Sediments. Models, Mechanisms, and Consequences*. SEPM Special Publication 82: 165–189. <https://doi.org/10.2110/pec.05.82.0165>
- Rübsam W, Al-Husseini M (2020) Calibrating the Early Toarcian (Early Jurassic) with stratigraphic black holes (SBH). *Gondwana Research* 82: 317–336. <https://doi.org/10.1016/j.gr.2020.01.011>
- Rulleau L (2007) *Biostratigraphie et paléontologie du Lias supérieur et du Dogger de la région Lyonnaise. Tome 1*. Dédale Editions, Lafarge Ciments, 129 pp.
- Salger M, Schmid H (1982) Die Forschungsbohrung Eschertshofen 1981 (Vorläufige Mitteilung). *Geologica Bavaria* 83: 145–161.
- Schmidt-Kaler H (1974) *Geologischen Karte von Bayern 1:250000, Erläuterungen zu Blatt Nr. 6634 Altdorf b. Nürnberg [mit Beiträgen von Apel, R., Bader, K., Berger, K., Diez, T., Gauckler, P.]*. Bayerisches Geologisches Landesamt, München, 152 pp.
- Schulbert C (2001a) Die Ammonitenfauna und Stratigraphie der Tongrubbe Mistelgau bei Bayreuth (Oberfranken). Beihefte zu den Berichten der Naturwissenschaftlichen Gesellschaft Bayreuth 4: 1–183.
- Schulbert C (2001b) Geologische Kartierung der Umgebung von Mistelgau bei Bayreuth (Oberfranken). Diploma mapping, Friedrich-Alexander-Universität Erlangen-Nürnberg, 58 pp. [+ XXVIII pp., 1 map]
- Simmons MD (2012) Sequence Stratigraphy and Sea-Level Change. In: Gradstein FM, Ogg JG, Schmitz M, Ogg GM (Eds) *The geologic time scale 2012*, vol 1. Elsevier, Amsterdam, 239–267. <https://doi.org/10.1016/B978-0-444-59425-9.00013-5>
- Simonsen S (2013) Fossilien aus dem Posidonienschifer der Tongrubbe Mistelgau. *Der Steinkern* 15: 28–46.
- Stankievitch ES (1964) *Amoniti yurskikh peschano-glinitovih otlojenii severo-zapadnogo Kavkaza [Ammonites in the Jurassic sandy clay deposits of the northwestern Caucasus]*. Nauka, Moscow-Leningrad, 99 pp. [in Russian]
- Stier K (1922) Vorläufige Mitteilung über das Ergebnis der Untersuchung der württemb. Ölschiefer-und Eisenerzvorkommen. *Jahresberichte und Mitteilungen des oberrheinischen geologischen Vereins, Neue Folge* 11: 94–97. <https://doi.org/10.1127/jmogr/11/1922/94>
- Straub W (1946) Stratigraphie und Bildungsgeschichte des Lias z. in Mittelwürttemberg und Südbaden. Dissertation Technische Hochschule Stuttgart, 72 pp.
- Teichert BMA, Luppold FW (2013) Glendonites from an Early Jurassic methane seep – Climate or methane indicators? *Palaeogeography, Palaeoclimatology, Palaeoecology* 390: 81–93. <https://doi.org/10.1016/j.palaeo.2013.03.001>
- Ulrichs M (1971) Alter und Genese des Belemniteschlachtfeldes im Toarcium von Franken. *Geologische Blätter für Nordost-Bayern* 21: 65–83.

- Urbachs M (1977a) The Lower Jurassic in Southwestern Germany. Stuttgarter Beiträge zur Naturkunde B 24: 1–41.
- Urbachs M (1977b) Stratigraphy, ammonite fauna and some os-tracodes of the Upper Pliensbachian at the type locality (Lias, SW-Germany). Stuttgarter Beiträge zur Naturkunde B 28: 1–13.
- Venturi F, Ferri R (2001) Ammoniti lassici dell'Appennino Centrale. Medesimi, Città di Castello, 268 pp.
- von Freyberg B (1958a) 250 Jahre geologische Forschung in der Fränkischen Alb. Geologische Blätter für Nordost-Bayern 8: 34–43.
- von Freyberg B (1958b) Johann Friedrich Bauder (1713–1791) und seine Bedeutung für die Versteinerungskunde in Franken. Geologische Blätter für Nordost-Bayern 8: 76–106.
- von Freyberg B (1958c) Johann Jacob Baiers Oryctographia Norica nebst Supplementen. Erlanger Geologische Abhandlungen 29, 133 pp.
- von Freyberg B (1972) Funde und Fortschritte zur Erdgeschichte beim Bau des Ludwig-Donau-Main-Kanals (1836–1845). Geologische Blätter für Nordost-Bayern 22: 100–125.
- von Gümbel CW (1891) Geognostische Beschreibung des Koenigreichs Bayern. 4. Abtheilung, Geognostische Beschreibung der Fränkischen Alb (Frankenalb) mit dem anstossenden Fränkischen Keupergebiete. Fischer, Kassel, 763 pp.
- Wagner G (1960) Einführung in die Erd- und Landschaftsgeschichte: mit besonderer Berücksichtigung Süddeutschlands. Ferdinand Rau, Öhringen, 694 pp.
- Weiß KP, Freitag D (1991) *Frechiella subcarinata* (Young and Bird, 1822), ein bemerkenswerter Ammonit aus dem höheren Untertoarcium (*bifrons*-Zone) der Fränkischen Alb. Geologische Blätter für Nordost-Bayern 41: 125–132.
- Weißenmüller M (2017) Eine Reise in den unteren Jura der Region Altdorf. Self publisher, Berg, 200 pp.
- Wiedemann HU (1966) Die Geologie der Blätter Göppingen (7223) und Lorch (7224) in Württemberg mit Nachträgen zu Blatt Weilheim (7323) 1:25000. Arbeiten aus dem Geologisch-Paläontologischen Institut der Technischen Hochschule Stuttgart, Neue Folge 53, 226 pp.
- Wunstorf W (1904) Die Fauna der Schichten mit Harpoceras dispansum Lyc. vom Gallberg bei Salzgitter. Jahrbuch der Königlich Preussischen Geologischen Landesanstalt und Bergakademie zu Berlin 25: 488–525. [+ pls 17–20]
- Zeiss A, Schirmer W (1965) Ober den obersten Lias delta bei Hetzles ostwärts Erlangen. Geologische Blätter für Nordost-Bayern 15: 189–193.
- Zimmermann J, Franz M, Heunisch C, Luppold FW, Mönnig E, Wolfgramm M (2015) Sequence stratigraphic framework of the Lower and Middle Jurassic in the North German Basin: Epicontinental sequences controlled by Boreal cycles. Palaeogeography, Palaeoclimatology, Palaeoecology 440: 395–416. <https://doi.org/10.1016/j.palaeo.2015.08.045>